



MAX-PLANCK-GESellschaft

Regulation of the neuronal SNARE-complex by accessory proteins

Dissertation for the award of the degree
“Doctor rerum naturalium”
of the Georg-August-Universität Göttingen
within the doctoral program (*IMPRS Molecular Biology*)
of the Georg-August University School of Science (GAUSS)

Submitted by
Shrutee Jakhanwal

from New Delhi, India
Göttingen, 2017



MAX-PLANCK-GESellschaft



MAX-PLANCK-GESELLSCHAFT

Thesis Committee

Prof. Dr. Reinhard Jahn

Department of Neurobiology,
Max Planck Institute for Biophysical Chemistry, Göttingen.

Prof. Dr. Claudia Steinem

Department of Biomolecular Chemistry,
Institute for Organic and Biomolecular Chemistry, Göttingen.

Prof. Dr. Silvio Rizzoli

Department of Neuro- and Sensory Physiology,
University Medical Center, Göttingen.

Members of the Examination Board

Referee: Prof. Dr. Reinhard Jahn

2nd Referee: Prof. Dr. Claudia Steinem

Further members of the Examination Board

Prof. Dr. Silvio Rizzoli

Department of Neuro- and Sensory Physiology,
University Medical Center, Göttingen.

Prof. Dr. Camin Dean

Trans-synaptic Signaling Group,
European Neuroscience Institute, Göttingen.

Prof. Dr. Henning Urlaub

Bioanalytical Mass Spectrometry Group,
Max Planck Institute for Biophysical Chemistry, Göttingen.

Prof. Dr. Blanche Schwappach

Department of Molecular Biology,
University Medical Center, Göttingen.

Date of oral examination: July 13, 2017.



MAX-PLANCK-GESellschaft



Declaration in the Lieu of Oath

I hereby declare that the thesis entitled "*Regulation of the neuronal SNARE-complex by accessory proteins*" has been compiled by me, with the aid of no sources other than quoted.

-Shrutee Jakhanwal



MAX-PLANCK-GESellschaft



Acknowledgements

“Saying ‘thank you’ is the only way to keep love alive”

The journey of my PhD studies, in Göttingen has been quite an amazing experience, both in terms of science and life in general. And, the first person whom I would like to thank here is, Professor Reinhard Jahn, for being a brilliant supervisor and a pillar of support throughout the ups and downs of the journey. A big, big thank you! If not for you, I would never have found the little scientist in me. I want you to know that you are a huge source of inspiration, both as a human-being and as a scientist. To all the good times, good discussions and good results-“PROST”!

Another very important person who has been a source of inspiration and support, and to whom I am really thankful for his guidance through these years is Dr. Steffen Burkhardt. He has contributed a lot by making my experience in Göttingen, ‘a lot like home’.

I would like to extend my most heart-felt thanks to my parents, to whom I am ever grateful. I thank them for their immense love and affection and most of all, for being there for me, ALWAYS! Be it via a Skype chat or a phone call, they have made sure that I never forget to believe in myself. Thank you Papa, thank you Mummy...I love you!

A big vote of thanks also goes to my sister (Aditi), my brother-in-law (Charu) and my brother (Suyash) for cheering me up whenever anything stupid tried to stress me and for never stopping to say “You can do it!”. A special thanks to my little niece (Dhaani), whose cute smile has always been enough to make me forget all my worries. And, I do not want to forget Abhishek, whose love and companionship is a bliss. Thank you all for making the journey so beautiful!

I also want to thank my grandparents (Late) Rama Prasad and Vinodini Prasad for their blessings.

Science of course requires hard-work, but more often than that, it requires a peace of mind. A special thanks goes to Hans Dieter Schmitt, for providing an extremely kind and generous company during the thesis-writing phase. And, cheers to the bond of friendship I have shared with Marcelo, Wolfgang, Sasha and Mahi. My thanks also goes to my flatmates, Pratibha and Sindhu for the random talks, tons of laughter and a lot of good memories. I would also like to thank some people for being critical-it helped me grow ☺ And, not to forget some very dear people who are miles apart but always in the heart- Thank you, thank you, thank you.

And, thank you God for answering my prayers!



MAX-PLANCK-GESELLSCHAFT

DEDICATION

I would like to dedicate this thesis to my parents, **Mr. Anil Kumar and Mrs. Saroj Sinha**, who always encouraged me to go on every adventure, *especially this one!*

*For their patience, faith and love,
Because, they always understood....*

!! ॐ साई राम!!



Table of Contents

1	INTRODUCTION	11
1.1	INTRACELLULAR MEMBRANE-TRAFFICKING.....	11
1.2	SYNAPTIC-VESICLE EXOCYTOSIS.....	13
1.3	SPECIFICITY AND STAGES OF SNARE-MEDIATED MEMBRANE-FUSION.....	15
1.4	SNARE-HYPOTHESIS AND SNARE-CYCLE.....	16
1.5	ROLE OF ACCESSORY PROTEINS IN NEURONAL EXOCYTOSIS.....	18
1.5.1	MUNC18-1.....	18
1.5.2	MUNC13.....	21
1.5.3	SYNAPTOTAGMIN	22
1.5.4	COMPLEXIN.....	23
1.6	SM-PROTEINS AS REGULATORS OF SNARE-MEDIATED MEMBRANE FUSION.....	23
1.7	PROPOSED ROLES OF MUNC18-1 IN SYNAPTIC VESICLE EXOCYTOSIS.....	25
1.7.1	MUNC18-1 AS A CHAPERONE FOR SYNTAXIN1A TRANSPORT.....	25
1.7.2	MUNC18-1 AS A TEMPLATE FOR SNARE-COMPLEX ASSEMBLY.....	26
1.7.2.1	SYNTAXIN1A/MUNC18-1 COMPLEX AS A STARTING POINT FOR SNARE-COMPLEX ASSEMBLY.....	26
1.7.2.2	SYNTAXIN1A/SNAP25A/MUNC18-1 COMPLEX AS AN INTERMEDIATE FOR SNARE-COMPLEX ASSEMBLY.....	26
1.7.2.3	SYNTAXIN1A/MUNC18-1/SYNAPTOBREVIN COMPLEX AS AN INTERMEDIATE IN SNARE-COMPLEX ASSEMBLY.....	28
1.7.3	ROLE OF MUNC18-1 IN ACCELERATING SNARE-MEDIATED FUSION.....	28
1.8	AIMS AND HYPOTHESIS	29
2	MATERIALS AND METHODS.....	31
2.1	PROTEIN CONSTRUCTS.....	31

2.2	PROTEIN EXPRESSION AND EXTRACTION FOR THE INDIVIDUAL NEURONAL SNARES AND MUNC18-1.....	35
2.3	CHROMATOGRAPHIC PURIFICATION OF PROTEINS.....	36
2.4	PROTEIN EXPRESSION AND EXTRACTION PROCEDURE FOR THE C-TERMINALLY STABILIZED ΔN-COMPLEX.....	36
2.5	ASSEMBLY AND PURIFICATION OF THE BINARY SYNTAXIN1A/SNAP25A COMPLEX.....	36
2.6	ASSEMBLY AND PURIFICATION OF THE SYNTAXIN1A/SNAP25A/MUNC18-1 COMPLEX.....	37
2.7	FLUORESCENT-LABELING OF SNARE-PROTEINS.....	37
2.8	FLUORESCENCE ANISOTROPY.....	38
2.9	FÖRSTER RESONANCE ENERGY TRANSFER (FRET).....	38
2.10	HETERONUCLEAR SINGLE QUANTUM COHERENCE SPECTROSCOPY (HSQC).....	39
2.11	LIPOSOME/PROTEOLIPOSOME PREPARATION.....	39
2.12	CO-FLOTATION ASSAY.....	40
2.13	SDS-PAGE AND COOMASSIE BLUE STAINING/ FLUORESCENCE SCANNING.....	41
2.14	WESTERN BLOT ANALYSIS.....	42
2.15	CHEMICAL CROSS-LINKING.....	42
2.16	MASS SPECTROMETRY (MS/MS).....	43
2.17	TRYPsin-DIGESTION ASSAY.....	44
3	RESULTS.....	45
3.1	EFFECT OF MUNC18-1 ON THE SYNTAXIN1A/SNAP25A (2:1) COMPLEX.....	45
3.2	OPTIMIZATION OF THE IN-VITRO ASSEMBLY AND PURIFICATION OF THE TERNARY SYNTAXIN1A/SNAP25A/MUNC18-1 COMPLEX.....	52
3.3	SYNTAXIN1A/SNAP25A/MUNC18-1 AS AN EFFICIENT ACCEPTOR-COMPLEX FOR SYNAPTOBREVIN-BINDING.....	54
3.3.1	STUDYING SYNAPTOBREVIN-BINDING TO THE SYNTAXIN1A/SNAP25A/MUNC18-1 COMPLEX USING FLUORESCENCE ANISOTROPY.....	54
3.3.2	FÖRSTER RESONANCE ENERGY TRANSFER (FRET).....	56
3.4	COMPARISON OF SYNTAXIN1A/SNAP25A/MUNC18-1 COMPLEX WITH THE PREVIOUSLY CHARACTERIZED ACCEPTOR COMPLEXES.....	57



3.5	STABILITY OF THE SYNTAXIN1A/SNAP25A/MUNC18-1 COMPLEX.	62
3.6	ARCHITECTURE OF THE SYNTAXIN1A/SNAP25A/MUNC18-1 COMPLEX.....	66
3.7	IS MUNC18-1 DISPLACED AFTER THE BINDING OF SYNAPTOBREVIN TO THE SYNTAXIN1A/SNAP25A/MUNC18-1 COMPLEX?.....	73
3.8	FULL-LENGTH SYNAPTOBREVIN IS REQUIRED FOR EFFICIENT BINDING TO THE SYNTAXIN1A/SNAP25A/MUNC18-1 COMPLEX.....	84
3.9	IS THE SYNTAXIN1A/SNAP25A/MUNC18-1 COMPLEX RESISTANT TO DISASSEMBLY BY NSF AND ASNAP?	90
4	DISCUSSION	96
4.1	STRUCTURAL PRECISION FINE-TUNES PROTEIN-PROTEIN INTERACTIONS.	96
4.2	MUNC18-1 AS A KEY PLAYER FOR SNARE-COMPLEX ASSEMBLY.	101
4.3	UNDERSTANDING THE TRANSITION OF AN ACCEPTOR-COMPLEX TO A FULLY-ASSEMBLED SNARE-COMPLEX.....	104
4.4	PHYSIOLOGICAL RELEVANCE OF THE SYNTAXIN1A/SNAP25A/MUNC18-1 COMPLEX.	105
5	CONCLUSIONS AND PERSPECTIVES.....	109
6	REFERENCES.....	111
	APPENDIX	121
	LIST OF FIGURES	128
	CURRICULUM VITAE	132
	LIST OF PUBLICATIONS.....	135

LIST OF ABBREVIATIONS

SNAREs	Soluble N-ethylmaleimide-sensitive factor attachment protein receptor
NSF	N-ethylmaleimide-sensitive factor
αSNAP	N-ethylmaleimide-sensitive factor attachment protein-alpha
SM	Sec1/Munc18-1
CATCHR	Complexes associated with tethering containing helical rods
Syx	Syntaxin1a
SN25	Synaptosomal-associated protein 25 (SNAP25)
Syb	Synaptobrevin
VAMP	Vesicle-associated membrane protein
M18	Munc18-1
PC12	Pheochromocytoma cells
AAA-ATPase	ATPases associated with diverse cellular activities
HOPS	Homotypic fusion and vacuole protein sorting
BS3	Bis(sulfosuccinimidyl)suberate
DDM	n-Dodecyl β -D-maltopyranoside
OG	Octyl β -D-glucopyranoside
CHAPS	3-((3-cholamidopropyl) dimethylammonio)-1-propanesulfonate



ATP	Adenosine triphosphate
IPTG	Isopropyl β -D-1-thiogalactopyranoside
DTT	Dithiothreitol
EDTA	Ethylenediamine tetra-acetic acid
HEPES	4-(2-hydroxyethyl)-1-piperazineethanesulfonic acid
TCEP	Tris-(2-carboxyethyl)phosphine
MES	2-(N-morpholino)ethanesulfonic acid
KCl	Potassium chloride
NaCl	Sodium chloride
MgCl₂	Magnesium chloride
TBST	Tris buffered saline, supplemented with Tween20
IEC	Ion-exchange chromatography
SDS-PAGE	Sodium dodecyl sulfate polyacrylamide gel electrophoresis

1 Introduction

1.1 Intracellular membrane-trafficcking.

The structural integrity of a cell is maintained by the continuous transport of proteins and lipids from one compartment of the cell to the other. Intracellular protein trafficking is mediated by a large plethora of proteins, each of which are specific to a given cellular compartment. The final step involves fusion of vesicles and membrane merger, which in most of the intracellular trafficking events is mediated by a special family of proteins called the SNARE (soluble N-ethylmaleimide sensitive factor attachment protein receptor) proteins. The discovery of the SNARE-proteins dates back to the 1980s, when they had been identified from a series of temperature-sensitive secretion-deficient mutants ('*sec-mutants*') in *Saccharomyces cerevisiae*, which showed accumulation of secretory vesicles in yeast cells (1). In subsequent years, a large number of SNARE-proteins have been identified in several different organisms. SNARE-proteins are the key components of most of the membrane fusion events in a cell and despite their sequence divergence, their mechanisms of actions have highly been conserved through evolution.

SNAREs belong to a superfamily of proteins, which are characterized by a special motif termed the 'SNARE-motif'. It consists of 60-70 amino-acid residues containing heptad repeats in their membrane-proximal regions (2, 3). Most of the SNARE-proteins also contain a transmembrane domain. This feature however, is not universal, with some of the SNARE-proteins lacking a transmembrane anchor. A classic example of this case is represented by the neuronal SNARE, SNAP25a which lacks a transmembrane domain, and is attached to the membrane by palmitoylation (4). Apart from the characteristic SNARE-motifs and the transmembrane-domains, some SNARE-proteins (for example, the yeast Sso1p and the neuronal syntaxin1a) also feature an autonomously folded N-terminal domain that have been implicated to have a regulatory role in SNARE-mediated membrane-fusion.

SNAREs are topologically distributed on opposing membranes, and the SNARE-motifs of the cognate SNAREs interact with each other to assemble into a parallel four-helical bundle. This core complex brings the two membranes in very close apposition with each other, and helps in membrane merger by using the free-energy released during the formation of the four-helical bundle (5). The core SNARE-complex exhibits peculiar biochemical characteristics like resistance to cleavage by botulinum neurotoxins, resistance to digestion by proteolytic enzymes (e.g. Trypsin), SDS-resistance and partial heat-resistance above a temperature of 70°C.

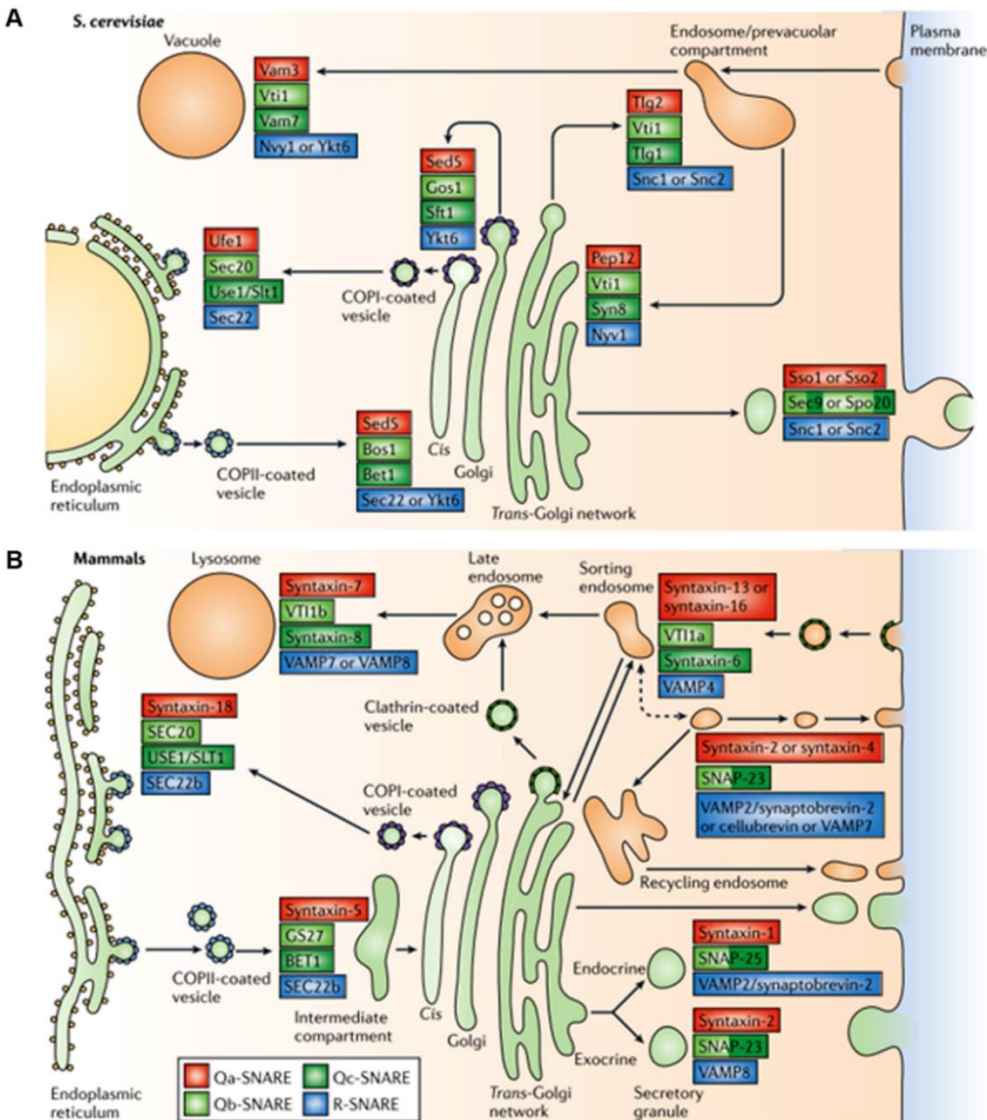


Figure 1.1-1. SNARE-proteins involved at different steps of intracellular trafficking in a yeast cell and a mammalian cell.

(A) A yeast cell represents a simplistic eukaryotic model for intracellular trafficking. Specific sets of SNARE-proteins have been assigned to each step of the pathway. However, the R-SNAREs Nvy1 and Ykt6 can substitute each other during vacuole fusion. Likewise, Sec22 and Ykt6 can substitute each other in the fusion of the ER-derived vesicles with the Golgi apparatus. (B) In a mammalian cell, distinct SNAREs are assigned to the different compartments of the trafficking pathway. A partial overlap of function, however, does exist for some compartments, as depicted for the sorting and recycling endosomes. [Taken from (5)].

Introduction

In a eukaryotic cell, distinct SNARE-proteins mediate membrane fusion in different intracellular compartments. Some SNAREs (for example syntaxin7), however are involved in more than one intracellular compartments. A summarized view of the SNAREs involved at the different stages of intracellular trafficking in the yeast and mammalian cells have been represented in Figure 1.1-1.

1.2 Synaptic-vesicle exocytosis

Membrane fusion is critical not only for intracellular trafficking pathways, but also for cell-cell communication. The cells of the nervous system represent a specialized example in this case, where the fusion of neurotransmitter-containing synaptic vesicles with the neuronal plasma membrane leads to neurotransmitter-release. The process of synaptic vesicle exocytosis is central to the formation of a core-SNARE complex by the three neuronal SNAREs namely syntaxin1a, SNAP25a and synaptobrevin2. Syntaxin1a and synaptobrevin-2 (also known as VAMP-2) are transmembrane proteins, containing one SNARE-motif each, whereas SNAP25a (containing two SNARE-motifs) lacks a transmembrane domain and is attached to the neuronal plasma membrane by a palmitoylation anchor. The two SNARE-motifs of SNAP25a are attached by a linker domain, and this covalent linkage between the domains has been implicated to be evolutionarily important for increasing the local effective concentration of SNAREs on the neuronal plasma membrane, for achieving rapid rates of neurotransmission (6). On similar lines, in non-synaptic cells, where the speed of fusion is not so crucial, the Qb and Qc SNARE motifs are often distributed between two different proteins (7). In a neuronal cell, syntaxin1a and SNAP25a are present on the neuronal plasma membrane, whereas synaptobrevin is present on the synaptic vesicles. The membrane-insertion of all the transmembrane SNARE-proteins are mediated by a specialized trafficking pathway called the GET-pathway (8).

The neurotransmitter-containing synaptic vesicles in the brain cells are roughly 40nm in diameter and are broadly maintained in three different pools, namely (i) readily-releasable pool (1-2% of all synaptic vesicles) (ii) recycling pool (10-20% of all synaptic vesicles) and (iii)reserve pool (80-90% of all synaptic vesicles) (9). The readily-releasable pool is depleted rapidly (requiring less than a second) upon stimulation of a nerve cell, whereas the recycling pool and the reserve pool require prolonged stimulation, with depletion occurring only after a few seconds (for the recycling pool) or even minutes (for the reserve pool) (9). In the readily-releasable pool, the synaptic vesicles are docked with the plasma-membrane in a release-ready state, at specialized sites called the 'active-zone'. The 'active-zone' contains several tethering and scaffolding factors, including Bassoon, Piccolo, RIMs, ELKs, α -liprin and Munc13-1 (10), that help in bringing the synaptic vesicles closer to the plasma membrane.

During neurotransmitter release, the SNARE motifs of the three neuronal SNAREs interact to form a four helical bundle, which is extremely critical for membrane fusion. The crystal structure of the cis-SNARE complex suggests that the interaction of the SNARE-proteins extend to the bilayer, thereby coupling the final state of SNARE-complex formation with membrane merger (2). The SNARE-complex consists of a hydrophobic core containing 16 layers of amino-acid residues numbered from -7 to +8. The central 'zero'-layer is however, ionic in nature, consisting of one polar residue contributed by each of the SNARE-motifs. Syntaxin1a and SNAP25a contribute one or, two glutamine (Q) residues respectively to this layer and, are hence called 'Q-SNAREs', with syntaxin1a being the Qa-SNARE, and SNAP25a being the Qb/Qc SNARE, respectively. Synaptobrevin2 contributes an arginine side-chain to the 'zero-layer' and is hence called the 'R-SNARE' (11).

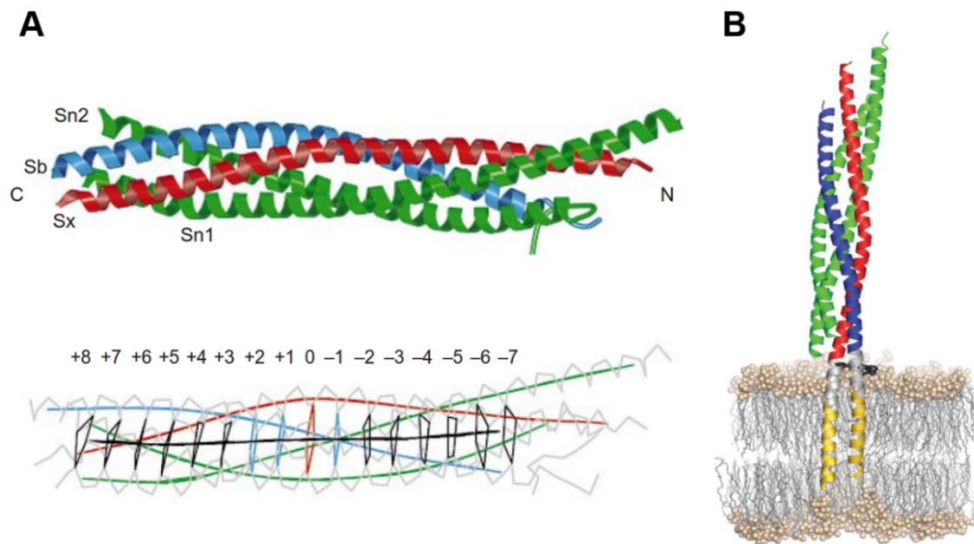


Figure 1.2-1. SNARE-core complex and the central layers of the interacting side-chains.

(A) (*Top*) Crystal structure of the SNARE-core complex containing the cytoplasmic fragments of the SNARE-proteins. (*Bottom*) The core of the SNARE-complex is extremely hydrophobic, containing 16 layers of amino-acids numbered from -7 to +8, with only one ionic layer at the center, termed the 'zero'-layer. (B) The crystal structure of the 'cis'-SNARE-complex containing the respective transmembrane domains of the SNARE-proteins. This model indicated that the energy from SNARE-zippering can be directly communicated to the bilayer via the linker regions connecting the SNARE-motif and transmembrane domain of the SNARE-proteins, thereby causing membrane fusion. *Color codes: syntaxin1a is represented in red, SNAP25a in green and synaptobrevin2 in blue.* [(A) has been adapted from (3) and (B) is taken from (2)].

Introduction

1.3 Specificity and stages of SNARE-mediated membrane-fusion.

The intracellular trafficking event is a highly coordinated process and requires extreme precision for the directional targeting of a donor vesicle to the correct target membrane. It was earlier believed that the topological (12) and pairing specificity (13) between the cognate SNAREs alone is responsible for conferring compartmental specificity for fusion. This view has been supported by *in-vitro* studies in PC12 cells, where the fusion of dense-core vesicles with the plasma membrane occur much faster in the presence of the cognate SNAREs, as compared to the non-cognate SNAREs (14). However, additional studies using *in-vitro* liposome fusion assays have indicated that some R-SNAREs can mediate fusion even with non-cognate Q-SNAREs, rendering the hypothesis of SNARE-specificity rather tenuous (13). Electron microscopy studies of giant squid synapses after treatment with botulinum B or tetanus neurotoxins (which cleave the neuronal R-SNARE, synaptobrevin (15)), showed normal vesicle docking, but a complete abolishment of evoked neurotransmitter release, as measured by electrophysiology (16). These observations indicated that the SNARE proteins might not be crucial for docking, and they might have a significant role only at a later step in membrane fusion. A recent study of hippocampal organotypic slice cultures from mice using cryofixation and electron tomography has, however, reported that both Q- and R-SNAREs are required for synaptic vesicle docking (17).

Subsequent studies hinted on the role of another family of proteins called Rab-proteins (small GTPases) in mediating compartmental specificity for SNARE-mediated fusion (18). Rab3 and Rab27b are associated with synaptic vesicles and have been indicated to have a role in docking synaptic vesicles to the plasma membrane (19). A deletion mutant of Rab3A (the major Rab-protein present in the brain) in mice was shown to cause a marked decrease in vesicle docking after nerve stimulation leaving the total number of vesicles unaffected, thereby indicating the role of Rab-proteins upstream of vesicle fusion (20). Taking into account the role of Rab-proteins in vesicle-docking and the cognate-specificity exhibited by the SNARE-proteins, it has collectively been proposed that both the Rab-proteins and the SNARE-proteins together, help in creating a check-point for preventing fusion between mismatched compartments (21).

SNARE-mediated membrane-fusion proceeds in stages with gradual changes in contacts between the proteins and lipids of the two compartments. As depicted in Figure 1.3-1, during the most initial phase, vesicles approach the plasma membrane but the SNAREs are not in contact with each other. This is followed by an initial contact of the SNARE-proteins that is expected to proceed from the N-terminus towards the C-terminus. The zippering reaction results in the formation of a loosely docked state, followed by a tightly docked state, which in turn increases the lateral tension on the membrane leading to hemi-fusion (22). The unfavorable

interaction between the bilayer interfaces results in the breaking of the membrane, creating a fusion-pore.

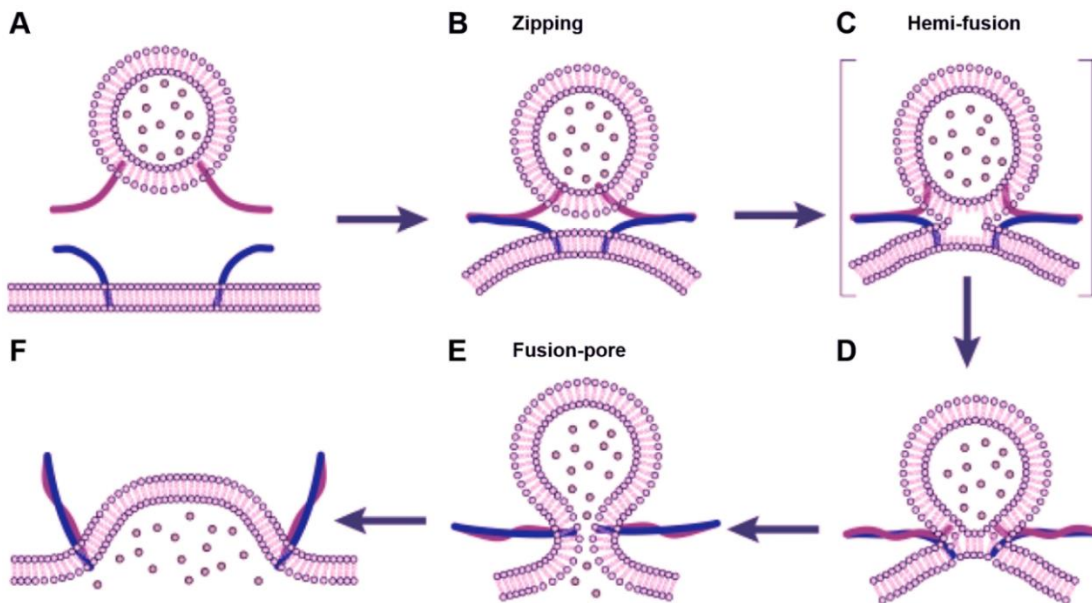


Figure 1.3-1. Steps involved in SNARE-mediated membrane fusion.

(A) The vesicles approach the target membrane, but the contact between the partner SNAREs is not yet established. (B) The SNAREs contact each other and start zipping from the N-terminus towards the C-terminus. (C) The zipping of the SNAREs increases the lateral tension, resulting in hemi-fusion. (D) The tight-zipping of the SNAREs brings the distal leaflets in contact with each other, resulting in (E) membrane breakage and the formation of a fusion pore. This is followed by (F) membrane-relaxation and expansion of the fusion-pore. [Taken from (22)].

1.4 SNARE-hypothesis and SNARE-cycle.

The SNARE-hypothesis, which was proposed in the year 1993 (19), states that each cellular compartment contains vesicles with specific ‘v-SNAREs’ that pair up with their cognate ‘t-SNAREs’ to bring about membrane fusion. In the context of the neuronal SNAREs, it has been proposed that the three SNAREs interact together with the AAA-ATPase NSF, and its co-factor α -SNAP to form a 20S fusion particle. The binding of α -SNAP to the SNARE-complex creates a binding-site for NSF. The

Introduction

energy released from the ATPase activity of NSF disassembles the SNARE-complex into individual proteins, thereby making them available for subsequent rounds of fusion (19). A schematic overview of the SNARE-cycle has been presented in Figure 1.4.1.

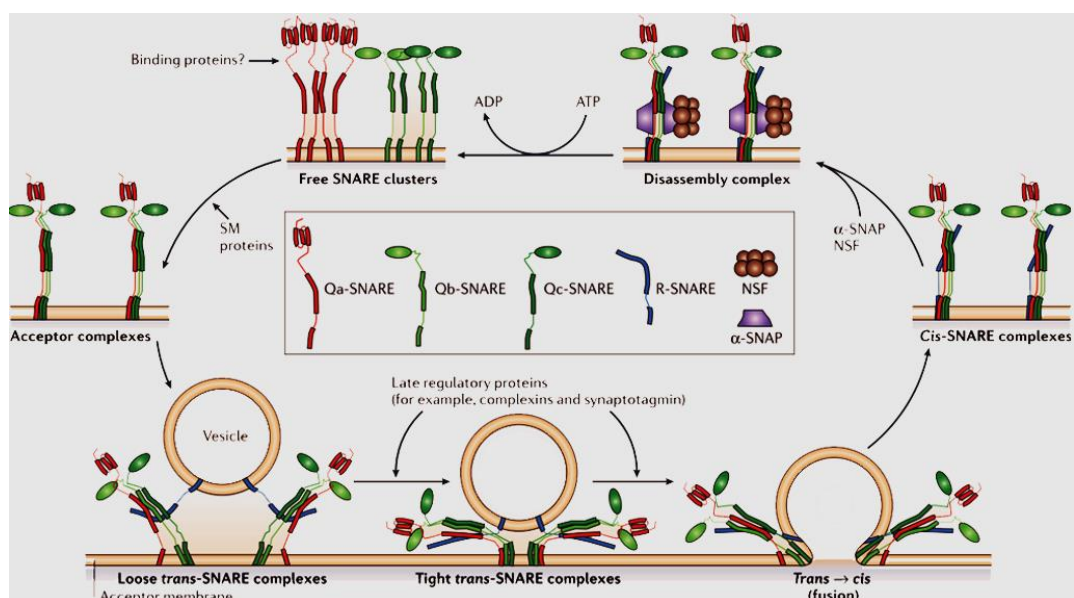


Figure 1.4-1. Steps involved in SNARE-complex assembly and subsequent SNARE-recycling.

SNARE-complex assembly initiates with the conformational reorganization of the Q-SNAREs, which is likely mediated by a member of the SM-protein family (*top left*). The so formed 'acceptor complexes' then interact with the R-SNAREs on the vesicles, proceeding from the N-terminus towards the C-terminus. The assembly progresses from a 'loose complex' (where the SNAREs are only partially assembled), towards a 'tight complex' (where the SNAREs are fully assembled), leading to fusion-pore formation and membrane-merger (*bottom*). In case of regulated exocytosis, the late-stages in the assembly process are controlled by accessory proteins like complexin and synaptotagmin, which are implicated to 'clamp' the SNAREs in a partially-zippered state, allowing membrane-fusion only upon calcium influx. Upon fusion, the SNARE complex transitions from a 'trans'-conformation to a 'cis'-conformation (*right*). The *cis*-SNARE-complex is disassembled by NSF- α SNAP, making the SNAREs available for subsequent rounds of fusion. [Adapted from(5)].

In regulated exocytosis, SNARE-complex assembly becomes irreversible after calcium-influx. The subsequent phase followed by full-zippering of the SNAREs and



formation of the four-helical bundle leads to the formation of the fusion-pore and membrane-merger.

1.5 Role of accessory proteins in neuronal exocytosis.

Since the discovery of the SNARE-proteins in late 1980s, major advances have been made in understanding the mechanism underlying the SNARE-machinery. Genetic approaches to screen for mutants showing defects in synaptic neurotransmission have provided a key tool to identify proteins that play a crucial role in the process. An understanding of the mechanistic details of the process has however, been gained through biochemical approaches. In this context, a wealth of knowledge has been provided by the isolation and characterization of native synaptic vesicles and by the purification of factors to reconstitute the fusion machinery *in-vitro*. The SNARE-proteins constitute a minimalistic system to mediate the *in-vitro* fusion between two sets of liposomes (23). Technical advancements have allowed the reconstitution studies to be performed in different membrane systems like small unilamellar vesicles (SUVs) (24), large unilamellar vesicles (LUVs) (25), giant unilamellar vesicle (GUVs) (26) and also supported bilayer systems like pore-spanning membranes (27). Electrophysiological measurements, on the other hand, have provided a significant tool to study synaptic vesicle exocytosis in intact cells (28).

A major discrepancy that has been observed while comparing SNARE-mediated membrane fusion *in-vitro* and *in-vivo*, is the speed at which the vesicle fusion occurs. Synaptic vesicle exocytosis occurs at a sub-millisecond time-scale in an intact neuronal cell (29), but requires several minutes for completion in an *in-vitro* bulk assay (25). One of the many reasons that can explain this discrepancy, is the absence of accessory proteins that are crucial for the regulation of the SNARE-machinery. The rates of vesicle fusion *in-vitro* have been observed to be altered substantially by accessory proteins like synaptotagmin-1 (30), Munc18-1 (31) and according to a recent report, also by Munc13-1 (32). The four major accessory proteins that are speculated to play crucial roles at different stages of SNARE-mediated membrane fusion in synapses are Munc-13, Munc-18, complexin and synaptotagmin.

1.5.1 Munc18-1

Munc18 (**M**ammalian **unc**18) is an important regulatory protein involved in the regulation of SNARE-mediated exocytosis. It belongs to the SM (**S**ec1/**M**unc18) family of proteins. It is a cytosolic protein that has been highly conserved from *Saccharomyces cerevisiae* to *Homo sapiens*. The first SM-protein, unc18 was

Introduction

identified as a product of the gene '*unc18*' whose mutation resulted in an 'uncoordinated' locomotion phenotype in *C.elegans* (33). Some years later, an orthologue of *unc18-1* was identified in *Saccharomyces cerevisiae*, and was referred to as 'Sec-1' (34). In subsequent years, orthologues of *unc18-1* were identified in several different organisms, like *Drosophila* (Rop) (35), plants (KEULE) (36) and mammals (Munc18). There are three homologues of Munc18 namely Munc18-1, Munc18-2 and Munc18-3 (also known as Munc18a, Munc18b and Munc18c, respectively). Munc18-1 is predominantly found in brain cells and is also referred to as 'neuronal Sec-1'. Munc18-2 shares 62% sequence homology with Munc18-1 and is predominantly present in kidney cells, intestine, testis, rat adipose tissue and 3T3-L1 cells (37). Munc18-3 only has 51% sequence homology with Munc18-1, and shows a rather ubiquitous pattern of expression (37).

Munc18-1 is a multi-domain cytosolic protein of 67 kDa, possessing an arch-shaped architecture (38). The affinity of interaction between the cytoplasmic variant of syntaxin1a (Syx1-262) and Munc18-1 is extremely high, with a dissociation constant (K_d) of 1.4 nM (39). Syntaxin1a is characterized by an N-terminal regulatory domain, which consists of an N-peptide and an Habc-domain. The Habc-domain of syntaxin1a forms an anti-parallel three-helical bundle, and can interact with its SNARE-motif, resulting in a '*closed*' conformation of syntaxin1a, which is incompatible for SNARE-complex assembly. Munc18-1 interacts via its domain 1 and domain 3 (designated the '*cleft*') with the '*closed*' conformation of syntaxin1a and '*locks*' it in this state (40). The N-peptide of syntaxin1a interacts with Munc18-1 via a spatially distinct region, termed the N-peptide binding site (39). As shown in Figure 1.5-1 C, this site is positioned directly opposite of the '*cleft*', on the outer surface of Munc18-1 (39). The interaction of Munc18-1 with the N-peptide *in-vitro* has been proposed to regulate the gating of syntaxin1a/Munc18-1 complexes into fully assembled SNARE-complexes, thereby acting as a switch to regulate SNARE-complex formation (41).

The role of Munc18-1 in neuronal exocytosis has long been investigated, but its precise mode of action remains unclear. Munc18-1 *null* mutations in mice were found to be embryonically lethal, causing a complete abrogation of neurotransmitter release (38). This observation was indicative of a stimulatory role of Munc18-1 in the process of neurotransmitter release, which was in stark contrast to the inhibitory sequestration of syntaxin1a by Munc18-1 observed *in-vitro* (39, 40, 42). Munc18-1 thus appears to play dual roles in neuronal exocytosis. Experimental evidence point toward different possible roles for Munc18-1 in regulating SNARE-mediated membrane fusion. Some studies indicate that Munc18-1 might have a role in structuring the acceptor complexes on the neuronal plasma membrane and setting the stage for SNARE-complex assembly (43–46). In yet another scenario, Munc18-1 has been speculated to act during the final step of the fusion reaction by helping in the enlargement of the fusion pore (31). The details of

the proposed roles of Munc18-1 in SNARE-mediated membrane fusion have been discussed in section 1.7.

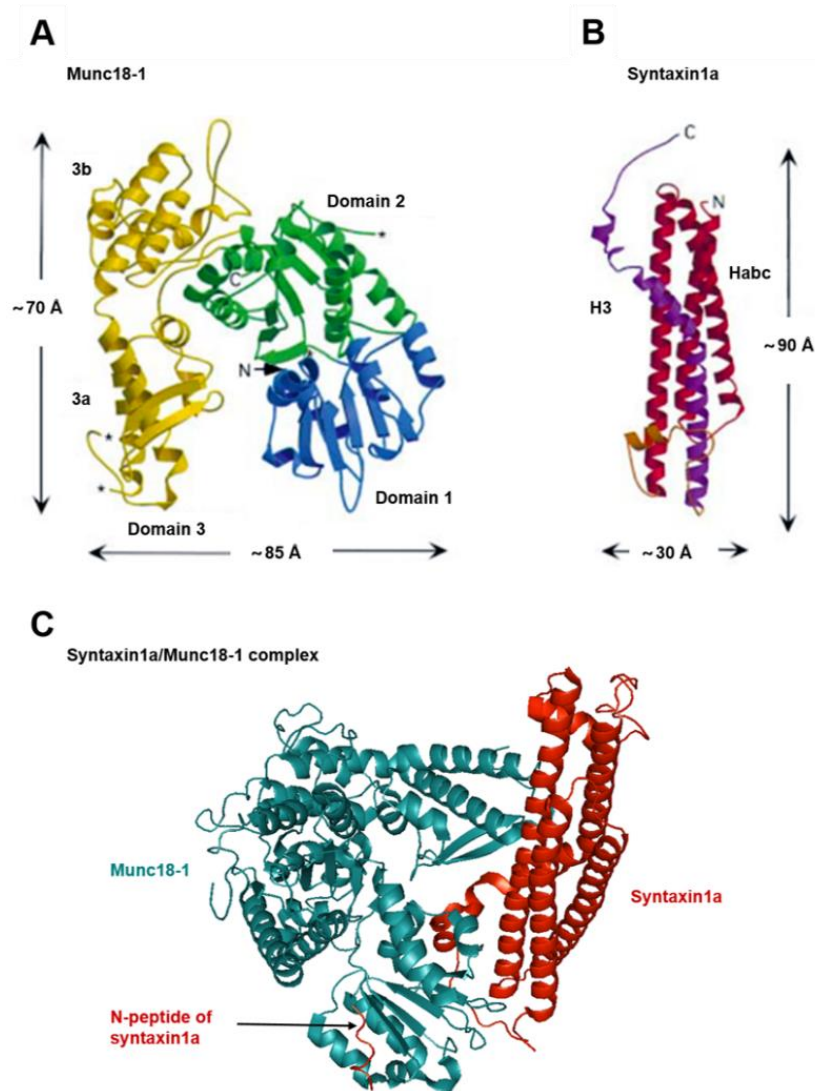


Figure 1.5-1. Ribbon diagrams of Munc18-1, syntaxin1a and the syntaxin1a/Munc18-1 complex.

(A) Ribbon diagram of Munc18-1 showing the arch-shaped arrangement of the three domains. (B) Ribbon diagram of syntaxin1a, depicting the Habc-domain and the SNARE-motif. Note that the N-peptide has not been presented in this diagram. (C) Syntaxin1a/Munc18-1 complex with syntaxin1a locked in the 'closed' conformation. Munc18-1 is shown in *cyan* and the N-peptide, Habc-domain and the SNARE-motif of syntaxin1a have been shown in *red*. [(A) and (B) have been adapted from (47), and (C) has been adapted from (39)].

Introduction

1.5.2 Munc13

Munc13 is another regulatory protein involved in SNARE-mediated exocytosis. It belongs to the CATCHR (Complexes associated with tethering containing helical rods) family of proteins. There are three isoforms of Munc13 namely Munc13-1, Munc13-2 and Munc13-3. These three isoforms show relatively different expression patterns in the rat brain, with overlaps between at least two isoforms in one particular compartment. Munc13-2 and Munc13-3 have been speculated to act together with Munc13-1, to help in the regulation of neurotransmitter release (48).

Munc13-1 is an elongated, cytosolic, multi-domain protein that is particularly expressed in the brain, with highest localization in the cerebral cortex, hippocampus, cerebellum and the olfactory bulb (49) and some expression also in pancreatic islet cells (50). It interacts with the N-terminus of the neuronal Qa-SNARE, syntaxin1a and with a calcium sensor Doc2, thereby helping in synaptic vesicle docking and priming. Additionally, it also interacts with active-zone proteins like RIM and ERC to help in tethering the synaptic vesicles to the neuronal plasma membrane at the active zone.

A double knock-out of Munc13-1/Munc13-2 in hippocampal neurons shows normal synaptogenesis, but causes a complete abrogation of spontaneous and evoked neurotransmitter release, underlining a key significance for the role of Munc13 in synaptic vesicle exocytosis (51). This phenotype, can, however, be rescued by the over-expression of the MUN-domain of Munc13-1 (52). The MUN-domain is an autonomously folded domain of Munc13-1 containing four sub-domains, the crystal structure of which has been reported only recently (53). The architecture of the MUN-domain resembles that of some homologous tethering factors like Tip20 and Exo70 (53).

A speculated key role of Munc13-1 in neuronal exocytosis is to bring about the transition of syntaxin1a from its 'closed' conformation in the syntaxin1a/Munc13-1 complex to an 'open' conformation, thereby making syntaxin1a available for SNARE-complex formation (54). A simplistic view of this transition mediated by Munc13-1 has been depicted in Figure 1.5-2. The interaction of Munc13-1 with syntaxin1a occurs via the linker region of syntaxin1a that connects the Habc-domain with its SNARE-motif (54).

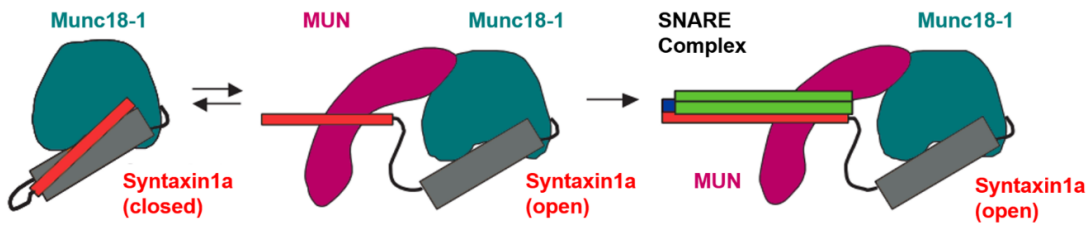


Figure 1.5-2. Munc13-1 causes the transition from the ‘closed’ syntaxin1a to ‘open’ syntaxin1a.

(*Left*) Munc13-1 interacts with syntaxin1a within the syntaxin1a/Munc18-1 complex, causing a conformational switch in syntaxin1a resulting in the formation of an intermediate consisting of syntaxin1a, Munc18-1 and Munc13-1, with syntaxin1a being in an open conformation (*middle*). The SNARE-motif of syntaxin1a then becomes available to interact with SNAP25 and synaptobrevin, leading to SNARE-complex assembly (*right*). Munc18-1 is depicted in *cyan*, syntaxin1a SNARE-motif in *red*, syntaxin1a Habc domain in *grey*, MUN-domain in *magenta*, SNAP25a SNARE-motif in *green* and synaptobrevin SNARE-motif in *blue*. [Adapted from (54)].

1.5.3 Synaptotagmin

Synaptotagmin is a membrane-trafficking protein, containing an N-terminal membrane anchor (unlike the SNARE-proteins) and two C-terminal C2-domains, namely C2A and C2B (55). The neuronal counterpart, synaptotagmin1 is a synaptic vesicle protein, and is commonly referred to as the ‘calcium-sensor’ for neuronal exocytosis (56). The C2B-domain contains a distinct patch comprising of basic amino-acids that binds to membranes containing phosphatidylinositol (4, 5) biphosphate (57). Synaptotagmin-1 also interacts with the Qa-SNARE syntaxin1a via its C2-domains (both in the monomeric form and as part of the SNARE-complex). This interaction, however, appears to be regulated by the intracellular calcium concentration (58). In a resting nerve cell with basal levels of calcium, synaptotagmin-1 has been hypothesized to ‘clamp’ the SNAREs in a partially-zipped state (59). The increase in the intracellular calcium levels, accompanied by the arrival of an action potential, results in binding of calcium ions to the C2-domains of synaptotagmin-1. The calcium-bound synaptotagmin then triggers SNARE-mediated fusion by either disengaging from the SNAREs (thereby releasing the clamp) (59) or by lowering the activation energy for membrane fusion by extensive membrane interactions via calcium-bridges (30).

Introduction

1.5.4 Complexin

Complexin belongs to a family of SNARE-binding proteins involved in the regulation of synaptic vesicle exocytosis. It is a cytosolic protein that can interact both with membrane phospholipids via its C-terminal amphipathic helix (60) as well as with (partially) assembled SNARE-complexes via its central helix (5). Complexin has been implicated in clamping SNARE-complex assembly by two alternate mechanisms: (i) by binding to the C-terminus of the syntaxin1a/SNAP25a complex, thereby interfering with the assembly of a fully-zippered SNARE-complex (61) and (ii) by forming cross-links between two adjacent pre-fusion complexes (62). The former clamping model is, however, debatable because it has been argued that the strong-binding of synaptobrevin to the pre-fusion complex is strong enough to cause the displacement of any downstream clamping agent, indicating that if at all, complexin-mediated clamping must occur at a stage that precedes initial contacts between the Q-SNAREs and the R-SNARE (63, 64). A deletion mutant of complexin causes a marked decrease in calcium-evoked synchronous release but leaves the asynchronous release unaltered (65). These observations implicate the role of complexin in calcium-triggered neurotransmission. The precise role of complexin in regulating the SNARE-fusion machinery, however, remains incompletely understood.

1.6 SM-proteins as regulators of SNARE-mediated membrane fusion.

As discussed in section 1.5.1, SM-proteins are highly conserved cytosolic proteins that play a critical role in SNARE-mediated membrane fusion. It is, however, important to mention that despite the high degree of sequence conservation, the mechanisms of actions of the different SM-proteins remain quite diverse. The modes of interaction of the SM-proteins can be grouped into three major categories: (i) interaction with the respective Qa-SNAREs involving the N-terminal regulatory domain, (ii) interaction with the fully-assembled SNARE-complexes, and (iii) simultaneous interactions with more than one partner SNARE at a given point of time. The different modes of interaction of some of the SM-proteins with their respective SNAREs or the SNARE-complex has been tabulated in Table 1. The difference in the modes of interactions of the SM-proteins can be attributed to their fine structural details. For example, the yeast Sec1 contains a peculiar C-terminal tail that is absent in all other SM-proteins, which favors its interaction with a fully-assembled SNARE-complex (66).

**Table 1. A summarized view of the interaction of some of the SM-proteins with components of their respective SNARE-machinery.**

<i>SM-protein</i>	<i>Compartment-specific Qa-SNARE</i>	<i>Cellular localization</i>	<i>Organism</i>	<i>Mode of interaction</i>
<i>Sly1</i>	Sed5	Sites of vesicular transport between ER and the Golgi apparatus.	<i>Saccharomyces cerevisiae</i>	Interacts with the N-peptide of Sed5 (67) and the assembled SNARE complex (68).
<i>Vps45</i>	Tlg2	Sites of vacuolar protein-sorting from the Golgi.	<i>Saccharomyces cerevisiae</i>	Interacts with the N-peptide of Tlg2 and the assembled SNARE-complex (69).
<i>Vps33</i>	Vam3 (on the vacuoles)/ Pep12 (at the endosomes)	Sites of protein sorting from Golgi to the yeast vacuole/lysosomes	<i>Saccharomyces cerevisiae</i>	Interacts with the Qa-SNARE (Vam3), Qc-SNARE (Vam7), R-SNARE (Nyv1) and the assembled SNARE-complex (70).
<i>Sec1</i>	Sso1	Budding sites on the yeast plasma membrane.	<i>Saccharomyces cerevisiae</i>	Interacts with the Qb/Qc SNARE, Sec9 (71) and the assembled SNARE-complex (72).
<i>Munc18-1</i>	Syntaxin1a	Sites of exocytosis on the neuronal plasma membrane.	<i>Rattus norvegicus</i>	Interacts with the 'closed' conformation of syntaxin1a (73), with the Q-SNARE complex (syntaxin1a/SNAP25a) (46), with the R-SNARE, synaptobrevin (74) and the assembled SNARE-complex (42, 75).
<i>Munc18-2</i>	Syntaxin3	Secretion sites on the plasma membrane of epithelial cells	<i>Rattus norvegicus</i>	Interacts with the Q-SNARE complex (syntaxin 3 / SNAP25) (76).
<i>Munc18-3</i>	Syntaxin4	Secretion sites on the plasma membrane of adipocytes	<i>Rattus norvegicus</i>	Interacts with the Qa-SNARE, syntaxin 4 and the assembled SNARE-complex (77).

Introduction

1.7 Proposed roles of Munc18-1 in synaptic vesicle exocytosis.

Despite major efforts in understanding the role of Munc18-1 in neuronal exocytosis, its precise mode of action remains enigmatic. Concisely, Munc18-1 has been proposed to act at multiple stages of SNARE-complex assembly, with several evidence of its significance both at the *'pre-docking'* as well as *'post-docking'* stage of the process of neurotransmitter release. Furthermore, Munc18-1 has been speculated to act as a *'chaperone'* for the transport of syntaxin1a from the Golgi-compartment to the neuronal plasma membrane.

As discussed in section 1.5.1, Munc18-1 enters into a very tight interaction with syntaxin1a (73). The syntaxin1a/Munc18-1 complex has, however been hypothesized to undergo substantial changes after being targeted to the neuronal plasma membrane, in order to mediate SNARE-complex assembly (40). The role of Munc18-1 in structuring the SNAREs for SNARE-complex assembly had been proposed almost a decade ago (41, 78) and has recently been revisited (44, 46, 79). A consensus view on how Munc18-1 lays the foundation for SNARE-complex formation, however, is still unclear. Alternatively, Munc18-1 has been speculated to accelerate the rate of SNARE-mediated membrane-fusion by its interacting with the fully assembled SNARE-complexes (42, 80). The details associated with each of the proposed roles for Munc18-1 have been discussed in the following sub-sections.

1.7.1 Munc18-1 as a chaperone for syntaxin1a transport.

First and foremost, Munc18-1 has been proposed to act as a *'chaperone'* for targeting syntaxin1a from the endoplasmic reticulum to the neuronal plasma membrane. This transport occurs with syntaxin1a in a *'closed'* conformation, and poses an important regulatory step by minimizing any futile interactions of syntaxin1a with its partner SNAREs during the transport process (81).

In PC12 cells, a downregulation of Munc18-1 drastically lowers syntaxin 1a expression and also affects its targeting to the plasma membrane, with syntaxin1a now being localized to the perinuclear regions of the cell (82). In addition to this, the docking and secretion ability of the dense-core vesicles were also seen to be compromised in these cells. These observations highlighted the role of Munc18-1 in maintaining syntaxin1a stability and targeting, as well as synaptic vesicle docking. Subsequent studies performed in mice showed that a double *knock-out* of Munc18-1 results in a 70% reduction in the expression levels of syntaxin1a (83), consistent with the observations in PC12 cells. The low amount of syntaxin1a synthesized was, however, seen to be correctly targeted to the plasma membrane for successful participation in SNARE-complex assembly. This observation raised a contradiction to the previously reported role of Munc18-1 (82) and suggested that



Munc18-1 is important for the stability of syntaxin1a but not for its intracellular targeting (83).

1.7.2 Munc18-1 as a template for SNARE-complex assembly.

Three different mechanisms for Munc18-1-mediated SNARE-complex assembly have been proposed so far. According to these hypotheses, Munc18-1 could provide a template for SNARE-complex assembly either (i) by interacting with the Qa-SNARE syntaxin1a (84), (ii) by interacting simultaneously with the Qa-SNARE syntaxin1a and the Qb/Qc SNARE SNAP25a (46, 79) or, (iii) by a simultaneous interaction with the Qa-SNARE syntaxin1a and the R-SNARE synaptobrevin2 (44).

1.7.2.1 Syntaxin1a/Munc18-1 complex as a starting point for SNARE-complex assembly.

Till date, the precise composition and conformation of the acceptor complexes on the neuronal plasma membrane for receiving the incoming synaptic vesicles, largely remains unknown. The syntaxin1a/SNAP25a complex, which is one of the candidates for forming this acceptor complex, is susceptible to disassembly by NSF- α SNAP(43), making the proposition rather tenuous. Additionally, a recent study has shown that the SNAP25a in the syntaxin1a/SNAP25a complex can be completely displaced by the action of Munc18-1, causing the formation of syntaxin1a/Munc18-1 complex (85). Moreover, biochemical characterization of the syntaxin1a/Munc18-1 complex has reported that this complex cannot be disassembled by NSF- α SNAP (85). *In-vitro* vesicle fusion starting with liposomes containing syntaxin1a/Munc18-1, could be reconstituted in the presence of all the important components of the SNARE-machinery, namely the SNARE-proteins (syntaxin1a, SNAP25a and synaptobrevin2), Munc18-1, Munc13-1, synaptotagmin, NSF and α SNAP. Based on these findings, it has been suggested that syntaxin1a/Munc18-1 complexes can possibly act as the starting point for SNARE-complex assembly, allowing SNARE-assembly to progress in an NSF- α SNAP-resistant manner (85).

1.7.2.2 Syntaxin1a/SNAP25a/Munc18-1 complex as an intermediate for SNARE-complex assembly.

In an alternative scenario, Munc18-1 has been speculated to set the stage for SNARE-complex assembly by interacting with both syntaxin1a and SNAP25a simultaneously.

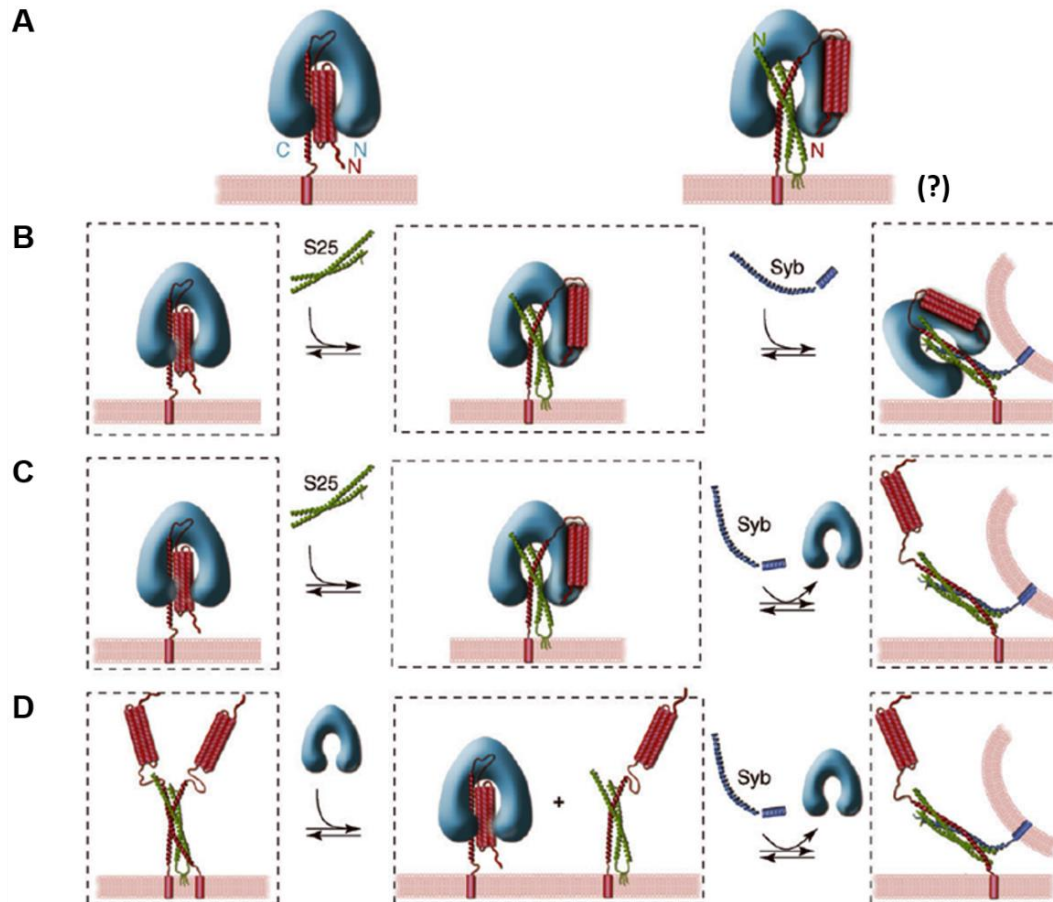


Figure 1.7-1. Schematic representations of the association of Munc18-1 with SNARE-proteins during the process of SNARE-complex assembly.

(A) The well characterized syntaxin1a/Munc18-1 complex is shown on the left and a speculated binding of Munc18-1 (*not yet characterized*) with both syntaxin1a and SNAP25a has been shown on the right. The mechanisms for transition of the syntaxin1a/Munc18-1 to a fully assembled SNARE-complex remains unknown (B) A proposed model for the gating of syntaxin1a/Munc18-1 complex to SNARE-complex assembly. Through yet unknown mechanisms, Munc18-1 is speculated to undergo alterations in its interaction with syntaxin1a, allowing SNAP25a to bind to this complex. The subsequent binding of synaptobrevin to the syntaxin1a/SNAP25a/Munc18-1 complex results in SNARE-complex assembly, with Munc18-1 bound to it. (C) The binding of synaptobrevin to the syntaxin1a/SNAP25a/Munc18-1 complex can, however, also lead to the displacement of Munc18-1. (D) An alternative model of SNARE-complex assembly assumes that the syntaxin1a/SNAP25a (2:1) complex can be acted upon by Munc18-1, shifting the equilibrium towards syntaxin1a/Munc18-1 complex or 1:1 syntaxin1a/SNAP25a complex. Both of these complexes can then bind synaptobrevin, resulting in SNARE-complex formation. [Adapted from (78)].



Single-molecule experiments have shown that the association of accessory proteins with the syntaxin1a/SNAP25a complex can stabilize the 1:1 acceptor complex, thereby preventing the formation of the “*off-pathway*” 2:1 syntaxin1a/SNAP25a complexes (45). On similar lines, distance measurements using electron paramagnetic resonance (EPR) have been reported, showing that the association of Munc18-1 with the syntaxin1a/SNAP25a complex results in the formation of a syntaxin1a/SNAP25a/Munc18-1 complex in a 1:1:1 stoichiometry, with syntaxin1a being shifted towards a more ‘*open*’ conformation. In addition to this, nano-domains containing clusters of syntaxin1a/SNAP25a/Munc18-1 have been observed on the neuronal plasma membrane (46). The presence of this tripartite assembly on the neuronal plasma membrane provided further support to the role of Munc18-1 in providing a facilitated template for SNARE-complex assembly via its interaction with both the Q-SNAREs (46).

1.7.2.3 Syntaxin1a/Munc18-1/synaptobrevin complex as an intermediate in SNARE-complex assembly.

In addition to the high-affinity interaction of Munc18-1 with syntaxin1a, Munc18-1 has been reported to interact with the R-SNARE, synaptobrevin, *albeit* with much lower affinity (74). Cross-linking studies have shown contacts between the membrane-proximal regions of synaptobrevin and residues in the outer surface of the domain 3b of Munc18-1 (74). Additionally, mutations of Munc18-1 that disrupt its interaction with synaptobrevin have been proposed to alter fusion kinetics in reconstituted systems (86). Likewise, a recent study using single-molecule force experiments to study SNARE-complex assembly has indicated that Munc18-1 can provide a template for SNARE-complex assembly via its simultaneous interaction with the Qa-SNARE, syntaxin1a and the R-SNARE, synaptobrevin2 (44).

Support for this hypothesis has been derived from a similar mechanism of SNARE-complex assembly that has lately been proposed for Vps33, a yeast orthologue of Munc18-1. Crystal structures of the vacuolar SM-protein, Vps33 have been obtained in complex with the Qa-SNARE, Vam3 and the R-SNARE, Nyv1. An overlay of these two structures has shown stark resemblance to a partially-zipped SNARE-complex, leading to the proposal of a model for SNARE-assembly via a SM-protein/Qa-SNARE/R-SNARE-template (87).

1.7.3 Role of Munc18-1 in accelerating SNARE-mediated fusion.

Last but not the least, *in-vitro* liposome fusion assays have indicated the role of Munc18-1 in accelerating the rate of SNARE-mediated liposome fusion (31). This function of Munc18-1, however, remains debatable. Biochemical characterizations

Introduction

have indicated that Munc18-1 forms a complex with the (cytosolic) core SNARE-complex that contains syntaxin1a in an 'open' conformation (80, 88). The functional implication of this association has been implicated in the enlargement of fusion pore by Munc18-1 (31). The affinity of Munc18-1 for the SNARE-complex is, however, quite low (74), thereby attenuating the physiological relevance of this interaction. Contradiction of this role of Munc18-1 has surfaced from studies showing the interaction of Munc18-1 with only the N-terminus of syntaxin1a, without any implications for contact with the core helical bundle (39, 41). The significance of Munc18-1 at the fusion-step of neuronal exocytosis still remains to be understood.

1.8 Aims and hypothesis

As summarized in the previous section, despite extensive research to understand the mechanistic details underlying the SNARE-machinery, many important questions in the field still remain unanswered. Amongst the many open questions, one of the major concern that remains to be addressed, is the composition and precise conformation of the acceptor complex present on the neuronal plasma membrane. In the light of the most recent research, the SM-protein Munc18-1 has been implicated to provide a template for SNARE-complex assembly. As indicated in the previous section, a consensus view on how Munc18-1 sets the stage for SNARE-complex assembly largely remains missing.

Several approaches indicate towards the formation of a ternary complex between syntaxin1a, SNAP25a and Munc18-1. Although evidence for the existence of this ternary complex on the plasma membrane do exist, a syntaxin1a/SNAP25a/Munc18-1 complex containing full-length proteins, has till date, not been isolated and characterized *in-vitro*. Therefore, one of the major aims of this project was to perform the *in-vitro* assembly and purification of this ternary complex, in order to attain a thorough knowledge about its biochemical properties.

In this work, a detailed characterization of the syntaxin1a/SNAP25a/Munc18-1 complex has been performed, using several different biophysical and biochemical approaches. The major questions to be addressed in this regard, were:

- To test the efficiency of synaptobrevin-binding to the syntaxin1a/SNAP25a/Munc18-1 complex
- To determine the molecular architecture of the syntaxin1a/SNAP25a/Munc18-1 complex
- To check whether synaptobrevin-binding to the syntaxin1a/SNAP25a/Munc18-1 complex results in the formation of a fully assembled SNARE-complex.



- To check the conformational status of Munc18-1 after binding of synaptobrevin to the syntaxin1a/SNAP25a/Munc18-1 complex.
- To check whether the association of Munc18-1 with the Q-SNAREs (syntaxin1a and SNAP25a) can protect the syntaxin1a/SNAP25a/Munc18-1 complex against disassembly by NSF- α SNAP.

I have tried to achieve the above-mentioned goals using diverse techniques like fluorescence anisotropy, FRET, HSQC-NMR, chemical cross-linking and MS/MS amongst others. This study is thus important, not only for gaining an insight into the conformational status of the acceptor complexes required for synaptic vesicle exocytosis, but also for clarifying the long-debated role of Munc18-1 in neuronal exocytosis.

2 Materials and Methods

2.1 Protein constructs

The sequences for all the recombinant proteins used in this work were obtained from *Rattus norvegicus*. All the constructs for the SNARE-proteins and the SM-protein, Munc18-1 had been cloned into a pET28a vector, containing an N-terminal His₆-tag, designed for protein purification using Ni⁺⁺-NTA affinity chromatography. Schematic representations of the wild-type proteins used in this study have been represented in Figure 2.1-1.

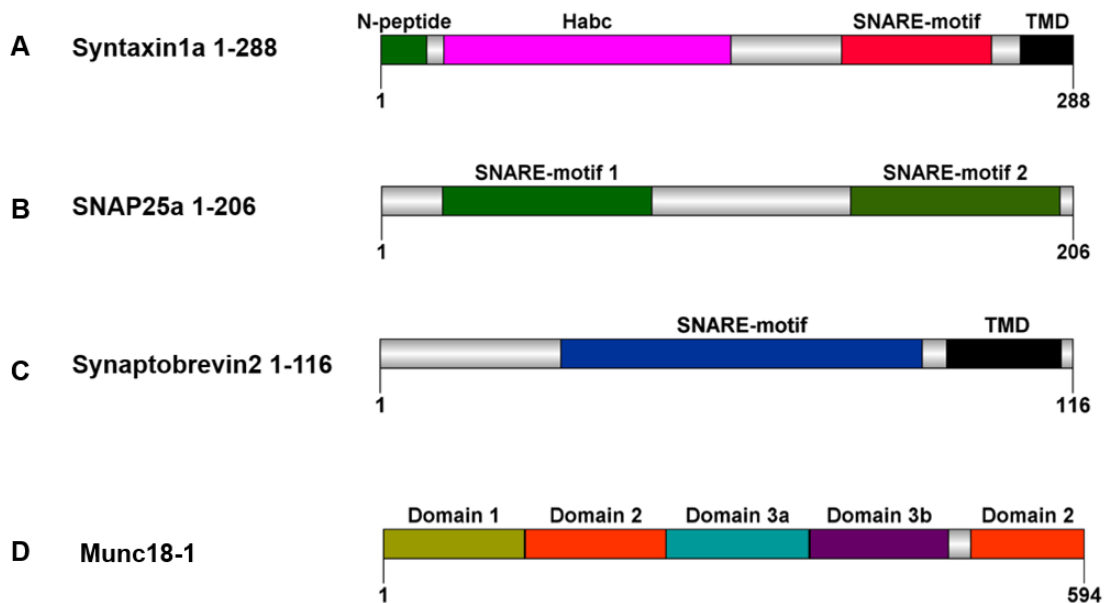


Figure 2.1-1. Wild-type constructs for neuronal SNARE proteins and SM-protein used in this study.

(A) Full-length syntaxin1a (Qa-SNARE) (B) full-length SNAP25a (Qb- and Qc- SNARE) and (C) full-length synaptobrevin (R-SNARE) (D) full-length Munc18-1 (SM-protein).

In addition to the full-length wild-type SNARE-constructs, single cysteine-mutants of both Q-SNAREs as well as R-SNAREs were used in this study for fluorescence-based (FRET and anisotropy) experiments. The cysteine mutants of the Q-SNAREs used in this study have been depicted in Figure 2.1-2.

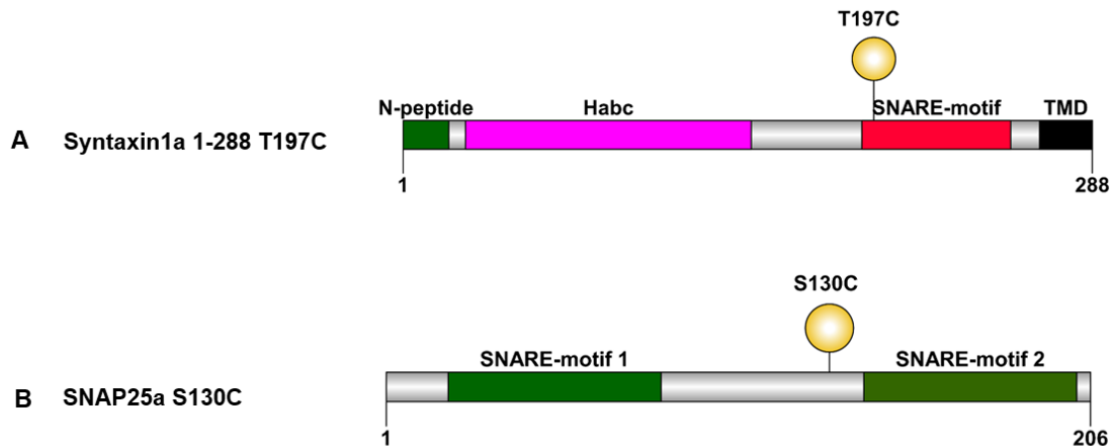


Figure 2.1-2. Representation of the cysteine mutants of syntaxin1a and SNAP25a used in this study.

(A) Single-cysteine mutant of syntaxin1a containing a point mutation T197C and (B) Single-cysteine mutant of SNAP25a containing a serine to cysteine mutation at position 130. In both the cases, all the native cysteines had been mutated to serine residues.

Different fragments of the neuronal R-SNARE, synaptobrevin (as shown in Figure 2.1-3) were also employed during the course of this study. For the purification of the Δ N-complex by co-expression, a pETduet 1 vector containing syntaxin1a (183-288) and a cytoplasmic fragment of synaptobrevin (residues 49-96) was used. All the above-mentioned constructs had been previously cloned and have been summarized in Table 2.

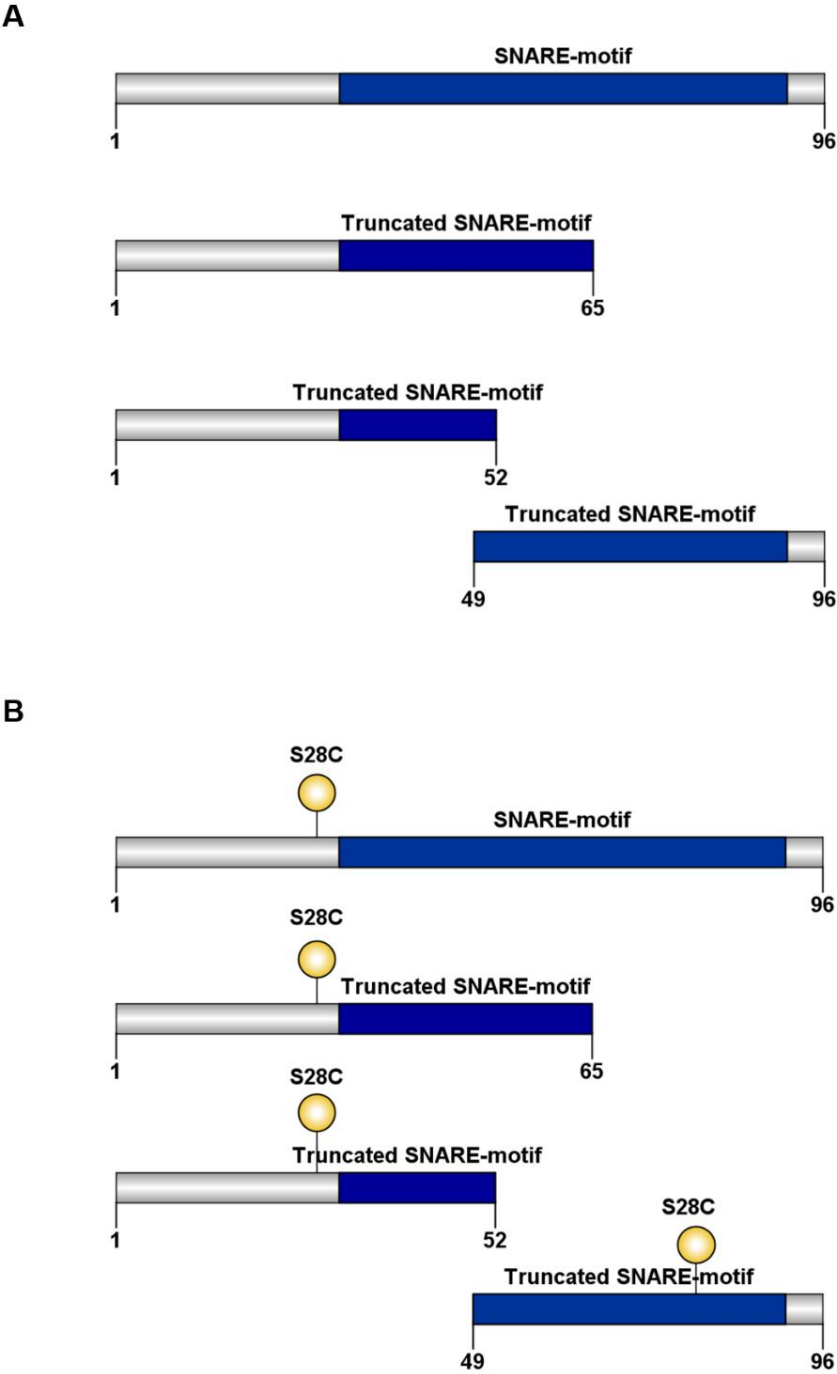


Figure 2.1-3. Different fragments of wild-type synaptobrevin and the corresponding cysteine-mutants used in this study.
(A) Truncated cytoplasmic fragments of the wild-type synaptobrevin and (B) Single-cysteine mutants of the different cytoplasmic fragments of synaptobrevin used in this study.

**Table 2. Tabulated view of all the protein constructs used in this study.**

Protein construct	Construct	Length of amino-acids	Reference
Syntaxin 1a	pET28a	1-288	(24)
		1-288 (T197C)	(89)
SNAP25a	pET28a	1-206 (no cysteine)	(90)
		1-206 S130C	(91)
Synaptobrevin2	pET28a	1-116	(24)
		1-96	(24)
		1-96 (S28C)	(89)
		1-65	(92)
		1-65 (S28C)	(92)
		1-52	(93)
		1-52 (S28C)	(93)
		49-96	(92)
49-96 (T79C)	(92)		
Munc18-1	pET28a	1-594	(39)
ΔN complex	pETduet	Syx 1-288, Syb 49-96	(94)
		Syx 183-288, Syb 49-96	(92)

Materials and Methods

2.2 Protein expression and extraction for the individual neuronal SNAREs and Munc18-1.

The constructs of the respective proteins contained in the pET28a vector were transformed into BL21 cells and the transformed cells were used for large-scale expression in *E.coli* cells. A primary culture of the *E.coli* cells was used for subsequent large-scale expression by inducing the cells with 0.25 mM IPTG, overnight at 25°C. The cells expressing the respective proteins were harvested by centrifuging the cells at 4,000 rpm for 20 minutes in a Beckman centrifuge (*J6-MI*). The supernatant was discarded and the pellets were subsequently resuspended in a buffer containing 20 mM HEPES, 500 mM NaCl and 8 mM imidazole, maintained at a pH of 7.4. The resuspended pellets were stored at -20°C.

Protein extraction was started with the addition of an extraction buffer containing 20 mM HEPES, 500 mM NaCl, 20 mM imidazole and 10% (w/v) sodium cholate at a pH of 7.4. The extraction buffer was added in a 1:1 (v/v) ratio of the resuspended pellets and incubated at room temperature for 30 minutes. Thereafter, the cells were incubated with a freshly prepared lysozyme solution (4 mg/L of the initial culture), 1 mM MgCl₂, DNase (1 mg/L of the initial culture) and complete EDTA-free protease inhibitor (1 tablet/3L of initial culture) and incubated at room temperature for 20 minutes. The cells were then sonicated using a Branson Sonifier with a 50% duty cycle at the micro-tip limit. Sonication was performed four times, with forty strokes each and the cells were thereafter incubated with 6M Urea for 15 minutes at room temperature. The cell-lysate was then centrifuged at 11000 rpm for 45 minutes (*Thermo Fisher, F12S-6X-500 LEX rotor*).

For the purification of all the proteins, the supernatant of the cell lysates were incubated with nitrilotriacetic acid (Ni-NTA) agarose resin (*Qiagen*) at 4°C for 2 hours, with rotational shaking. The lysate-bead suspension was then loaded onto a BioRad econo-column (3cm x 13cm) and the flow-through was discarded. The beads were then extensively washed with a buffer containing 20 mM HEPES, 500 mM NaCl and 20 mM imidazole at a pH of 7.4. For proteins containing transmembrane domains, the washing buffer was supplemented with detergents (1% (w/v) CHAPS or 0.03% (w/v) DDM). Elution of the proteins was performed using a buffer containing 20 mM HEPES, 500mM NaCl and 400 mM imidazole (pH 7.4) and the eluants were immediately supplemented with 10 mM DTT. The protein concentration of the eluants was measured using the molecular weights and the extinction co-efficients of the respective protein/protein complex in the Nano-drop machine (*Nano-Drop 1000, Thermo Scientific*). The purity of the samples were checked using SDS-PAGE and Coomassie Blue staining. The eluants containing the highest protein concentrations were pooled and subsequently dialyzed overnight to remove excess imidazole. The dialysis buffer contained 20 mM HEPES, 1 mM DTT and an appropriate salt concentration to support the stability of the respective protein. During the dialysis procedure, the proteins were also supplemented with 1Unit/ μ L of thrombin (*Merck*), prepared as a stock of 5mg/mL in



50% (v/v) glycerol, in order to facilitate the removal of the His-tag present in the respective proteins. Detergents were supplemented in the dialysis buffers for proteins containing transmembrane domains.

2.3 Chromatographic purification of proteins

All the three neuronal SNAREs were purified using ion-exchange chromatography on an Äkta system (*GE Healthcare*) (39, 89). Anion-exchange columns (*MonoQ, GE Healthcare*) were used for the purification of all the above-mentioned proteins except synaptobrevin, for which a cation-exchange column (*MonoS, GE Healthcare*) was used. The dialyzed samples were filtered using a 0.45µm filter and loaded onto the respective ion-exchange columns. For proteins containing a transmembrane domain, the buffers were supplemented with either 1% CHAPS, 1% OG or 0.03% DDM. The proteins were eluted over a salt gradient of 0-1000 mM NaCl (20 mM HEPES, 1 mM EDTA, 0.5 mM TCEP, pH 7.4). After elution, the concentrations of the proteins were checked by nano-drop measurements using the respective extinction co-efficients. The fractions containing the highest protein concentrations were pooled and stored at -80°C or, were immediately used for subsequent experiments. Munc18-1 was purified using size-exclusion chromatography in a buffer containing 20 mM HEPES, 200 mM NaCl, 1mM DTT, 1 mM EDTA and 10% (w/v) glycerol. The purity of the purified sample was assessed as mentioned in the previous sections.

2.4 Protein expression and extraction procedure for the C-terminally stabilized ΔN-complex

The C-terminally stabilized ΔN-complex was prepared using the strategy of co-expression by co-transforming BL21 cells with pETduet vectors containing full-length syntaxin1a and the 49-96 fragment of synaptobrevin2 with a pET28a plasmid containing full-length SNAP25a with a His-tag (94). The cells were induced overnight with IPTG at 25°C and the extraction was performed using nitrilotriacetic acid (Ni-NTA) agarose resin as described in the previous section.

2.5 Assembly and purification of the binary syntaxin1a/SNAP25a complex

The binary syntaxin1a/SNAP25a complexes were prepared from purified monomeric full-length syntaxin (1-288) and SNAP25a (1-206), using a previously described procedure (94). The complex was purified using ion-exchange chromatography (*MonoQ, GE Healthcare*), in buffers supplemented with 50 mM OG. The purity of the

samples was assessed by subjecting the samples to SDS-PAGE analysis and subsequent Coomassie Blue staining.

2.6 Assembly and purification of the syntaxin1a/SNAP25a/Munc18-1 complex

The ternary syntaxin1a/SNAP25a/Munc18-1 complex was also assembled from purified full-length monomeric proteins. Syntaxin1a and SNAP25a were first mixed together and incubated overnight with shaking at 4°C. The following day, a 2-fold molar excess of Munc18-1 was added to the mixture and the protein-mix was subjected to a further incubation of 3 hours at room temperature. The resulting ternary complex between syntaxin1a, SNAP25a and Munc18-1 was further purified by ion-exchange chromatography (*MonoQ, GE Healthcare*). The formation of the ternary complex was assessed by SDS-PAGE and Coomassie Blue staining. For qualitative assessments, the ternary complex that had been purified using ion-exchange chromatography was further purified by size-exclusion chromatography (*Superdex 200, GE Healthcare*). The presence of a single elution peak containing all the three constituent proteins further validated the formation of a ternary complex.

2.7 Fluorescent-labeling of SNARE-proteins

The single cysteine mutants of syntaxin1a, SNAP25a and synaptobrevin2 were fluorescently labeled with dyes like Oregon Green (*Oregon Green488 Iodoacetamide, mixed isomers, Thermo Fisher Scientific*) or Texas Red (*Texas Red-C5-bromoacetamide, Thermo Fisher Scientific*) by incubating the proteins with a six-times molar excess of the fluorescent dye and incubating them either for 2 hours at room temperature or overnight at 4°C, with rotation. The excess unreacted dye was removed from the proteins by performing a subsequent purification step by size exclusion chromatography, using commercially available PD-10 columns (*GE Healthcare*). The purification step was performed using a buffer composition of 20 mM HEPES, 150 mM NaCl and 1 mM EDTA, at a pH of 7.4. For proteins containing transmembrane domains, the buffer was supplemented with 1% (*w/v*) OG. The column was equilibrated with 25 mL of the buffer before loading the protein sample on the column. Elution was performed with 3.5 mL of the buffer. The concentrations of the fluorescently-labeled proteins were determined using Nano-Drop and the efficiency of labeling was calculated using the given formula:

$$\left[\frac{A_x}{\epsilon} \right] \times \left[\frac{MW \text{ of protein}}{mg \text{ protein/mL}} \right] = \frac{\text{moles of dye}}{\text{moles of protein}} \quad \text{Eq. (1)}$$

where, A_x is the absorbance value of the dye at the maximum absorbance wavelength,



ϵ is the molar extinction co-efficient of the dye, and
MW denotes the molecular weight of the protein.

2.8 Fluorescence anisotropy

Fluorescence anisotropy is a widely used tool to study the rotational freedom a fluorescently-labeled molecule, using linearly polarized light (95). All the fluorescence anisotropy measurements in this study were performed in a fluorimeter with an in-built T-configuration, equipped for polarization (*Model FL322, Jobin Yvon*). For binding experiments, 200 nM of synaptobrevin labeled with the fluorophore Oregon Green was used. Unlabeled acceptor complexes (the syntaxin1a/SNAP25a/Munc18-1 complex or the Δ N-complex) were added to the reaction mixture at a concentration of 400 nM. For each set of experiments, the *g-factor* was calculated. The *g-factor* (g) is a factor for correcting the polarization bias of the instrument, and is represented by the formula:

$$g = \frac{I_{hv}}{I_{hh}} \quad \text{Eq. (2)}$$

The buffer used for the anisotropy experiments included 20 mM HEPES, 150 mM KCl, 1 mM DTT and 50 mM OG, at a pH of 7.4. Anisotropy of the samples were calculated using the formula:

$$r = \frac{I_{vv} - gI_{vh}}{I_{vv} + 2gI_{vh}} \quad \text{Eq. (3)}$$

where, 'I' denotes the fluorescence intensity, and the first and second subscript letter indicate the polarization of the exciting light and the emitting light, respectively.

2.9 Förster Resonance Energy Transfer (FRET)

Förster resonance energy transfer (FRET) provides an excellent tool for studying protein-protein interactions between two fluorescently-labeled probes (96). The major determinant of FRET is the spectral overlap between the donor emission and the acceptor absorption (97). It however, also depends on other factors like the quantum

yield of the donor, the extinction co-efficient of the acceptor, and the relative spatial orientation between the donor and the acceptor fluorophore (98). FRET efficiency is inversely related to the sixth power of the distance, making it extremely sensitive to distance measurements (97) and can be used to calculate distances ranging from 10-100Å.

FRET measurements in this study were performed in a fluorimeter (*FluoroMax 3, Horiba Jovin Yvon*) equipped with a magnetic stirrer. For monitoring SNARE-zippering, FRET was measured between synaptobrevin (S28C) labeled with the fluorophore Oregon Green and SNAP25a (S130C) labeled with the fluorophore Texas Red.

All the reactions were performed in a volume of 600 µL, at a temperature of 37°C. Oregon Green served as the donor fluorophore and Texas Red served as the acceptor fluorophore. The measurements were obtained by setting the excitation wavelength to 460nm and the emission wavelength to 520nm, which correspond to the excitation and emission maximums of Oregon Green respectively. The quenching of the donor emission was reported as a measure of FRET during the course of the reactions. For recording fluorescence spectra, the excitation was set to 460nm and the spectra were recorded in a wavelength range of 400 nm-700 nm. The buffer used for the FRET measurements included 20 mM HEPES, 150 mM KCl, 1 mM DTT and 50 mM OG.

2.10 Heteronuclear Single Quantum Coherence spectroscopy (HSQC)

HSQC-spectroscopy is a highly sensitive 2D-NMR experiment based on the transfer of magnetization from the proton to a second nucleus (¹⁵N or ¹³C), using an insensitive nuclei enhanced by polarization transfer (INEPT) pulse sequence (99). In the first step, the transfer occurs from the proton to the second nucleus and during the second step, the magnetization gets transferred from the second nucleus, back to the proton via a retro-INEPT step, and the corresponding signal is then recorded. A series of experiments are usually recorded using increments in the time-delay between the two transfers (99). Each peak in a HSQC-spectra represents a bonded-H pair, where every co-ordinate corresponds to the chemical shifts of each of the H and N-atoms. In this study, the HSQC-NMR spectra were recorded over a time-period of 8 hours, and at a frequency of either 600 Hz or, 800 Hz.

2.11 Liposome/proteoliposome preparation.

In this study, small unilamellar vesicles (SUVs) were used for the incorporation of proteins/protein complexes into a membrane compartment. These vesicles roughly have a diameter of 50 nm, which is similar to the diameter of synaptic vesicles present in the nervous system (100). For the preparation of SUVs, 1,2-dioleoyl-sn-glycero-3-phosphocholine (DOPC) , 1,2-dioleoyl-sn-glycero-3-phosphoethanolamine (DOPE) ,



1,2-dioleoyl-sn-glycero-3-phospho-L-serine (DOPS), cholesterol, 1-oleoyl-2-{12-[(7-nitro-2-1,3-benzoxadiazol-4-yl)amino]dodecanoyl}-sn-glycero-3-phosphoserine (NBD-PS) and 1,2-dioleoyl-sn-glycero-3-phosphoethanolamine-N-(lissamine rhodamine B sulfonyl) (Rhodamine PE) from *Avanti Polar lipids* were used, similar to an earlier report (101).

For the preparation of unlabeled liposomes, lipids were mixed in the given molar ratio: 50% (DOPC):20% (DOPE):20% (DOPS):10% (Cholesterol). For labeled liposomes, the ratio of the lipids mixed was 50% (DOPC): 18.5% (DOPE): 1.5% (Rhodamine PE): 18.5% (DOPS): 1.5% (NBD-PS): 10% (Cholesterol). After drying the lipids, the lipid film was resuspended in 20mM HEPES, 150mM KCl, 5% (w/v) sodium cholate solution and vortexed thoroughly. The lipid-mix was then mixed with the respective protein(s) in 20mM HEPES, 150mM KCl, 3% (w/v) sodium cholate (101). The resuspended lipid film was mixed with the respective protein(s), and the proteoliposomes were prepared by subsequent detergent removal, using gel-filtration chromatography on a column packed with Sephadex G-50. The buffer composition for proteoliposome preparation was 20 mM HEPES, 150 mM KCl and 1 mM DTT at a pH of 7.4. The protein: lipid (n/n) ratio was 1:1000 (for synaptobrevin liposomes) and 1:2000 (for liposomes containing syntaxin1a/SNAP25a/Munc18-1 complex), unless stated otherwise.

2.12 Co-flotation assay

Co-flotation assay is a well-established assay based on the separation of molecular components over a density-gradient, using high-speed centrifugation (102). After centrifugation, liposomes and the associated proteins float in the topmost fractions, attributed by the low density of liposomes. This assay is a widely used tool to monitor protein-lipid interactions (103). A schematic overview of this assay has been represented in Figure 2.12-1.

For all the co-flotation experiments carried out in this study, the density-gradient was prepared by carefully overlaying 40% Nycodenz with 30% Nycodenz and a final top layer containing the reconstitution buffer (20 mM HEPES, 150 mM KCl, pH 7.4). The density-gradient was then subjected to ultra-centrifugation (*Thermo scientific, Sorvall, M150 SE*) at a speed of 55,000 rpm in a S55S-rotor, for 1.5 hours at 4°C. After centrifugation, 25 µl samples were carefully taken from the top to the bottom of the gradient and analyzed by SDS-PAGE, followed by Coomassie Blue staining or western blotting.

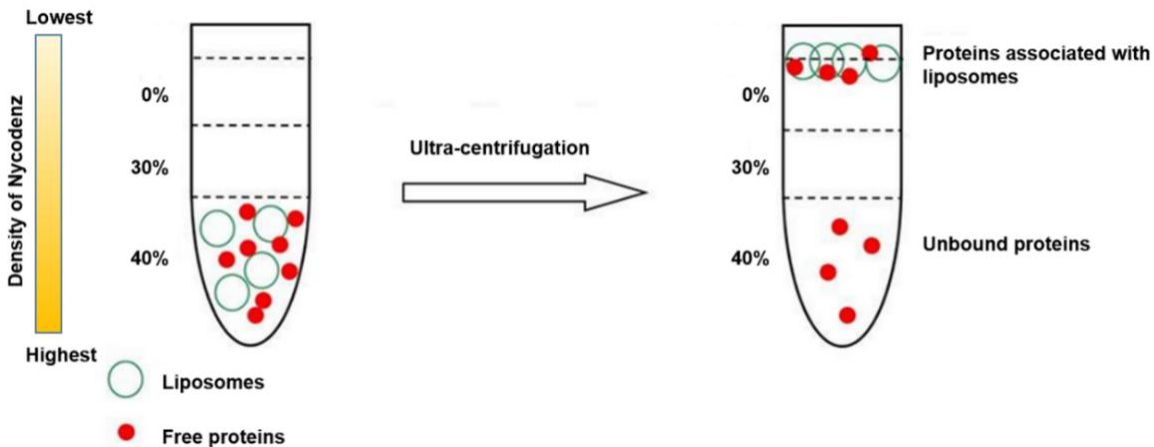


Figure 2.12-1. Scheme of a typical co-floitation assay.

A nycodenz density gradient is prepared by carefully overlaying nycodenz solutions. A mixture of liposomes and free proteins are mixed in the bottom layer of the gradient prior to centrifugation. Upon ultracentrifugation, liposomes and proteins associated with liposomes float at the top of the gradient due to the low density of the liposomes. Any unbound proteins, however, sediment at the bottom of the gradient after ultracentrifugation. [Adapted from (103)].

2.13 SDS-PAGE and Coomassie Blue staining/ fluorescence scanning

Sodium-dodecyl polyacrylamide gel electrophoresis is a classic technique in protein biochemistry for the separation of proteins/ protein complexes using an electric field (104). SDS-PAGE in this work was performed using pre-cast 4-12% Bis/Tris gels (Novagen) (105). MES (2-(N-morpholino)ethanesulfonic acid) was used as a running buffer for electrophoresis. After SDS-PAGE, the gels were stained with Coomassie Brilliant Blue R-250. Staining of the gels was performed by a brief heating of the gel in the staining solution followed by incubation for 10 minutes at room temperature, with slow shaking. Thereafter, the gels were incubated with a destaining solution comprised of 40% (v/v) ethanol and 10% (v/v) acetic acid. The gels were incubated with the destaining solution for 2-3 times, each for an incubation period of 10 minutes at room temperature, with shaking.

In addition to the qualitative assessment of the purified proteins, SDS-PAGE can be employed as a tool to monitor the formation of SDS-resistant SNARE-complexes (106). In this study, it was used to test whether the addition of synaptobrevin to the syntaxin1a/SNAP25a/Munc18-1 complex can result in the formation of SDS-resistant SNARE-complexes. For this purpose, freshly-prepared syntaxin1a/SNAP25a/Munc18-



1 complexes were briefly incubated with synaptobrevin and the resulting mixture was then mixed with a sample buffer, followed by SDS-PAGE, without prior boiling of the samples. Coomassie Blue staining of the gel was performed to monitor the formation of SNARE-complexes.

In this study, the formation of SDS-resistant SNARE-complexes was also assessed using SDS-PAGE, followed by fluorescence-scanning of the gels. For this, a fluorescently-labeled synaptobrevin (Syb 1-96 C28-Oregon Green) was mixed with freshly prepared syntaxin1a/SNAP25a/Munc18-1 complex and the mixture was then incorporated into liposomes. The proteoliposomes were further purified using the co-floitation assay. 25 μ L fractions of proteoliposomes from top to the bottom of the gradient were mixed with SDS-sample buffer and subjected to SDS-PAGE, without prior boiling of the samples. Presence of SDS-resistant bands in the liposomal fractions were observed by scanning the gels in a *TECAN* fluorescence scanner (*FLA-7000*).

2.14 Western blot analysis

Western blot analysis was performed after SDS-PAGE, by transferring proteins from a gel onto a nitrocellulose membrane in an electric field, at 100 Volts for one hour in transfer buffer [25mM Tris, 190mM glycine and 20% isopropanol]. The transfer of proteins to the membrane was checked by performing Ponceau staining, i.e. by incubating the membrane with Ponceau stain [0.1% (w/v) of Ponceau S in 5% (v/v) acetic acid] for 10 minutes (107). The nitrocellulose membranes were then washed with double-distilled water to remove the Ponceau stain completely. The membranes were then incubated with blocking buffer (5% milk in 1X TBST) for 1 hour at room temperature. The blocking buffer was then discarded and the membranes were incubated with the respective primary antibodies (usually used at a dilution of 1:1000), overnight at 4°C. The following day, any excess primary antibodies were removed from the membrane by washing with 1X TBST (three times, for 10 minutes each). Thereafter, the membranes were incubated in the secondary antibodies (1:10000), for 1 hour at room temperature. After repeated washing of the membranes to remove any unbound secondary antibodies, the membranes were developed using enhanced chemiluminescence. The blots were visualized in the luminescent scanner *Fujifilm FAS-1000*, equipped with a CCD camera.

2.15 Chemical cross-linking

Chemical cross-linking of proteins/protein complexes is an informative method to determine the structural details of protein-protein interactions (108). The general principle of a cross-linking reaction involves the formation of a covalent bond with specific reactive groups (for example, primary amine group, sulfhydryl group, carboxyl

Materials and Methods

group or carbonyl group) of proteins resulting in a bio-conjugate that can be used for attaining structural information using mass spectrometry (MS/MS) (108).

In this study, the chemical cross-linker, bis(sulfosuccinimidyl)suberate (*BS3, Thermo Scientific*) was used for crosslinking of the syntaxin1a/SNAP25a/Munc18-1 complex. BS3 has a spacer arm-length of 11.4Å and crosslinks the amino side-chains of the lysine residues and the free amino-terminus of proteins. The optimal amount of cross-linker to be used was determined by performing a titration with different concentrations of the cross-linker (see Figure 3.6-1). Having determined the optimal concentration, the syntaxin1a/SNAP25a/Munc18-1 complex was cross-linked using that particular concentration of the cross-linker and the sample was then subjected to SDS-PAGE, followed by in-gel trypsin digestion (109) and subsequent analysis by mass spectrometry (MS/MS).

2.16 Mass spectrometry (MS/MS)

The reconstituted proteolytic peptides were separated by a nano-liquid chromatography system (*UltiMate™ 3000RSLCnano system*). The system comprised of a C18-trapping column of 3 cm × 150 µm inner diameter, in-line with a 30 cm × 75 µm inner diameter C18 analytical column (both packed in-house with 1.9-µm C18 material, from *Dr. Maisch GmbH*). Subsequently, the peptides were loaded on the trapping column and desalted for 3 minutes at a flow rate of 10 µL/min in 95% of mobile phase A (0.1% FA in H₂O, v/v) and 5% of mobile phase B (80% ACN and 0.05% FA in H₂O, v/v). Thereafter, the peptides were eluted and separated on the analytical column using a 43-minutes linear gradient of 15-46% mobile phase B, at a flow rate of 300 nL/min (109). The separated peptides were analyzed by Orbitrap Fusion mass spectrometer (*Thermo Scientific*).

A method called ‘top-20’ was employed, where the 20 most intense precursor ions with charge states 3-8 in the survey scan (380-1580 m/z scan range) were isolated in the quadrupole mass filter (isolation window 1.6 m/z) and fragmented in the higher energy collisional dissociation (HCD) cell with normalized energy. A dynamic exclusion of 20 seconds was used. Both the survey scan (MS1) and the product ion scan (MS2) were performed in the Orbitrap at 120,000 and 30,000 resolution, respectively. Spray voltage was set at 2.3 kV and 60% of S-lens RF level was used. Automatic gain control (AGC) targets were set at 5 × 10⁵ (MS1) and 5 × 10⁴ (MS2).

The raw data were converted to mgf files by Proteome Discoverer 2.0.0.802 software (*Thermo Scientific*). The mgf files were searched against a FASTA database containing the sequences of syntaxin1a, SNAP25a, synaptobrevin2 and Munc 18-1 from *Rattus norvegicus* by pLink 1.23 software using a target-decoy strategy (110). Database search parameters included mass accuracies of MS1 < 10 ppm and MS2 < 20 ppm,



carbamidomethylation on cysteine as a fixed modification, oxidation on methionine as variable modification. Number of residues of each peptide on a cross-link pair was set between 4 and 40. A maximum of two trypsin missed-cleavage site was allowed. The results were obtained with 1% false discovery rate.

2.17 Trypsin-digestion assay

Trypsin-digestion assay is a biochemical tool to determine the orientation of proteins/protein complexes after their insertion into liposomes (110). The technique involves limited proteolysis of proteins/protein complexes in the presence of a proteolytic enzyme and the absence of a detergent. The amount of protein(s) inserted facing the inside of the liposomes show resistance to proteolysis because they get protected by the membrane of the liposomes and thereby represent the fraction of proteins in the 'inside-out' orientation. The fraction of protein(s) inserted with the 'right-side out' orientation are exposed to the proteolytic activity of the enzyme and hence, get cleaved. A comparison of the cleaved and the uncleaved fraction of the proteins provides an estimate of the correctly oriented proteins on the liposomes.

In this study, limited proteolysis was employed to determine the orientation of the syntaxin1a/SNAP25a/Munc18-1 complex after its incorporation into the liposomes.

Proteoliposomes of specific lipid compositions were prepared as described in the previous section. Freshly prepared proteoliposomes were incubated with 0.1 mg of Trypsin (*Sigma Aldrich*) in the presence or absence of 0.3% (w/v) Triton X-100 at 37°C, for 2 hours. As a negative control, the proteoliposomes were incubated only with the reconstitution buffer (without Trypsin or TritonX-100), also for 2 hours at 37°C. The reconstitution buffer consisted of 20mM HEPES, 150mM KCl, and 1mM DTT (at a pH of 7.4). The reactions were performed in a 50 μ L reaction volume. After completion of the incubation period, the samples were analyzed by SDS-PAGE followed by western blotting. As a final step, the samples were probed using a polyclonal antibody against Munc18-1 (111).

3 Results

3.1 Effect of Munc18-1 on the syntaxin1a/SNAP25a (2:1) complex

The precise composition and conformation of the acceptor complexes present on the neuronal plasma membrane largely remain unknown. The two major propositions for the acceptor complexes for the reception of synaptic vesicles are (i) the syntaxin1a/SNAP25a complex (112) and (ii) the syntaxin1a/Munc18-1 complex (84). As highlighted in one of the previous sections, the syntaxin1a/SNAP25a complex is susceptible to disassembly by NSF and α SNAP. Moreover, according to a recent study, it has been proposed that the syntaxin1a/SNAP25a complex can be acted upon by the SM-protein Munc18-1, to result in the formation of syntaxin1a/Munc18-1 complex (85). In this report, however, a cytoplasmic variant of syntaxin1a (Syx 2-253) had been used. Several studies have reported that the interaction of syntaxin1a with its partner proteins get altered in the presence of the transmembrane segment of syntaxin1a (113–115). Therefore, it becomes important to revisit the mechanistic details of SNARE-mediated fusion in a system incorporating the transmembrane segment of syntaxin1a. In this study, a full-length construct of syntaxin1a, containing its transmembrane domain has been used for most of the experiments, *unless stated otherwise*.

As a starting point, I wanted to establish the effect of Munc18-1 on the syntaxin1a/SNAP25a (2:1) complex. The questions to be addressed in this section were:

- a) Does Munc18-1 cause a complete displacement of SNAP25a from the syntaxin1a/SNAP25a complex to form syntaxin1a/Munc18-1 complex? or,
- b) Does Munc18-1 interact with the syntaxin1a/SNAP25a complex to form a ternary syntaxin1a/SNAP25a/Munc18-1 complex?

To address these questions, I employed FRET-based measurements as a first step to monitor the impact of Munc18-1 on the syntaxin1a/SNAP25a complex. For this purpose, fluorescently labeled syntaxin1a (Syx 1-288, C197-Oregon Green) and fluorescently labeled SNAP25a (1-206, C130- Texas Red) were used to assemble the syntaxin1a/SNAP25a (2:1) complex. Oregon Green and Texas Red are fluorescent dyes that form a FRET-pair and have widely been used for *in-vitro* FRET-based measurements (116). The assembled complex was further purified by ion-exchange chromatography and used for the subsequent experiments.

The changes in FRET between the two fluorophores in the syntaxin1a/SNAP25a (2:1) complex were studied upon the addition of Munc18-1. In the first set of experiments, the dequenching of the donor emission (syntaxin1a labeled with Oregon Green) was recorded upon the addition of Munc18-1. A slow dequenching of the donor emission was observed upon the addition of Munc18-1 (Figure 3.1-1 A, *black curve*). As a control experiment, syntaxin1a that had been pre-incubated with Munc18-1 was added to the double-labeled syntaxin1a/SNAP25a complex. In this case, no dequenching of the donor emission was observed (Figure 3.1-1 A, *red curve*). These observations indicated that Munc18-1 alters the interaction between syntaxin1a and SNAP25a in the complex, but the magnitude of this effect remained unclear. In order to assess the dependence of the dequenching reaction on the concentration of Munc18-1, a titration was performed with increasing concentrations of Munc18-1. The reaction seemed to saturate at a concentration of $0.5\mu\text{M}$ of Munc18-1 (Figure 3.1-1 B, *red curve*). This concentration of Munc18-1 was, therefore, used for all subsequent experiments.

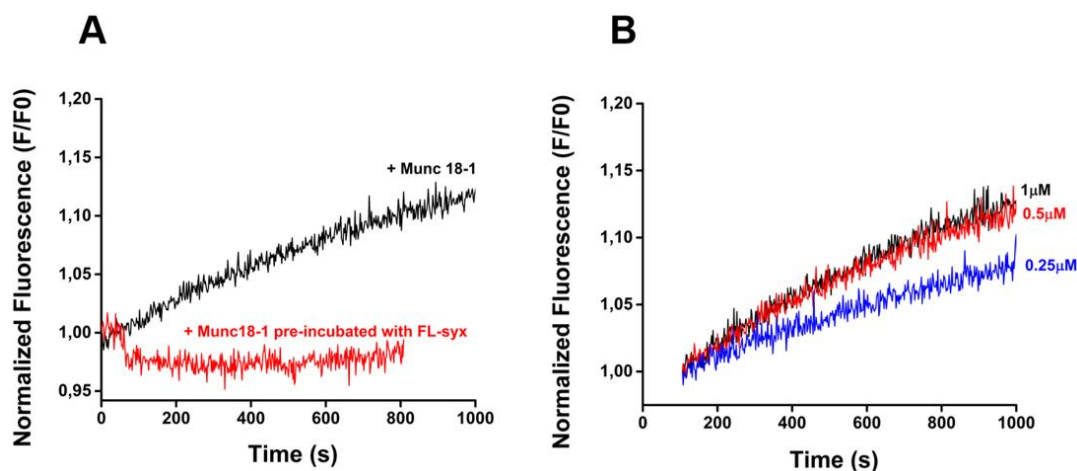


Figure 3.1-1. Effect of Munc18-1 on the syntaxin1a/SNAP25a (2:1) complex in solution.

(A) Addition of Munc18-1 to the syntaxin1a/SNAP25a (2:1) complex resulted in a slow dequenching of the donor emission (*black curve*). No increase in the donor emission was recorded upon the addition of Munc18-1 that had been previously incubated with full-length syntaxin1a. (B) Titration showing the effect of increasing concentrations of Munc18-1 on the syntaxin1a/SNAP25a complex. The reaction reached saturation at a $0.5\mu\text{M}$ concentration of Munc18-1 (*red curve*).

The next important question to be addressed was to assess the degree of effect caused by Munc18-1 on the syntaxin1a/SNAP25a complex. To address this issue, the SNARE-disassembly machinery, NSF and α SNAP were incorporated in the above assay. NSF- α SNAP have been known to completely disassemble the syntaxin1a/SNAP25a complex (106). Thus, a comparison of the effect of Munc18-1 and NSF- α SNAP on the syntaxin1a/SNAP25a complex would provide a rough estimate of the displacement of SNAP25a from the syntaxin1a/SNAP25a complex caused by Munc18-1. As shown in Figure 3.1-2, the extent of dequenching caused by Munc18-1 on the syntaxin1a/SNAP25a complex was much less as compared to that caused by NSF- α SNAP.

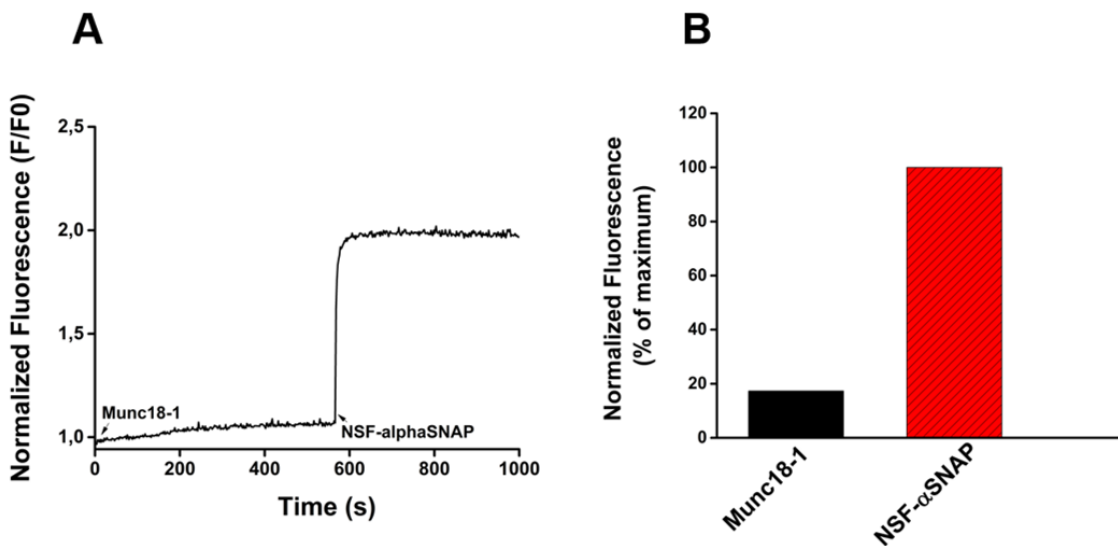


Figure 3.1-2 Determination of the magnitude of Munc18-1 effect on the syntaxin1a/SNAP25a complex.

(A) The degree of donor dequenching on a double-labeled syntaxin1a/SNAP25a complex was determined upon the addition of Munc18-1, followed by NSF- α SNAP, in the presence of ATP and magnesium. Subsequent addition of NSF- α SNAP, after Munc18-1 addition to the complex resulted in a very fast dequenching of the donor emission. (B) Assuming the effect of NSF- α SNAP to be 100%, the degree of dequenching caused by the addition of Munc18-1 was calculated to be only 20%.



Since, NSF- α SNAP can completely disassemble the syntaxin1a/SNAP25a complexes, the magnitude of its effect was assumed to be 100%. Based on this assumption, the effect of Munc18-1 on the binary complexes was calculated to be only about 20% (see Figure 3.1-2 B). Collectively, the above-experiments indicated that Munc18-1 only produces a mild effect on the syntaxin1a/SNAP25a (2:1) complex.

The slow dequenching of the donor emission observed upon Munc18-1 addition could be indicative of two possible phenomenon:

- a) The displacement of SNAP25a by Munc18-1 from the syntaxin1a/SNAP25a complex. OR
- b) The displacement of a second syntaxin1a from the 2:1 syntaxin1a/SNAP25a complex by Munc18-1, resulting in the formation of a ternary syntaxin1a/SNAP25a/Munc18-1 complex.

In order to gain further support in favor of either of these two hypotheses, I tried to study the effect of Munc18-1 on the syntaxin1a/SNAP25a complex using nuclear magnetic resonance (NMR). For this purpose, full-length SNAP25a (1-206) containing ^{15}N was purified and was subsequently used for the assembly and purification of syntaxin1a/SNAP25a complexes. I used heteronuclear single quantum coherence spectroscopy (HSQC) to compare the spectra of SNAP25a under three different conditions. HSQC-NMR spectra of SNAP25a were recorded to assess its conformational state in the syntaxin1a/SNAP25a complex and also after the addition of Munc18-1 to the syntaxin1a/SNAP25a complex. As a control, the HSQC-NMR spectrum of monomeric SNAP25a was also recorded.

The spectra of SNAP25a obtained under the three conditions mentioned above, have been represented in Figure 3.1-3. A large number of the cross-peaks of SNAP25a (as compared to its monomeric form, Figure 3.1-3 A) were seen to disappear upon the formation of syntaxin1a/SNAP25a complex (Figure 3.1-3 B). Upon addition of Munc18-1 to the syntaxin1a/SNAP25a complex, a partial reappearance of some of the cross-peaks of SNAP25a was observed (Figure 3.1-3 C). The spectra however remained quite different as compared to that of unbound SNAP25a (see Figure 3.1-3 A). These observations suggested that the addition of Munc18-1 does not completely displace SNAP25a from the syntaxin1a/SNAP25a (2:1) complex.

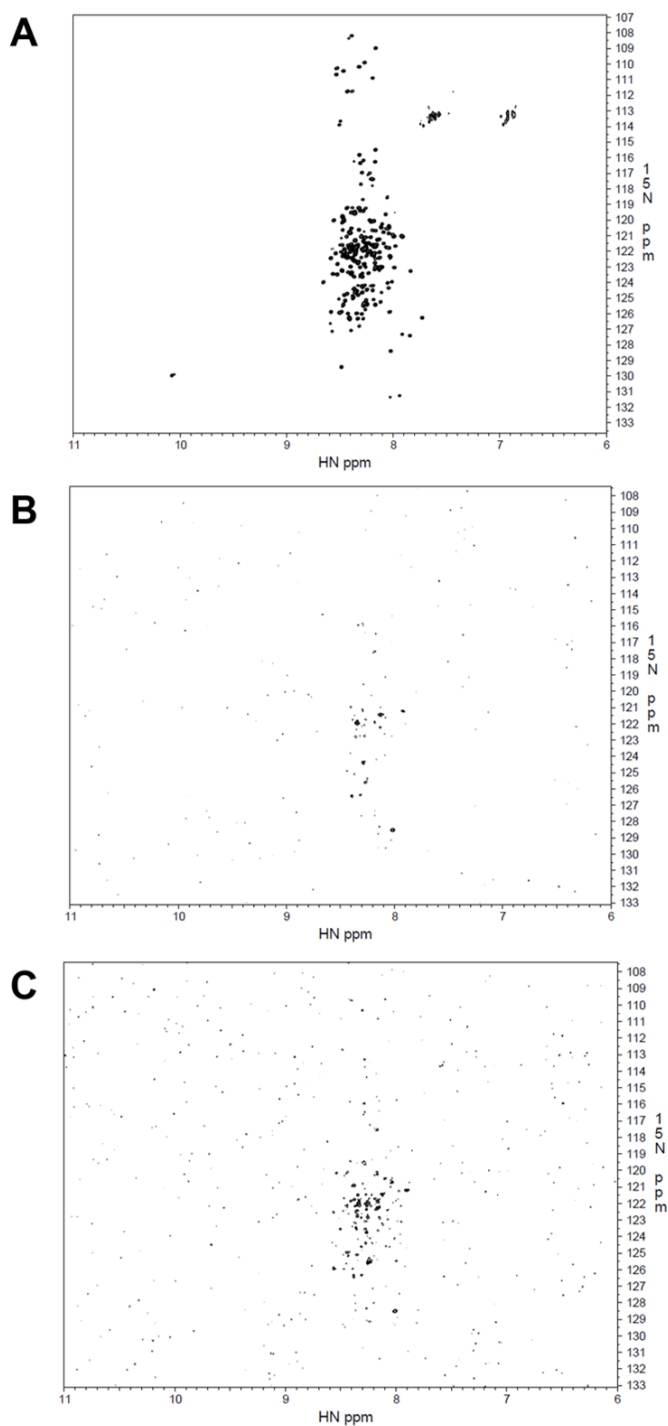


Figure 3.1-3 HSQC-NMR spectra of ^{15}N -SNAP25a under different conditions.

HSQC-NMR spectra of (A) unbound SNAP25a, (B) SNAP25a in the syntaxin1a/SNAP25a complex and, (C) SNAP25a after addition of Munc18-1 to the syntaxin1a/SNAP25a. [These experiments were performed in collaboration with Dr. Nils Alexander Lakomek].



In summary, both the NMR spectra and the FRET measurements were indicative of mild structural effects of Munc18-1 on the syntaxin1a/SNAP25a (2:1) complex. HSQC-NMR measurements, however, made it more reasonable to believe that Munc18-1 does not completely displace SNAP25a from the syntaxin1a/SNAP25a complex. Had this been the case, the HSQC-NMR spectrum of SNAP25a upon the addition of Munc18-1 to the syntaxin1a/SNAP25a complex would have been similar to the HSQC-NMR spectrum of unbound SNAP25a. Based on these observations, it was concluded, that the addition of Munc18-1 to syntaxin1a/SNAP25a complex likely results in the displacement of the second syntaxin1a molecule, resulting in the subsequent formation of a ternary syntaxin1a/SNAP25a/Munc18-1 complex.

In the subsequent time-course, efforts were made to perform the peak-assignment for the cross-peaks observed in the HSQC-NMR spectra of SNAP25a. The peak assignments were performed by Dr. Nils Alexander Lakomek, and have been represented in Figure 3.1-4 A. Figure 3.1-4 B shows an overlay of SNAP25a in the syntaxin1a/SNAP25a complex (*blue dots*) and upon addition of Munc18-1 to the syntaxin1a/SNAP25a complex (*red dots*). The residues of SNAP25a which showed reappearance upon the addition of Munc18-1 to the syntaxin1a/SNAP25a complex have been labeled in Figure 3.1-4 B. These residues were found to be positioned on the SNARE-motif1 (SN1) as well as SNARE motif2 (SN2) of SNAP25a. It, however, needs to be mentioned that the assignments are tentative, because the frequency used for recording the spectra were not identical in all the three cases. The assignments, are nonetheless important since they provide a broad overview of the structural effect of Munc18-1 on the syntaxin1a/SNAP25a complexes.

The reappearance of the residues lying in the first SNARE-motif of SNAP25a can be explained by a conformational change in SNAP25a accompanied by the formation of a ternary syntaxin1a/SNAP25a/Munc18-1 complex. And, the reappearance of the peaks in the second SNARE-motif of SNAP25a can be explained by the displacement of the second syntaxin1a molecule from the syntaxin1a/SNAP25a (2:1 complex) upon addition of Munc18-1. Therefore, the assignments of the cross-peaks (*although tentative*), provided an additional support for the conclusions obtained from the FRET-measurements and the HSQC-NMR experiments.

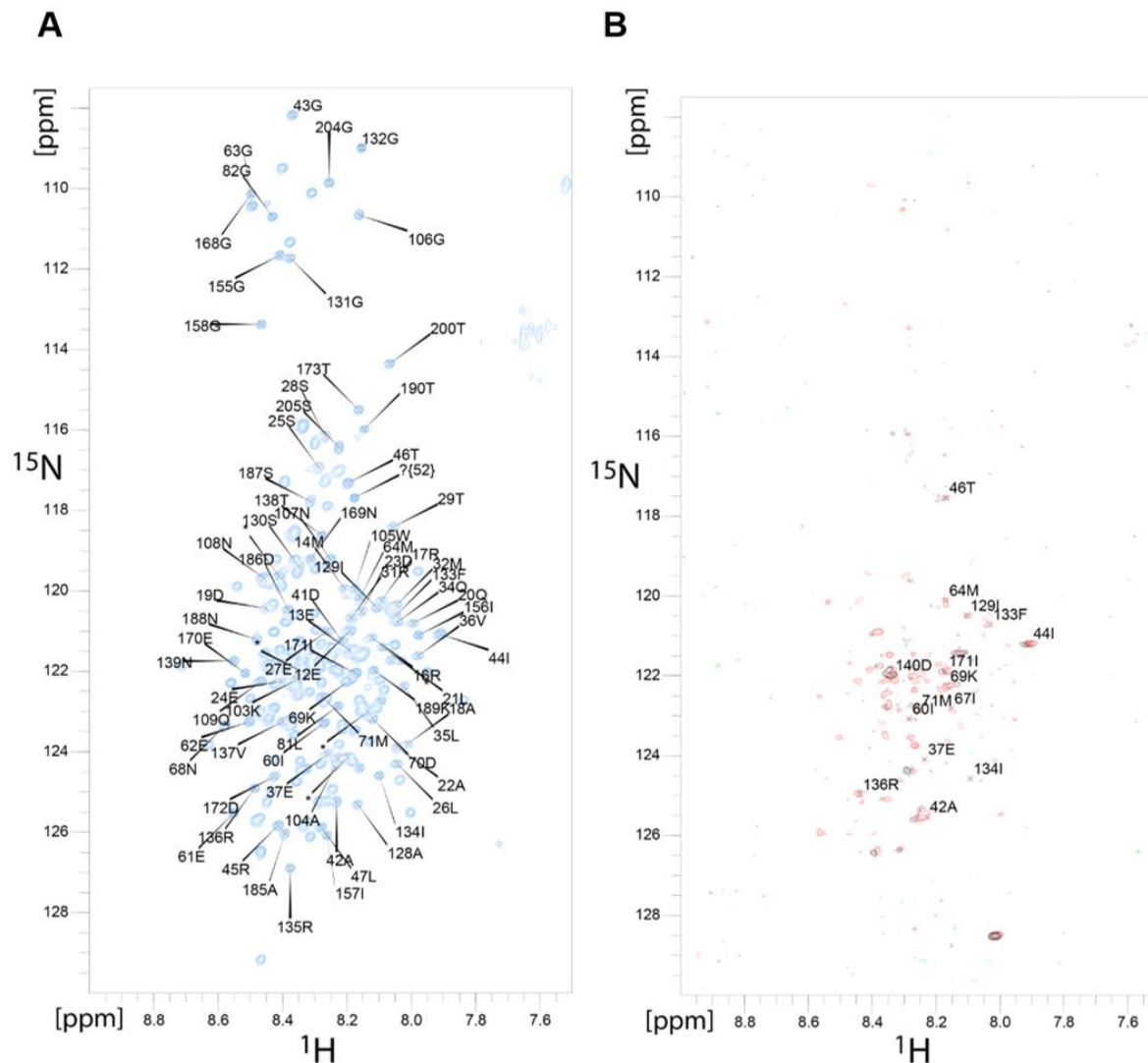


Figure 3.1-4. Peak assignments of SNAP25a for the cross-peaks observed in the HSQC-NMR spectra.

(A) Peak assignments for the unbound SNAP25a. (B) Peak assignments for the SNAP25a residues that showed reappearance upon the addition of Munc18-1 to the syntaxin1a/SNAP25a/Munc18-1 complex. [These experiments were performed in collaboration with Dr. Nils Alexander Lakomek].



3.2 Optimization of the *in-vitro* assembly and purification of the ternary syntaxin1a/SNAP25a/Munc18-1 complex.

As a next step, I wanted to perform the *in-vitro* assembly and the subsequent purification of the syntaxin1a/SNAP25a/Munc18-1 complex. The complex formation and purification was tested under different conditions which included:

- Order of addition of the constituent proteins
- Salt concentration
- Buffer conditions

To start with, I tried to reconstitute the complex using simultaneous mixing of all the three proteins namely syntaxin1a, SNAP25a and Munc18-1. This method, however resulted in the precipitation of the protein complex and hence could not be used for successful complex assembly. As a next step, I tried to constitute the proteins by subsequent mixing of the proteins. To this end, syntaxin1a and SNAP25a were mixed together and incubated overnight at 4°C, followed by the mixing of a 2-fold molar excess of Munc18-1 on the following day, and a further incubation for 3 hours at room temperature. The resulting complex was then further purified by chromatographic procedures like ion-exchange chromatography and/or size-exclusion chromatography. Both ion-exchange chromatography and size-exclusion chromatography resulted in a peak fraction containing syntaxin1a, SNAP25a and Munc18-1, thereby indicating that these three proteins can assemble together to form a ternary syntaxin1a/SNAP25a/Munc18-1 complex. Using ion-exchange chromatography, the complex was purified over a salt gradient of 0-1000mM NaCl, and the complex was seen to elute at a salt concentration of ≈ 300 mM (Figure 3.2-1 A, B). As a quality check to test for the presence of aggregates in the purified sample, the syntaxin1a/SNAP25a/Munc18-1 complex was also purified using size-exclusion chromatography. As shown in Figure 3.2-1 C, there was no elution of proteins in the void volume of the column (*before 8mL*), thereby indicating the absence of protein aggregates in the purified protein sample. Size-exclusion chromatography was performed at a salt concentration of 200 mM NaCl.

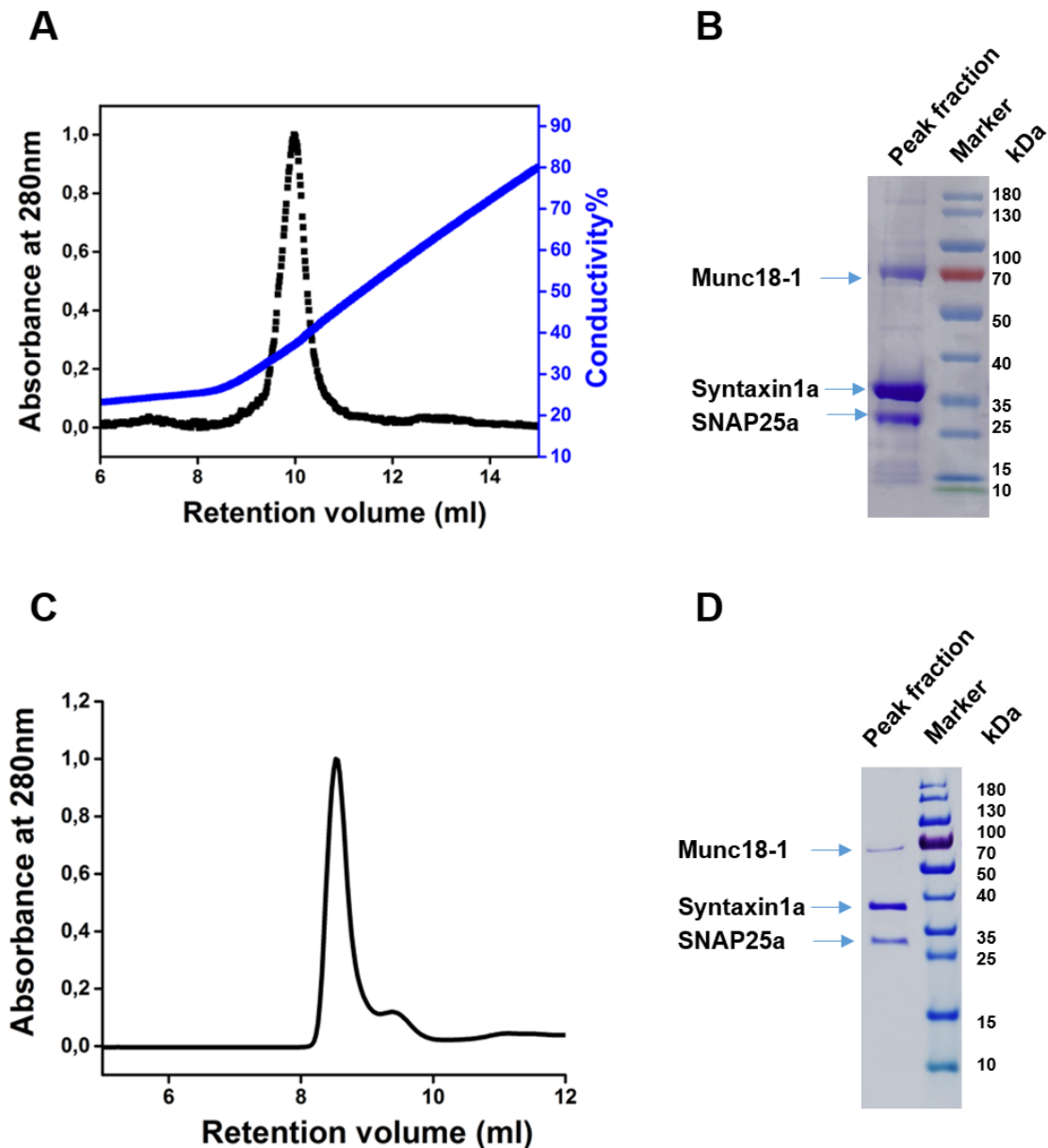


Figure 3.2-1. Purification of the syntaxin1a/SNAP25a/Munc18-1 complex.

(A) Purification of the syntaxin1a/SNAP25a/Munc18-1 complex using ion-exchange chromatography. (B) SDS-PAGE and Coomassie Blue staining showed the presence of all the three proteins in the elution peak. (C) Purification of the complex using size-exclusion chromatography. (D) Analysis of the purified samples by SDS-PAGE and Coomassie Blue staining. [Refer to Figure 3.5-3 for the elution profiles of the monomeric constituents of the syntaxin1a/SNAP25a/Munc18-1 complex].

3.3 Syntaxin1a/SNAP25a/Munc18-1 as an efficient acceptor-complex for synaptobrevin-binding.

After the successful optimization of purification of the ternary syntaxin1a/SNAP25a/Munc18-1 complex, I wanted to test whether this complex can serve as an efficient acceptor for synaptobrevin-binding and subsequent SNARE-complex assembly.

3.3.1 Studying synaptobrevin-binding to the syntaxin1a/SNAP25a/Munc18-1 complex using fluorescence anisotropy

As a first step towards this approach, I used fluorescence anisotropy to monitor the binding of synaptobrevin to the syntaxin1a/SNAP25a/Munc18-1 complex. Fluorescence anisotropy measurements report the freedom of rotation of a fluorescently-labeled molecule and hence can be used to study protein-protein interactions (117). The synaptobrevin used for this assay consisted of a single-cysteine mutant of the full-length cytoplasmic variant of synaptobrevin (1-96), labeled at position 28 with the fluorophore Oregon Green.

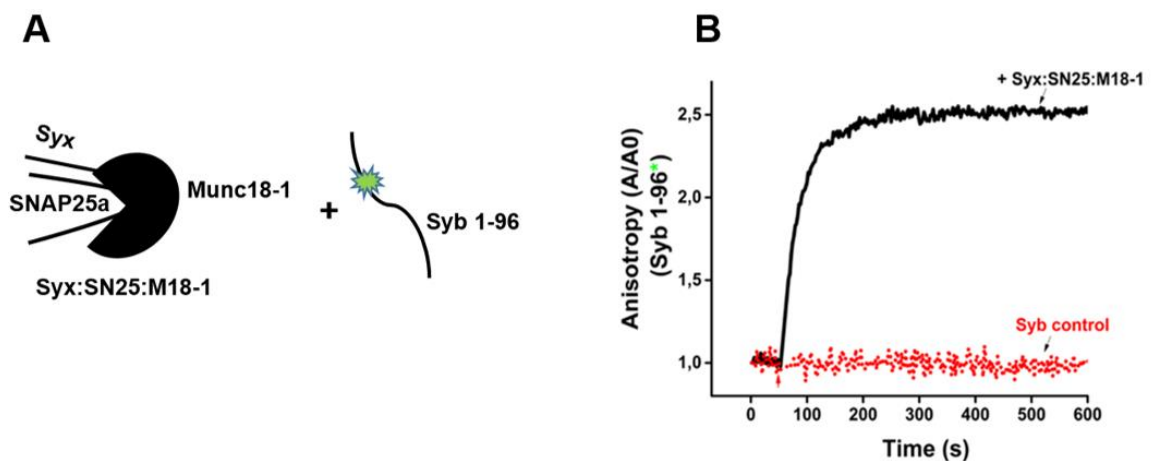


Figure 3.3.1-1. Syntaxin1a/SNAP25a/Munc18-1 complex binds efficiently to synaptobrevin.

(A) Schematic representation of the fluorescence anisotropy experiment. (B) Addition of the syntaxin1a/SNAP25a/Munc18-1 complex to synaptobrevin resulted in a very fast increase in anisotropy (*black curve*). No increase in anisotropy was recorded when excess of unlabeled synaptobrevin was added to the reaction mixture (*red curve*).

As shown in Figure 3.3.1-1 B (*black curve*), the addition of unlabeled syntaxin1a/SNAP25a/Munc18-1 complex to fluorescently-labeled synaptobrevin resulted in a fast increase in the anisotropy of synaptobrevin, thereby indicating a fast binding of synaptobrevin to the syntaxin1a/SNAP25a/Munc18-1 complex.

As a control reaction, the acceptor complex was added in the presence of excess amounts of unlabeled synaptobrevin. In this case, no increase in the anisotropy of synaptobrevin was recorded (Figure 3.3.1-1 B, *red curve*). As a next step, the anisotropy reaction was also performed over a range of concentrations of the syntaxin1a/SNAP25a/Munc18-1 complex. The complex exhibited a dose-dependent response for the syntaxin1a/SNAP25a/Munc18-1 complex as shown in Figure 3.3.1-2.

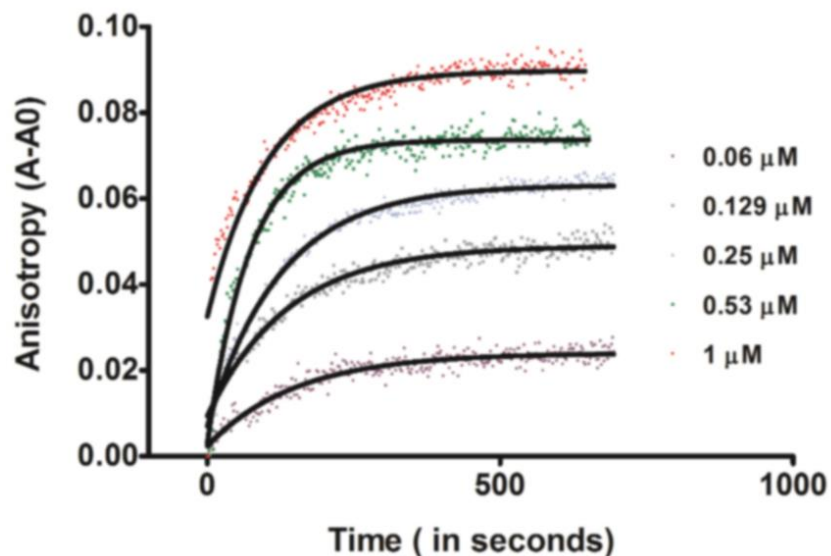


Figure 3.3.1-2. Dose-dependent response for the syntaxin1a/SNAP25a/Munc18-1 complex.

Addition of increasing concentrations of the syntaxin1a/SNAP25a/Munc18-1 complex resulted in a dose-dependent increase of the anisotropy of the fluorescently-labeled synaptobrevin. The range of concentrations of the acceptor complex used for the fluorescence anisotropy measurements was 0.06 μM - 1 μM.

3.3.2 Förster Resonance Energy Transfer (FRET)

In order to gain a deeper understanding of the kinetics of synaptobrevin-binding to the syntaxin1a/SNAP25a/Munc18-1 complex, I tried to confirm the results from fluorescence anisotropy using FRET-measurements.

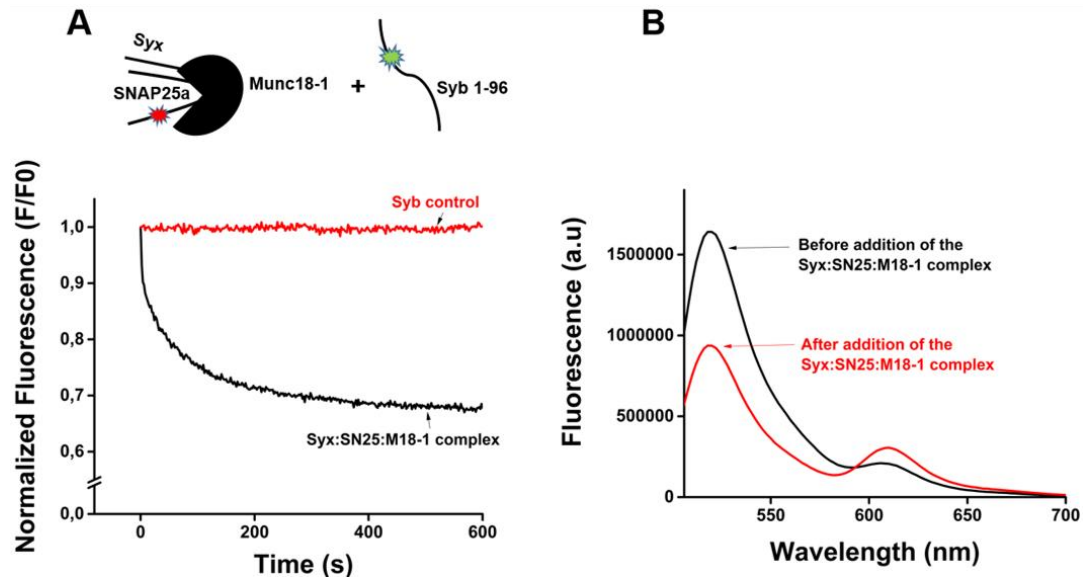


Figure 3.3.2-1. Monitoring SNARE-zippering between synaptobrevin and the syntaxin1a/SNAP25a/Munc18-1 complex using FRET.

(A) Addition of the acceptor syntaxin1a/SNAP25a/Munc18-1 complex to synaptobrevin resulted in a fast quenching of the donor emission (*black curve*). No quenching of the donor emission was observed when the acceptor complex was added in the presence of excess of unlabeled synaptobrevin (*red curve*). (B) Scans of the fluorescence spectrum were also recorded before (*black curve*) and after the addition of the ternary syntaxin1a/SNAP25a/Munc18-1 complex (*red curve*). The addition of the acceptor complex resulted in a decrease in the donor emission, followed by a subsequent increase in the acceptor emission, thereby indicating that the donor quenching takes place due to FRET. Fluorescent scans were performed by using an excitation wavelength of 460 nm and recording the emission spectrum in the wavelength range of 490 nm-700 nm.

Results

For this purpose, a single-cysteine mutant of SNAP25a was fluorescently labeled with the fluorophore Texas Red at position 130. The labeled SNAP25a was then used for the assembly and subsequent purification of a fluorescent version of the syntaxin1a/SNAP25a/Munc18-1 complex. The binding of the same cytoplasmic fragment of synaptobrevin (*as used in the previous section for anisotropy measurements*) was used to monitor SNARE-zippering with the labeled syntaxin1a/SNAP25a/Munc18-1 complex.

As shown in Figure 3.3.2-1 A, the addition of the syntaxin1a/SNAP25a/Munc18-1 complex to synaptobrevin, resulted in a fast quenching of the donor emission (*black curve*). The reaction could be completely inhibited when an excess of unlabeled synaptobrevin was present in the reaction mixture (*red curve*). As shown in Figure 3.3.2-1 B, the decrease in the emission of synaptobrevin (*donor*) was accompanied by a simultaneous decrease in the emission of the syntaxin1a/SNAP25a/Munc18-1 complex (*acceptor*), thereby validating the occurrence of FRET.

3.4 Comparison of syntaxin1a/SNAP25a/Munc18-1 complex with the previously characterized acceptor complexes.

After establishing the binding of synaptobrevin to the syntaxin1a/SNAP25a/Munc18-1 complex using both fluorescent anisotropy and FRET measurements, I wanted to establish its efficiency as an acceptor complex. To this end, I performed a comparison of its activity with the previously characterized acceptor complexes like the syntaxin1a/SNAP25a complex (118) and the C-terminally stabilized Δ N-complex (101). The syntaxin1a/SNAP25a (2:1) complex acts as a '*slow acceptor complex*' because in this complex, both the SNARE-motifs of syntaxin1a are occupied by SNAP25a. The second syntaxin1a molecule, poses a competition for synaptobrevin-binding, thereby lowering the speed of the reaction (118). On the other hand, the C-terminally stabilized Δ N-complex has been characterized as a '*fast acceptor complex*' because the presence of a C-terminal synaptobrevin fragment in this complex prevents the binding of a second syntaxin1a molecule, thereby facilitating synaptobrevin-binding (92).

In order to compare the efficiencies of the different complexes, I assembled and purified the unlabeled version of the syntaxin1a/SNAP25a complex as well as the labeled and unlabeled versions of both Δ N-complex and the syntaxin1a/SNAP25a/Munc18-1 complex. The unlabeled syntaxin1a/SNAP25a complex and syntaxin1a/SNAP25a/Munc18-1 complexes were used to test the binding of synaptobrevin, using fluorescence anisotropy measurements. As shown in Figure 3.4-1 A, the binding of synaptobrevin to the syntaxin1a/SNAP25a complex (*black curve*) was much slower as compared to that of the syntaxin1a/SNAP25a/Munc18-1 complex (*red curve*). Both of these reactions could be inhibited by the addition of excess of unlabeled synaptobrevin to the reaction mixture, thereby indicating that the

reactions were SNARE-specific. The quantification of the aforementioned fluorescence anisotropy measurements have been represented in Figure 3.4-2 B. Quantifications were performed at a time-point of 100 seconds (*black bars*) and 600 seconds (*red bars*), respectively. The error bars indicate the range of values from three independent set of experiments.

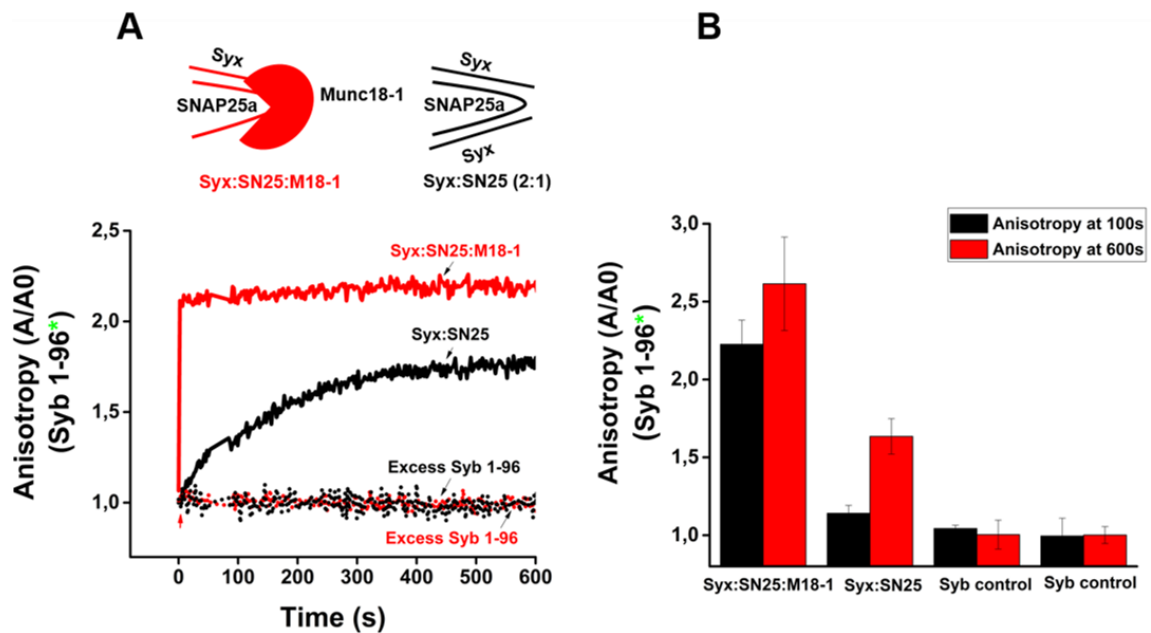


Figure 3.4-1 Comparison of the syntaxin1a/SNAP25a/Munc18-1 complex with the syntaxin1a/SNAP25a (2:1) complex.

(A) Addition of unlabeled syntaxin1a/SNAP25a complexes to fluorescently-labeled synaptobrevin resulted in a slow increase in anisotropy (*black curve*), in contrast to the fast increase observed upon the addition of the syntaxin1a/SNAP25a/Munc18-1 complex. Both of these reactions could be completely inhibited upon the addition of an excess of unlabeled synaptobrevin to the reaction mixture (*dotted curves*). (B) Quantification of the fluorescence anisotropy experiments. Quantifications were performed at 100 seconds (*black curve*) and 600 seconds (*red curve*) after addition of the acceptor complexes. Error bars indicate the range of values, $n=3$.

After having compared the efficiency of the syntaxin1a/SNAP25a/Munc18-1 complex with the 2:1 syntaxin1a/SNAP25a complex, I carried out the comparison with the Δ N-complex. The same approach using fluorescence anisotropy measurements (as described above) was employed to compare the synaptobrevin-binding efficiencies of the Δ N-complex and the syntaxin1a/SNAP25a/Munc18-1 complex.

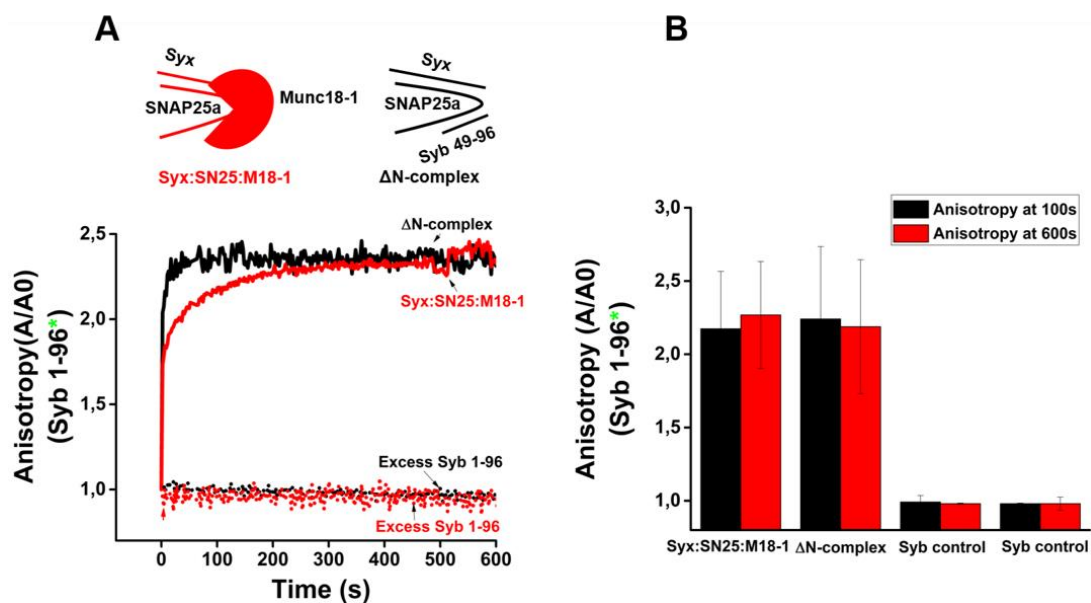


Figure 3.4-2 Comparison of the synaptobrevin-binding efficiency between the syntaxin1a/SNAP25a/Munc18-1 complex and the Δ N-complex.

(A) Synaptobrevin-binding to the Δ N-complex (black curve) and the syntaxin1a/SNAP25a/Munc18-1 complex (red curve) proceeded on a similar time-scale. Both of these reactions could be inhibited by addition of excess unlabeled synaptobrevin to the reaction mixture. (B) Quantification of the anisotropy measurements from three independent experiments, at 100 seconds (black bars) and 600 seconds (red bars) respectively. Error bars indicate the range of values.



The above comparison revealed that synaptobrevin-binding to both ΔN -complex and the syntaxin1a/SNAP25a/Munc18-1 complex proceeds with similar kinetics (Figure 3.4-2 A, *black and red curves*). Quantifications of the anisotropy measurements have been shown in Figure 3.4-2 B, where the error bars indicate the range of values from three independent experiments.

The remarkable similarity in the kinetics of synaptobrevin-binding exhibited by the ΔN -complex and the syntaxin1a/SNAP25a/Munc18-1 complex was quite interesting, providing clues to the role of Munc18-1 in structuring the Q-SNAREs for SNARE-complex assembly. I therefore wanted to study the association of synaptobrevin with these complexes using FRET-measurements, in order to gain more insights into the process of SNARE-zippering.

For this purpose, I used fluorescently-labeled version of a single-cysteine mutant of SNAP25a (C130), labeled with Texas Red to assemble and purify fluorescently-labeled versions of the syntaxin1a/SNAP25a/Munc18-1 complex and the ΔN -complex. These labeled acceptor complexes were subsequently used for monitoring SNARE-complex assembly by measuring FRET between SNAP25a (incorporated in the acceptor complexes) and the full cytoplasmic version of a single-cysteine mutant of synaptobrevin (Syb 1-96 C28), that had been fluorescently labeled with Oregon Green. SNARE-complex assembly was monitored as quenching of the donor emission observed upon the addition of the acceptor complexes. As shown in Figure 3.4-3 A, the addition of the fluorescently-labeled syntaxin1a/SNAP25a/Munc18-1 complex (*red curve*) as well as the ΔN -complex (*black curve*) to fluorescently-labeled synaptobrevin resulted in a fast quenching of the donor emission. The reaction could be inhibited by the addition of an excess unlabeled synaptobrevin to the reaction mixture (*dotted red curve*), indicating the SNARE-specificity of the reaction. Thereafter, the degree of quenching of the donor emission was also recorded over a range of concentrations of the syntaxin1a/SNAP25a/Munc18-1 complex. As shown in Figure 3.4-3 B, a dose-dependent response was observed for the FRET measurements using syntaxin1a/SNAP25a/Munc18-1 as an acceptor complex.

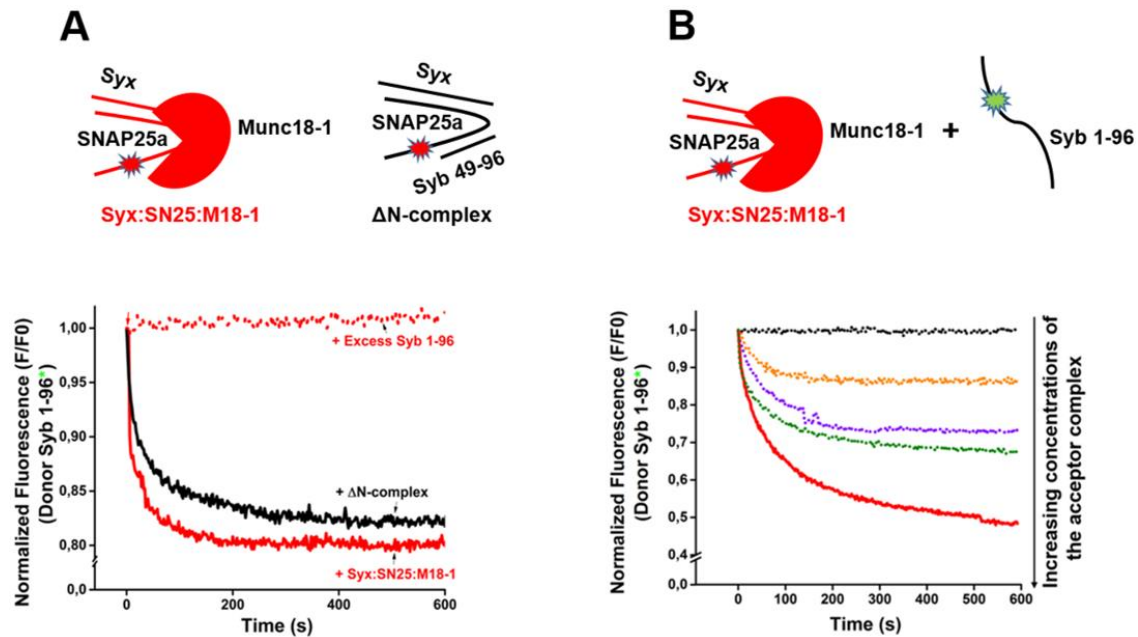


Figure 3.4-3. FRET measurements showing the kinetics of SNARE-complex formation, using the syntaxin1a/SNAP25a/Munc18-1 complex and the Δ N-complex.

(A) A fast dequenching of the donor emission was observed upon the addition of the syntaxin1a/SNAP25a/Munc18-1 complex (*red curve*) as well as the Δ N-complex (*black curve*). The reaction could be inhibited upon adding excess of unlabeled synaptobrevin to the reaction mixture (*red dotted curve*). (B) Increasing concentrations of the syntaxin1a/SNAP25a/Munc18-1 complexes resulted in an increasing quenching of the donor emission, thereby exhibiting a dose-dependent response.

Collectively, the experiments performed in this section could faithfully establish that the syntaxin1a/SNAP25a/Munc18-1 complex serves as an efficient acceptor complex, with its synaptobrevin-binding efficiency being similar to that of the non-physiological Δ N-complex.

3.5 Stability of the syntaxin1a/SNAP25a/Munc18-1 complex.

After having established the functional significance of the syntaxin1a/SNAP25a/Munc18-1 complex, I wanted to delve deeper into the biochemical characteristics of this complex. To this end, I wanted to determine the *in-vitro* stability of the syntaxin1a/SNAP25a/Munc18-1 complex.

The stability of the syntaxin1a/SNAP25a/Munc18-1 complex was determined using a time-based approach. This involved measurement of the synaptobrevin-binding activity of the syntaxin1a/SNAP25a/Munc18-1 complex at different time-intervals post-purification, using fluorescence anisotropy.

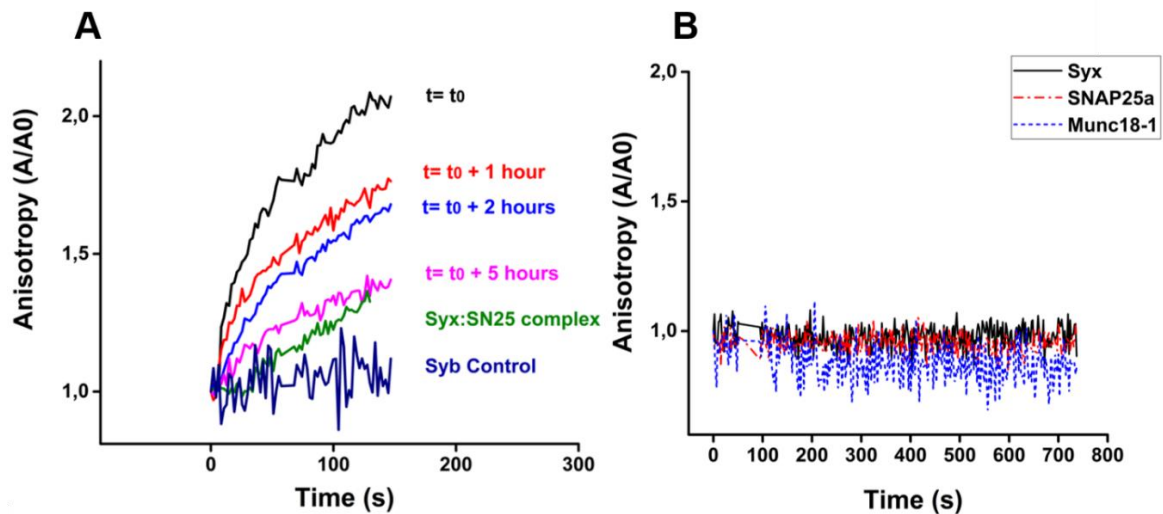


Figure 3.5-1. The syntaxin1a/SNAP25a/Munc18-1 complex loses its stability with time. (A) Time-dependent loss in the activity of the syntaxin1a/SNAP25a/Munc18-1 complex assessed by fluorescence anisotropy measurements. A considerable loss in the activity of the syntaxin1a/SNAP25a/Munc18-1 complex was observed after five hours of purification (B) Fluorescence anisotropy of synaptobrevin remained unaffected upon the addition of either monomeric syntaxin1a (*black curve*), SNAP25a (*blue curve*) or Munc18-1 (*red curve*).

As shown in Figure 3.5-1 A, the syntaxin1a/SNAP25a/Munc18-1 complex appeared to lose its synaptobrevin-binding activity over extended periods of time, with considerable loss in its activity five hours post-purification. This decrease indicated a loss of the integrity of the complex with increasing time-course.

Taking this into account, it became important to determine whether or not, the monomers formed due to the dissociation of the syntaxin1a/SNAP25a/Munc18-1 complex could contribute to any increase in the anisotropy of synaptobrevin. To test this, I used fluorescently-labeled synaptobrevin to monitor the changes in its anisotropy upon the addition of monomeric syntaxin1a, SNAP25a and Munc18-1 respectively.

As indicated in Figure 3.5-1 B, no increase in the anisotropy of synaptobrevin could be observed upon the addition of monomeric syntaxin1a (*black curve*), SNAP25a (*red curve*) or Munc18-1 (*blue curve*). This observation therefore asserted the fact that, irrespective of the unstable nature of the syntaxin1a/SNAP25a/Munc18-1 complex, it can be believed that the fast synaptobrevin-binding activity of the syntaxin1a/SNAP25a/Munc18-1 complex, is solely the property of the complex and is not attributed by any monomers that could be present in the solution at extended time-points.

As a next step, I wanted to further verify the dissociation of the syntaxin1a/SNAP25a/Munc18-1 complex into its constituent proteins, using an independent approach. To this end, I performed the *in-vitro* assembly and purification of the syntaxin1a/SNAP25a/Munc18-1 complex and subsequently injected the purified complex into an analytical column for size-exclusion chromatography (*Superdex 10/300 Increase, GE Healthcare*). The results of this experiment have been shown in Figure 3.5-2.

The elution profile from size-exclusion chromatography revealed the presence of one major peak that corresponded to the ternary complex but, also showed the presence of additional peaks at higher retention volumes (Figure 3.5-2 B). The presence of additional peaks were indicative of the unstable nature of the syntaxin1a/SNAP25a/Munc18-1 complex under the given experimental conditions.

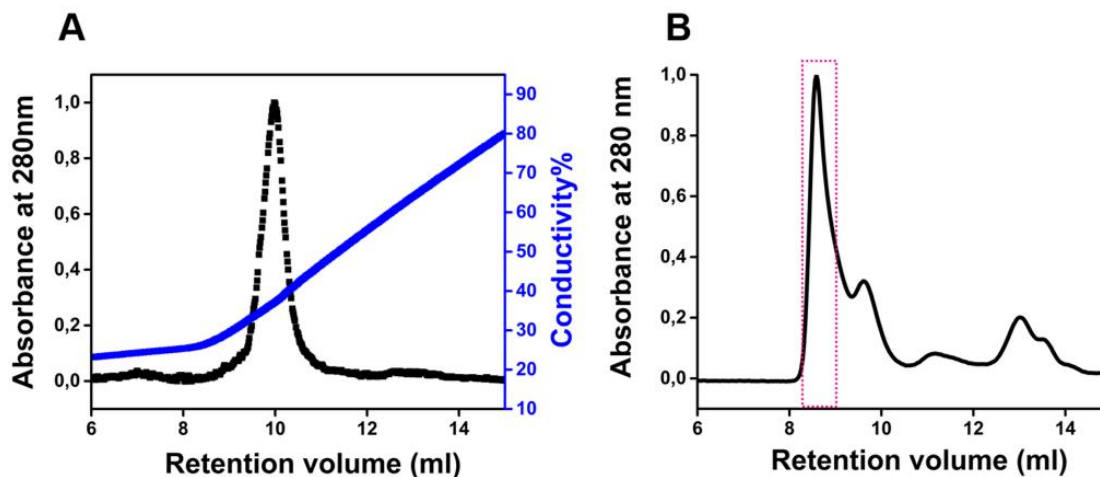


Figure 3.5-2. Stability of the syntaxin1a/SNAP25a/Munc18-1 complex.

(A) Purification of the syntaxin1a/SNAP25a/Munc18-1 using ion-exchange chromatography. (B) The subsequent injection of the purified sample into an analytical gel-filtration column showed the presence of a main peak (*pink dotted lines*) corresponding to the syntaxin1a/SNAP25a/Munc18-1 complex. Small additional peaks were, however, also observed that were later characterized to correspond to the monomeric constituents of the syntaxin1a/SNAP25a/Munc18-1 complex.

As a next step, I tried to validate whether the additional peaks observed upon size-exclusion chromatography corresponded to the respective monomers of the syntaxin1a/SNAP25a/Munc18-1. For this purpose, I used the same analytical gel-filtration column as indicated before (*Superdex 10/300 Increase, GE Healthcare*) to determine the retention volumes for the monomeric constituents of the syntaxin1a/SNAP25a/Munc18-1 complex.

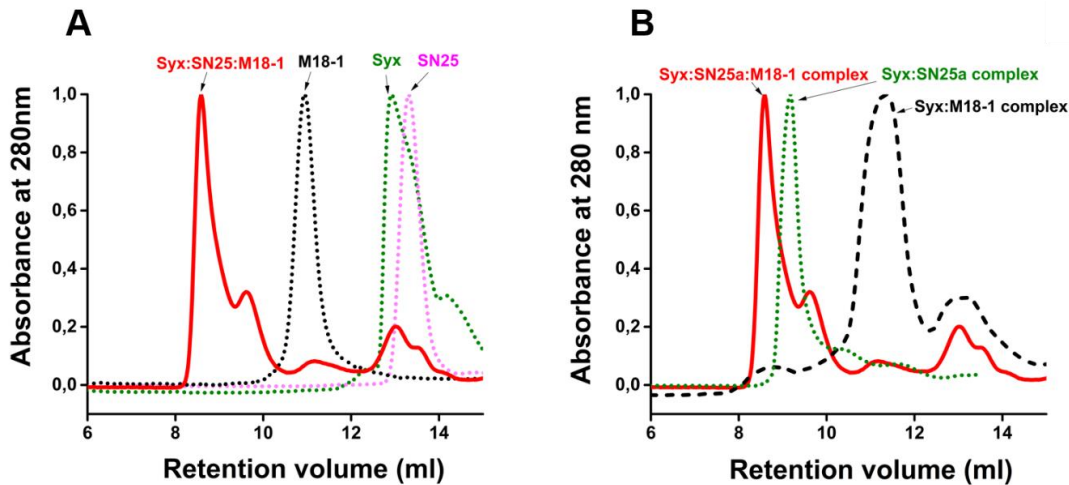


Figure 3.5-3. SEC-profiles of syntaxin1a, SNAP25a, Munc18-1, the binary syntaxin1a/SNAP25a complex and the syntaxin1a/Munc18-1 complex.

(A) An overlay of the re-injection profile of the syntaxin1a/SNAP25a /Munc18-1 complex with the elution profiles of the respective monomers and (B) with the binary syntaxin1a/SNAP25a (2:1) complex (*green curve*) and the syntaxin1a/Munc18-1 complex (*black curve*).

As indicated in Figure 3.5-3 A, the peaks corresponding to the retention volumes 11.3 mL, 13.2 mL and 13.5 mL corresponded to the proteins Munc18-1 (*black dotted curve*), syntaxin1a (*green dotted curve*) and SNAP25a (*pink dotted curve*) respectively. These three peaks showed perfect correlation with the three minor peaks observed upon the subsequent injection of the purified syntaxin1a/SNAP25a/Munc18-1 complex into size-exclusion chromatography (Figure 3.5-3 A, *red solid curve*). These observations therefore confirmed that the syntaxin1a/SNAP25a/Munc18-1 complex has a tendency to dissociate into its respective monomers.

For a more thorough analysis of the reaction, I also determined the elution profiles of the binary syntaxin1a/Munc18-1 complex and the syntaxin1a/SNAP25a complex. This was achieved by performing the *in-vitro* assembly and subsequent injection of the respective complexes into the same gel-filtration column (*Superdex 10/300 Increase, GE Healthcare*), and under the same buffer conditions that were used to perform the above-mentioned purifications. As shown in Figure 3.5-3 B, the elution of the syntaxin1a/SNAP25a (2:1) complex and the syntaxin1a/Munc18-1 complex corresponded to retention volumes of 9.3 ml and 11 ml respectively. Thus, the small shoulder peak observed at 9.3ml in Figure 3.5-2 B was identified to be syntaxin1a/SNAP25a complex that could possibly have been formed as a side-product from the dissociation of the syntaxin1a/SNAP25a/Munc18-1 complex.



3.6 Architecture of the syntaxin1a/SNAP25a/Munc18-1 complex.

The experiments performed in the previous sections established the ternary syntaxin1a/SNAP25a/Munc18-1 as a loose complex with a 1:1:1 stoichiometry, which exists in a dynamic equilibrium with its monomers and serves as a very efficient acceptor for synaptobrevin-binding. This finding was very interesting because it consolidated some earlier findings hinting at the existence of a syntaxin1a/SNAP25a/Munc18-1 complex as an intermediate in the SNARE-pathway (45, 46, 79, 119).

In order to gain a deeper understanding of this intermediate, it became very important to investigate the structural features of the syntaxin1a/SNAP25a/Munc18-1 complex that dictate its efficiency as an acceptor complex. Since this complex appeared to be labile under the experimental conditions, it was difficult to resort to X-ray crystallography as a tool to monitor its architecture. Another popular structural technique, cryo-electron microscopy could also not be used due to the small size of the ternary complex (120 kDa). I therefore used chemical cross-linking and mass spectrometry (MS/MS) as a tool to gain insight into the architecture of the syntaxin1a/SNAP25a/Munc18-1 complex.

The cross-linker used for this purpose was bis(sulfosuccinimidyl) suberate (BS3), which is a homo-bifunctional chemical cross-linker that cross-links the lysine residues and also the free amino-terminus of the proteins. The spacer arm-length of this cross-linker is 11.4 Å. As a first step in this approach, the protein complex was titrated with increasing amounts of the chemical cross-linker to determine the amount of cross-linker required for optimum cross-linking. The efficiency of cross-linking was determined by separation of the cross-linked products using SDS-PAGE and Coomassie Blue staining. Optimum cross-linking of the syntaxin1a/SNAP25a/Munc18-1 complex appeared to occur when a 50-fold molar excess of the chemical cross-linker (BS3) with respect to the syntaxin1a/SNAP25a/Munc18-1 complex was used. The molecular weight of the cross-linked syntaxin1a/SNAP25a/Munc18-1 complex was observed at 130kDa. A representative gel showing the titration of the ternary complex with BS3 has been depicted in Figure 3.6-1.

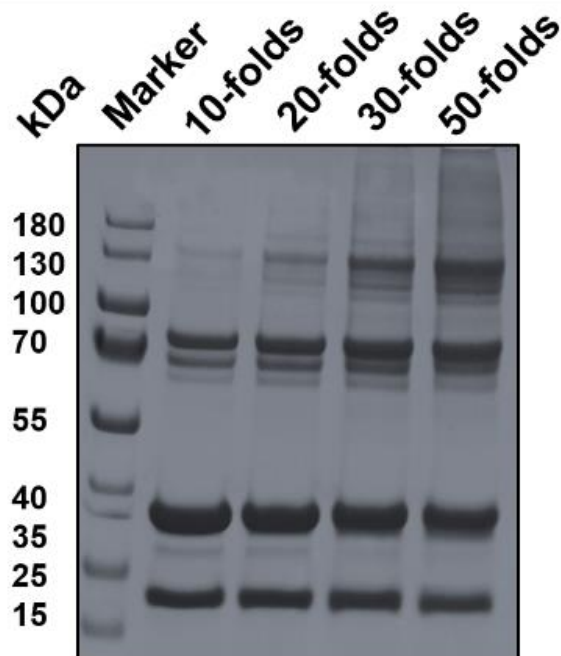


Figure 3.6-1. Titration of the syntaxin1a/SNAP25a/Munc18-1 complex with increasing amounts of the chemical cross-linker, BS3.

Freshly purified syntaxin1a/SNAP25a/Munc18-1 complex was titrated with different amounts of the cross-linker, ranging from a 10-fold molar excess to a 50-fold molar excess of BS3 with respect to the syntaxin1a/SNAP25a/Munc18-1 complex. The cross-linked samples were analyzed by SDS-PAGE and Coomassie Blue staining. Optimum cross-linking of the syntaxin1a/SNAP25a/Munc18-1 complex was obtained when a 50-fold molar excess of the cross-linker was used. The cross-linked band was observed at a molecular weight of 130 kDa.

Thereafter, cross-linking of the complex was performed at the optimum concentration of the cross-linker, and the cross-linked bands corresponding to the ternary complex were excised from the gel and subjected to in-gel trypsin digestion followed by peptide analysis by mass spectrometry (MS/MS). All the mass spectrometry experiments and analysis in this study were performed by Dr. Chung-Tien Lee. MS/MS analysis of the cross-linked samples revealed inter-crosslinks between all the three constituent proteins namely syntaxin1a, SNAP25a and Munc18-1. A pictorial representation of the major cross-links observed upon MS/MS analysis have been represented in Figure 3.6-2.

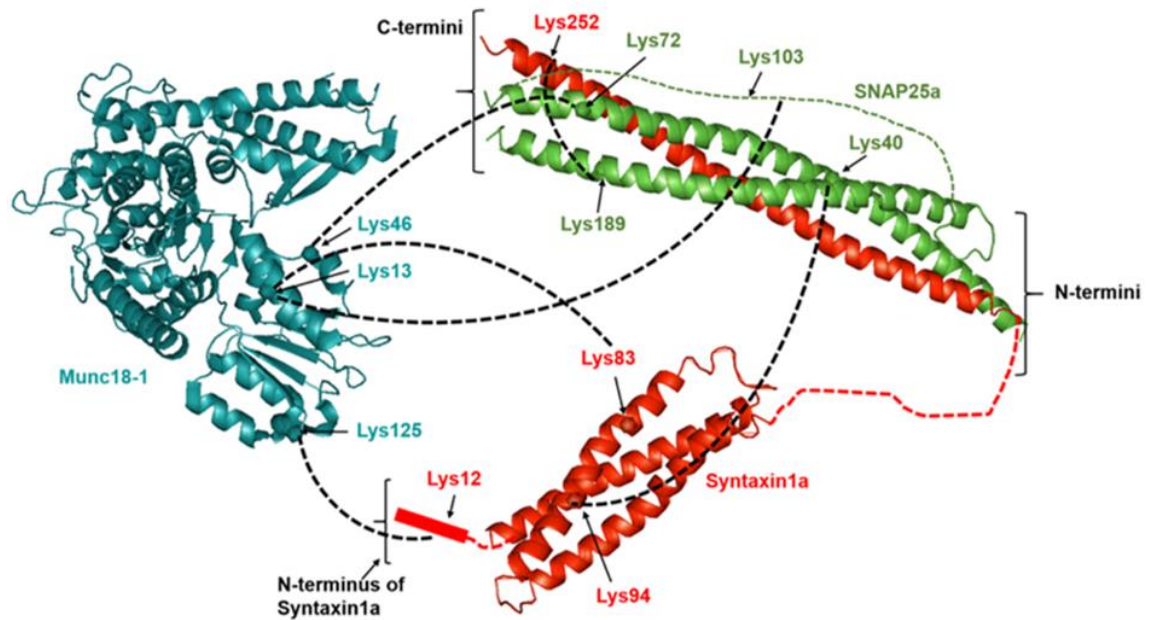


Figure 3.6-2. Inter cross-links obtained between syntaxin1a, SNAP25a and Munc18-1 upon chemical cross-linking of the syntaxin1a/SNAP25a/Munc18-1 complex.

Chemical cross-linking and the subsequent MS/MS analysis of the syntaxin1a/SNAP25a/Munc18-1 complex provided inter-cross-links between all the three constituents of the ternary complex. Munc18-1 was seen to be cross-linked to both syntaxin1a as well as SNAP25a. [This experiment was performed in collaboration with Dr. Chung-Tien Lee].

In the syntaxin1a/SNAP25a/Munc18-1 complex, Munc18-1 was seen to closely interact with the N-terminal domain of syntaxin1a, i.e. the N-peptide and the Habc-domain. Lysine 12, lying in the N-peptide of syntaxin1a was crosslinked to lysine 125 of Munc18-1 (positioned in domain1), consistent with the speculated role of N-peptide in mediating the interaction of syntaxin1a with Munc18-1 (39). Cross-links between lysine 83 (positioned in the Habc-domain of syntaxin1a) and lysine 13 (positioned in the domain3a of Munc18-1) were also observed. No crosslinks were, however, detected between the SNARE-motif of syntaxin1a and Munc18-1.

The most interesting insight that came from the cross-linking experiments, was the presence of cross-links between SNAP25a and Munc18-1. As shown in Figure 3.6-2, lysine 72 of SNAP25a and lysine 46 of Munc18-1 were seen to be crosslinked in the ternary complex. This cross-link provided a structural insight for the functional efficiency of the syntaxin1a/SNAP25a/Munc18-1 complex.

Lysine 46 of Munc18-1 is positioned in the syntaxin1a-binding 'cleft' of Munc18-1 (domain 1), a region in the syntaxin1a/Munc18-1 structure which closely interacts with the Habc-domain and the SNARE-motif of syntaxin1a (39, 73). For a clear demonstration, the residues of syntaxin1a that interact with Munc18-1 in the syntaxin1a/Munc18-1 structure have been represented in Figure 3.6-3. On the other hand, lysine 72 of SNAP25a is positioned towards the C-terminus of the first SNARE-motif (SN1) of SNAP25a. The relative orientation of Munc18-1 with respect to SNAP25a in the syntaxin1a/SNAP25a/Munc18-1 complex indicates that Munc18-1 could help in preventing the association of a second syntaxin1a molecule to the syntain1a/SNAP25a complex, thereby attributing to the efficiency of the syntaxin1a/SNAP25a/Munc18-1 complex as an acceptor for synaptobrevin-binding.

A comparison of the interaction interfaces between syntaxin1a and Munc18-1 in the syntaxin1a/SNAP25a/Munc18-1 complex with the previously reported structure of the syntaxin1a/Munc18-1 complex (39, 47) revealed significant differences. Most importantly, the contact sites between syntaxin1a and Munc18-1 in the syntaxin1a/SNAP25a/Munc18-1 complex appeared to be limited to the N-terminus of syntaxin1a, as opposed to the syntaxin1a/Munc18-1 complex, where extensive associations with the SNARE-motif are also present (see Figure 3.6-3). This loss of interaction could be caused due to the interaction of the SNARE-motif of syntaxin1a with its partner SNARE, SNAP25a thereby placing SNAP25a in close vicinity of Munc18-1. It thus, becomes conceivable that syntaxin1a in the syntaxin1a/SNAP25a/Munc18-1 complex has a tendency to exist in a more 'open' conformation, in contrast to the 'closed' conformation observed in the syntaxin1a/Munc18-1 complex (39, 47).

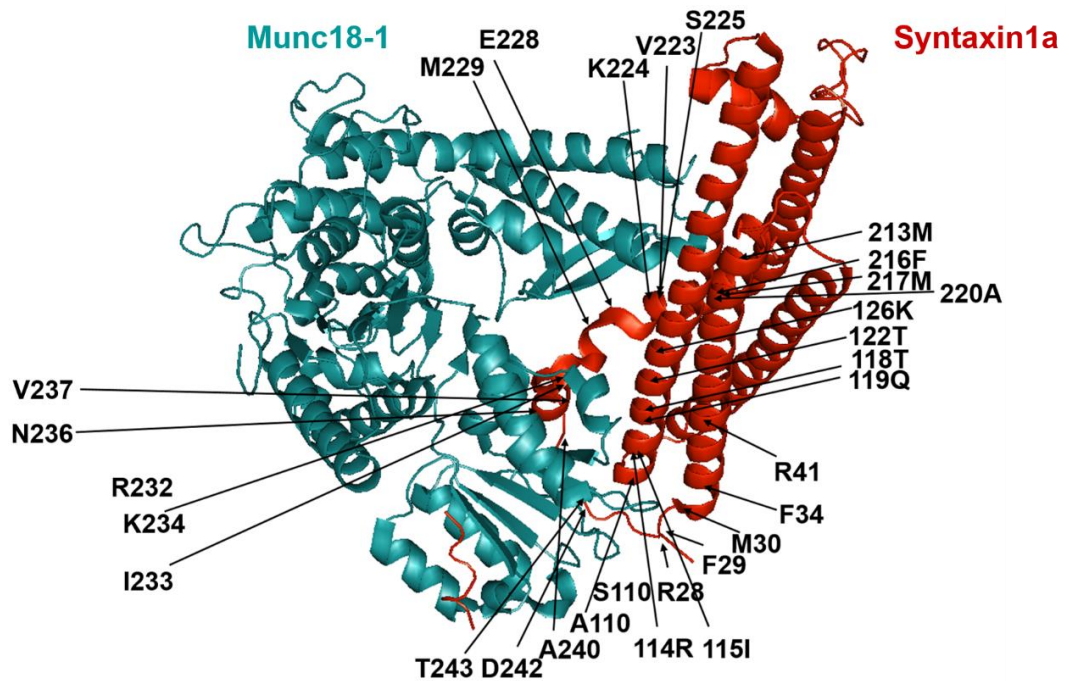


Figure 3.6-3. Ribbon diagram of the syntaxin1a/Munc18-1 complex.

Syntaxin1a is locked in a 'closed' conformation within the syntaxin1a/Munc18-1 complex. The Habc-domain of syntaxin1a (residues 30-150) fold back on its SNARE-motif (residues 195-254) and interact tightly with a binding pocket ('cleft') formed by the domain 1 and 3a of the Munc18-1. Residues of syntaxin1a that contact the 'syntaxin1a-binding cleft' of Munc18-1 in this binary complex have been indicated by the labels. Syntaxin1a is shown in *red* and Munc18-1 is shown in *cyan*. [Adapted from (39)]. [This experiment was performed in collaboration with Dr. Chung-Tien Lee].

A wealth of knowledge was also gained from the analysis of the intra-crosslinks observed within the monomeric constituents of the syntaxin1a/SNAP25a/Munc18-1 complex. The intra-crosslinks provided a measure of the domain-proximities of syntaxin1a, SNAP25a and Munc18-1, when they existed as part of the syntaxin1a/SNAP25a/Munc18-1 complex. A representative diagram of the obtained intra-crosslinks has been shown in Figure 3.6-4.

The intra-crosslinks for syntaxin1a indicated extensive contacts within the residues of the Habc-domain and the within the SNARE-motif respectively, but minimal contacts were found between the Habc-domain and the SNARE-motif of syntaxin1a. This observation also pointed towards syntaxin1a being in a more 'open' conformation in the syntaxin1a/SNAP25a/Munc18-1 complex. This structural information was quite consistent with the synaptobrevin-binding efficiency of the syntaxin1a/SNAP25a/Munc18-1 complex obtained from the anisotropy and FRET measurements, discussed previously. The intra-crosslinks obtained for SNAP25a were also very informative. Contacts were obtained between the SN1 and the linker regions of SNAP25a as well as the SN2 and the linker regions of SNAP25a. The absence of intra-crosslinks between the SN1 and SN2 of SNAP25a were indicative of the fact that in the syntaxin1a/SNAP25a/Munc18-1 complex, the SN2 of SNAP25a remains a little unstructured and dynamic with respect to the SN1 of SNAP25a, which probably gets structured due to association with syntaxin1a. Intra-crosslinks between the different domains of Munc18-1 were consistent with the three-dimensional structure of the protein, with crosslinks being obtained between lysine residues that constitute the domain2 of Munc18-1 and also between the domains 1 and 3a, respectively. The amino-acids that constitute these regions are separated by a stretch of amino-acids in the primary sequence, but are positioned closely in the three-dimensional space. The presence of these crosslinks added further belief to the fidelity of the conclusions obtained from the cross-linking experiments, by providing a proof of fact.

Collectively, the results obtained from the experiments in this section indicate that the association of Munc18-1 with syntaxin1a and SNAP25a in the ternary syntaxin1a/SNAP25a/Munc18-1 complex helps in structuring the Q-SNAREs for productive SNARE-complex assembly. The discovery of the close association between SNAP25a and Munc18-1 is quite novel, since such an interaction has not been reported for Munc18-1. A recent study with the yeast SM-protein, Sec1 (homologue of Munc18-1) has, however, indicated a groove on Sec1 that might participate in its interaction with Sec9 (the yeast homologue of SNAP25) (71).

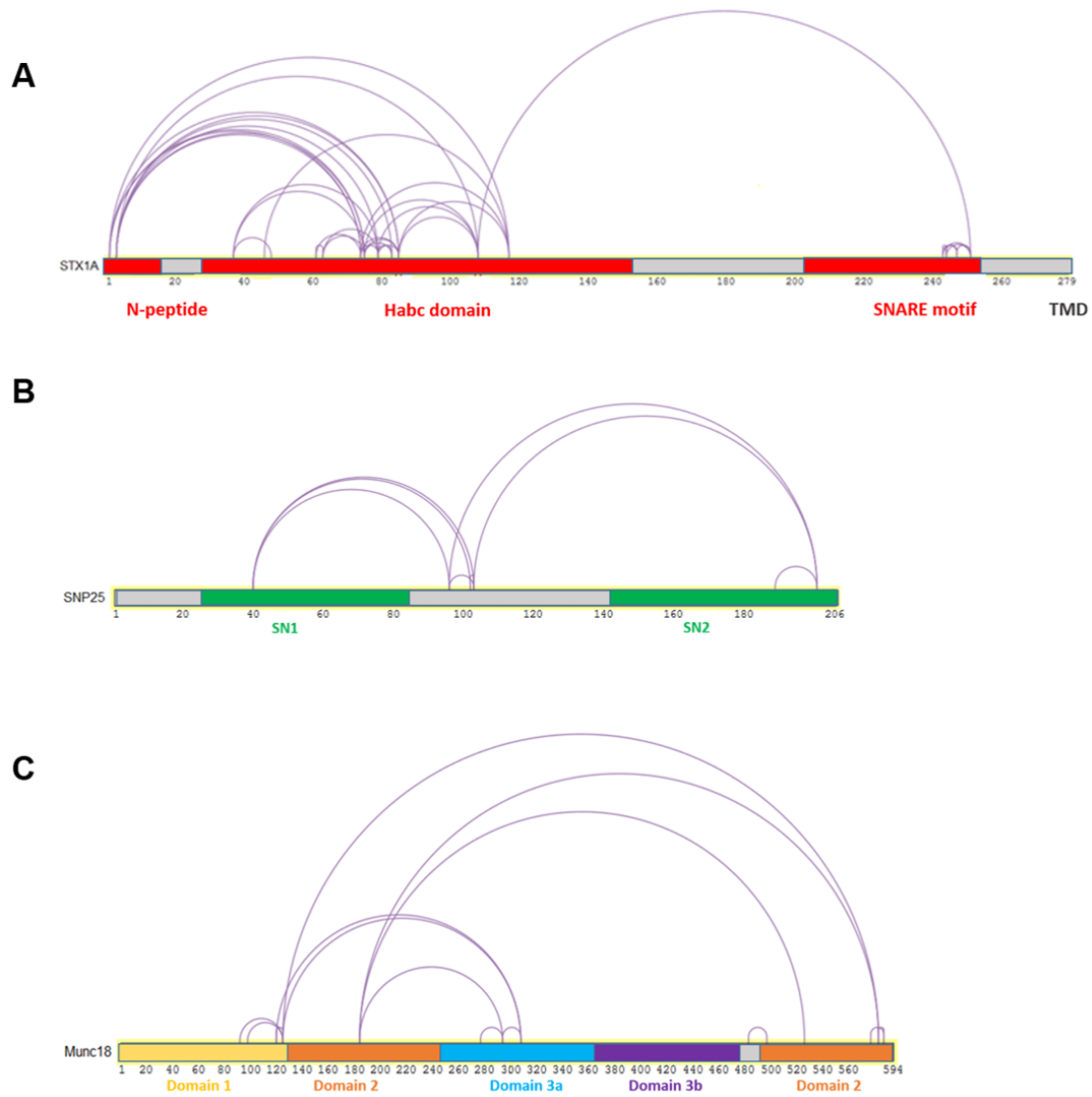


Figure 3.6-4. Representative intra-crosslinks between the monomeric constituents of the syntaxin1a/SNAP25a/Munc18-1 complex.

Intra-crosslinks obtained for (A) syntaxin1a, (B) SNAP25a and (C) Munc18-1, upon chemical cross-linking of the syntaxin1a/SNAP25a/Munc18-1 complex. [This experiment was performed in collaboration with Dr. Chung-Tien Lee].

3.7 Is Munc18-1 displaced after the binding of synaptobrevin to the syntaxin1a/SNAP25a/Munc18-1 complex?

The results from cross-linking experiments clearly established that the structural organization of the constituent proteins in the syntaxin1a/SNAP25a/Munc18-1 complex provide a facilitated pathway for synaptobrevin-binding and subsequent SNARE-complex assembly. After gaining some insights into the architecture of the syntaxin1a/SNAP25a/Munc18-1 complex, I attempted to address the changes in this complex upon synaptobrevin-binding, in terms of its composition and architecture.

To this end, I started with testing the impact of synaptobrevin-binding on Munc18-1, *i.e.* whether or not, Munc18-1 remains associated with the syntaxin1a/SNAP25a/Munc18-1 complex upon synaptobrevin-binding. I tried to address this question using three different biochemical techniques. As a starting approach, I used size-exclusion chromatography to monitor any changes in the molecular mass/hydrodynamic radius of the syntaxin1:SNAP25:Munc18-1 complex before and after synaptobrevin-addition. A direct measure of such changes can be obtained by assessing the retention volumes for the elution of the complex under different experimental conditions.

Freshly purified syntaxin1a/SNAP25a/Munc18-1 complex was injected into an analytical column for size-exclusion chromatography and the retention volume of the complex was monitored (Figure 3.7-1, *red curve*). Thereafter, the complex was subjected to a brief incubation with synaptobrevin and was again analyzed by analytical size-exclusion chromatography. The retention volume of this complex was seen to be slightly lower (Figure 3.7-1, *black curve*) as compared to the complex without synaptobrevin (Figure 3.7-1, *red curve*). These observations provided a first indication that the addition of synaptobrevin to the syntaxin1a/SNAP25a/Munc18-1 complex, probably does not lead to the dissociation of Munc18-1 from the complex.

Although, size-exclusion chromatography is a widely used technique for the assessment of changes in molecular masses of proteins/protein complexes, it is not the ideal choice of method in this case. This is mainly because the syntaxin1a in the ternary complex contained a transmembrane-domain, which in turn demanded the analysis to be performed in detergent micelles. The precise determination of the hydrodynamic radius/molecular mass of proteins under micellar conditions, using size-exclusion chromatography, however, is a little challenging. It therefore, became important to validate the above results, using a different technique.

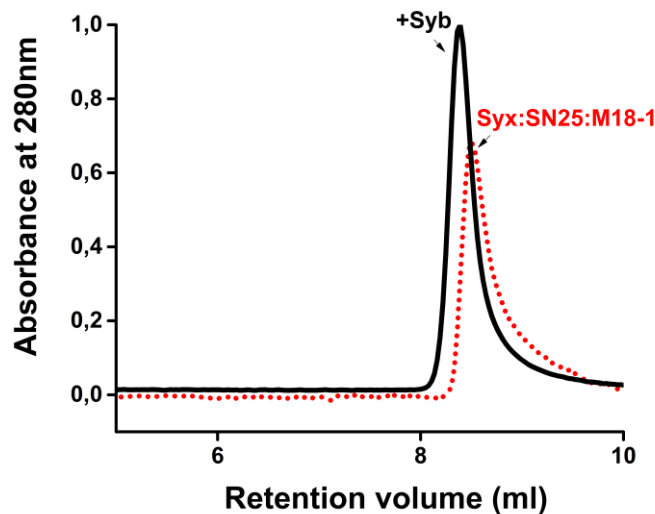


Figure 3.7-1. Synaptobrevin-binding to the syntaxin1a/SNAP25a/Munc18-1 complex causes a decrease in its retention volume.

The syntaxin1a/SNAP25a/Munc18-1 complex, after synaptobrevin addition, showed a lower retention volume (*black curve*) as compared to the complex without synaptobrevin -addition (*red curve*).

As an alternative approach, I tried to address this issue using a co-floitation assay (*see section 2.12*). To this end, I purified the syntaxin1a/SNAP25a/Munc18-1 complex and subjected it to a brief incubation with synaptobrevin. Thereafter, the protein mixture was incorporated into liposomes and the proteoliposomes were separated from the unbound/displaced proteins using ultra-centrifugation on a nycodenz density-gradient. The samples were thereafter analyzed by SDS-PAGE and subsequent western blotting using antibodies against synaptobrevin and Munc18-1. As shown in Figure 3.7-2, after incubation of the syntaxin1a/SNAP25a/Munc18-1 complex with synaptobrevin, both synaptobrevin and Munc18-1 were seen to co-float with the liposomes, thereby indicating that synaptobrevin successfully binds to the syntaxin1a/SNAP25a/Munc18-1, without displacing Munc18-1 from the complex. However, it remained very important to address whether the presence of Munc18-1 in the liposomal fractions was due to a SNARE-specific interaction or whether it was due to non-specific binding of Munc18-1 to the lipids present in the liposomes. To address this concern, I prepared liposomes lacking any SNARE-proteins and subjected them to incubation with Munc18-1. The liposomes were analyzed in the same way as mentioned previously. As shown in Figure 3.7-2 (*last lane*), the incubation of Munc18-

1 with liposomes lacking any SNARE proteins did not result in any specific binding with the liposomes. Here the pattern of association of Munc18-1 with the liposomes was rather diffuse, with the majority of Munc18-1 being present in the bottom fractions of the gradient after co-flotation. A small amount of Munc18-1 was however, seen to be present in the liposomal fractions. This was consistent with an earlier report demonstrating the weak affinity of Munc18-1 for membrane lipids (120).

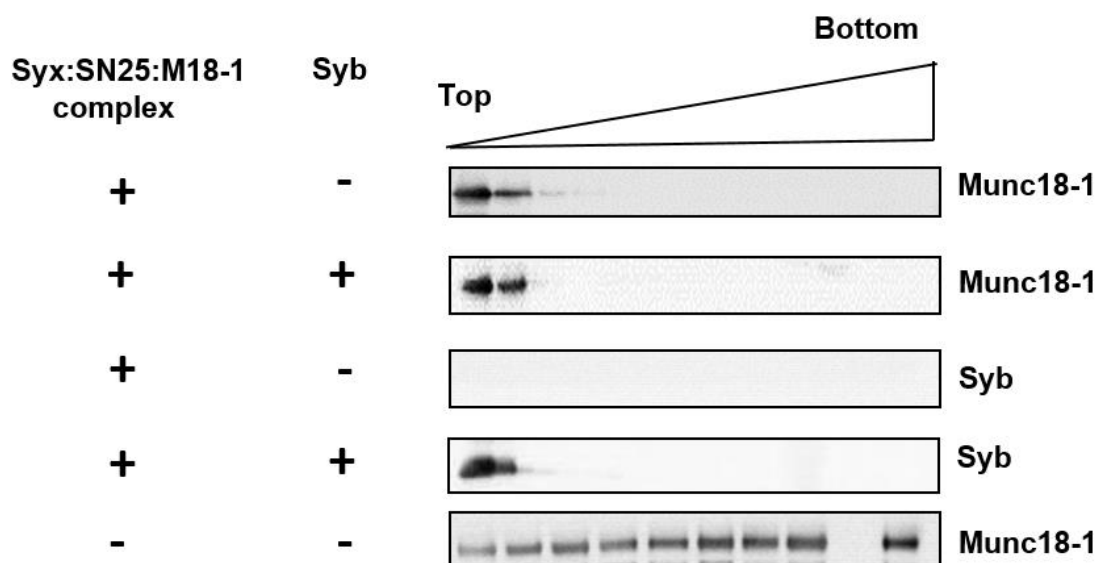


Figure 3.7-2. Munc18-1 does not get displaced upon synaptobrevin-binding to the syntaxin1a/SNAP25a/Munc18-1 complex.

Syntaxin1a/SNAP25a/Munc18-1 complex was incubated with synaptobrevin and the mixture was incorporated into liposomes, followed by a separation of unbound/displaced proteins from the liposomes using co-flotation assay. As a control, this assay was performed without synaptobrevin-incubation. Detection of Munc18-1 and synaptobrevin was performed by western blot analysis. The presence of Munc18-1 both in the absence (*lane 1*) and presence of synaptobrevin (*lane 2*) indicated that synaptobrevin-binding to the syntaxin1a/SNAP25a/Munc18-1 complex does not lead to the displacement of Munc18-1. Upon incubation of Munc18-1 with protein-free liposomes (*last lane*), Munc18-1 was seen to be only weakly associated with the liposomal fractions.



The results obtained both from size-exclusion chromatography (Figure 3.7-1) and the co-floitation assay (Figure 3.7-2), pointed towards the continued association of Munc18-1 after synaptobrevin-binding to the syntaxin1a/SNAP25a/Munc18-1 complex. This could result due to three different possibilities:

- Continued association of Munc18-1 with the N-terminal domain of syntaxin1a, after SNARE-complex formation
- Or, interaction of Munc18-1 with the core SNARE-complex
- Or, both.

The best way to approach this situation was to use a tool that would provide structural details of the syntaxin1a/SNAP25a/Munc18-1 complex upon its association with synaptobrevin. To this end, I resorted to the previously described chemical cross-linking approach with BS3. In this case, purified syntaxin1a/SNAP25a/Munc18-1 complex was incubated with synaptobrevin and the resulting complex was subjected to chemical crosslinking with BS3. The downstream processing of the sample was done in the same way as discussed in section 3.6, with the final step being the identification of the cross-linked peptides by mass spectrometry (MS/MS). The results of the cross-linking experiments gave very interesting insights into the conformational changes that occur upon synaptobrevin-binding to the syntaxin1/SNAP25a/Munc18-1 complex. A pictorial representation of the main results is provided in Figure 3.7-3.

Upon addition of synaptobrevin to the syntaxin1a/SNAP25a/Munc18-1 complex, crosslinks could be observed only between Munc18-1 and syntaxin1a. Cross-links were obtained between residues in domain 3b of Munc18-1 (lysine 384 and lysine 461) and the Habc-domain of syntaxin1a (lysine 70 and lysine 92). It becomes important to emphasize that although the Habc-domain of syntaxin1a could be observed to be associated with Munc18-1 after synaptobrevin-binding, the interaction-sites appeared to be altered considerably as compared to the case where no synaptobrevin was added to the syntaxin1a/SNAP25a/Munc18-1 complex (see Figure 3.6-2 for comparison). The residues of Munc18-1 which showed cross-linking with syntaxin1a were mapped to a region which is spatially very distinct from the '*syntaxin-binding cleft*' of Munc18-1. Altogether, these observations suggested that synaptobrevin-binding to the syntaxin1a/SNAP25a/Munc18-1 complex leads to major structural rearrangements, re-orienting Munc18-1 towards the N-terminus of syntaxin1a in a fully assembled SNARE-complex.

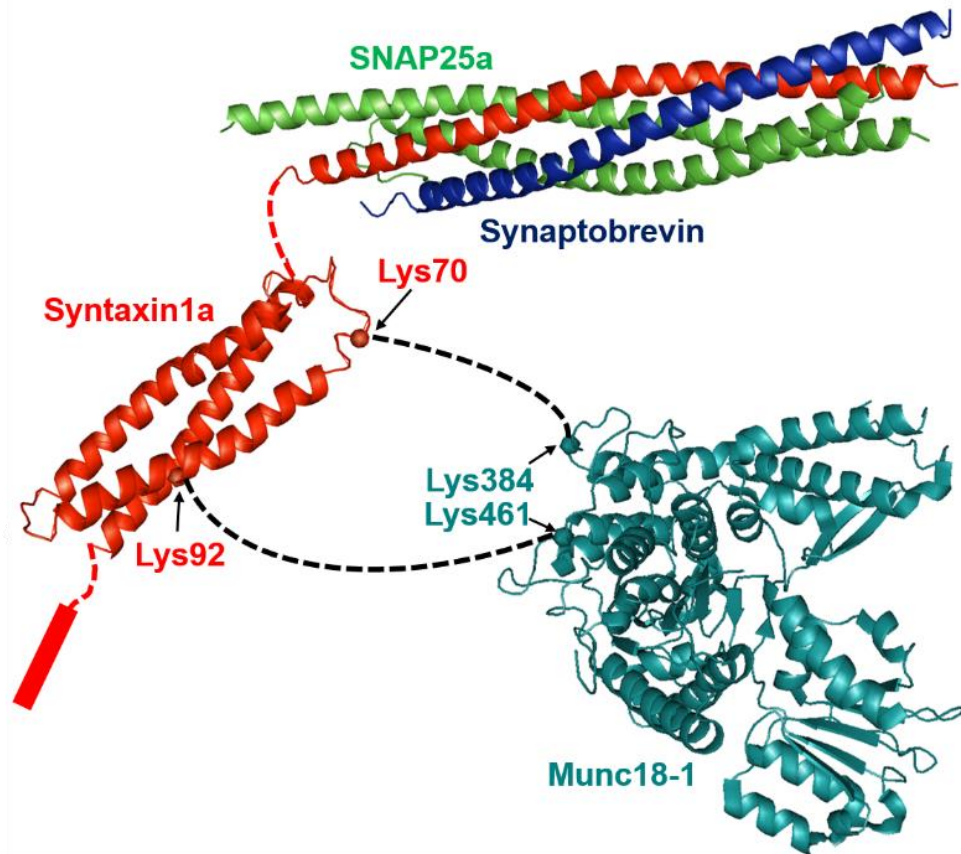


Figure 3.7-3. Inter-crosslinks between Munc18-1 and syntaxin1a after the addition of synaptobrevin to the syntaxin1a/SNAP25a/Munc18-1 complex.

Cross-links were obtained between lysine 70 and lysine 92 on the Habc-domain of syntaxin1a and lysine 384 and lysine 461 on Munc18-1, respectively. The cross-linked residues on Munc18-1 belong to its domain3b, which is spatially distal and distinct from the syntaxin-binding 'cleft' of Munc18-1. These observations support the notion that Munc18-1 remains tethered to the fully-assembled SNARE-complex via the N-terminus of syntaxin1a. [This experiment was performed in collaboration with Dr. Chung-Tien Lee].

For qualitative analysis, the retention volumes of the crosslinked syntaxin1a/SNAP25a/Munc18-1 complex with or without synaptobrevin addition was determined by size-exclusion chromatography using an analytical Superose column (GE Healthcare).

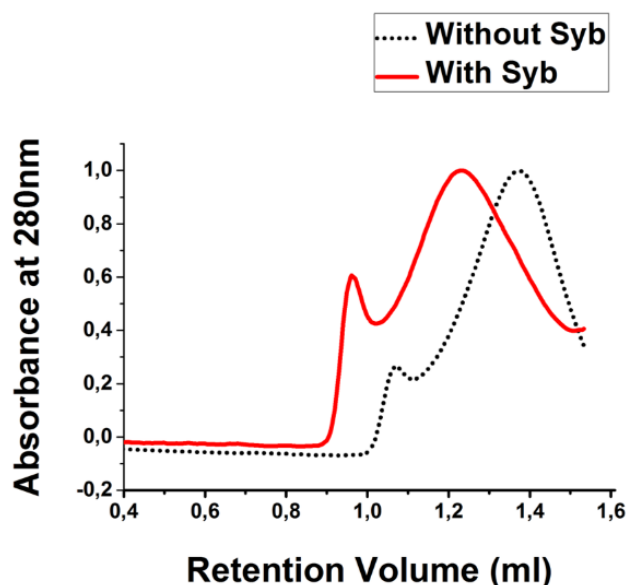


Figure 3.7-4. Synaptobrevin-binding to the syntaxin1a/SNAP25a/Munc18-1 complex leads to an increase in its molecular mass/hydrodynamic radius.

The crosslinked syntaxin1a/SNAP25a/Munc18-1 complex after synaptobrevin addition showed elution at a lower elution volume (*red curve*) as compared to the cross-linked complex without synaptobrevin addition (*black curve*).

As depicted in Figure 3.7-4, the crosslinked complex after synaptobrevin-addition eluted at a lower retention volume (*red curve*) as compared to the syntaxin1a/SNAP25a/Munc18-1 complex without synaptobrevin (*black curve*). The small shoulder observed in the purification profiles depicted above could have resulted because of the presence of some high-molecular weight complexes formed due to over cross-linking.

Results

The result from the analysis of the cross-linked complexes (with or without synaptobrevin addition) by size-exclusion chromatography corroborated the earlier finding on the increase of the hydrodynamic radius of the syntaxin1a/SNAP25a/Munc18-1 complex upon synaptobrevin addition, using non-crosslinked samples (see Figure 3.7-1 for comparison). These observations, together with the results of the co-floitation assay and the cross-linking experiments established that synaptobrevin-binding to the syntaxin1a/SNAP25a/Munc18-1 complex does not cause the dissociation of Munc18-1 from the SNARE-complex. Moreover, the obtained crosslinks established that Munc18-1 remains attached to the fully zippered SNARE-complex via its interaction with the N-terminus of syntaxin1a.

The next important question to be addressed was to check whether synaptobrevin-binding to the syntaxin1a/SNAP25a/Munc18-1 complex results in a fully-zippered SNARE-complex. I tried to address this question using different biochemical methods like SDS-PAGE, co-floitation assay, chemical crosslinking and fluorescence anisotropy.

As a simple step to determine SNARE-complex formation upon addition of synaptobrevin to the syntaxin1a/SNAP25a/Munc18-1 complex, I performed a gel-assay to check for the property of SDS-resistance, which is a gold-standard for assessing SNARE-complex formation (106). To this end, I purified the syntaxin1a/SNAP25a/Munc18-1 complex, and after its incubation with synaptobrevin, I analyzed the complex by SDS-PAGE (without prior boiling of the samples), followed by Coomassie Blue staining. As shown in Figure 3.7-5 A, multiple high-molecular weight, SDS-resistant bands were observed, indicating the formation of SNARE-complex upon synaptobrevin-binding to the syntaxin1a/SNAP25a/Munc18-1 complex.

As an alternative way to address the same question, I resorted to a classical co-floitation assay using a single cysteine mutant (C28) of the full cytoplasmic fragment of synaptobrevin, which had been fluorescently labeled with the reporter dye, Oregon Green. The fluorescently labeled synaptobrevin fragment was incubated with the syntaxin1a/SNAP25a/Munc18-1 complex and the resulting complex was incorporated into small unilamellar vesicles (SUVs). The proteoliposome preparation was then subjected to fractionation on a nycodenz density-gradient to separate the unbound/displaced proteins from the liposomes. Thereafter, samples from top to the bottom of the gradient were carefully collected and subjected to SDS-PAGE (without prior boiling of the samples), followed by fluorescence-scanning of the gels. As indicated in Figure 3.7-5 B, synaptobrevin was seen to be present in multiple high-molecular weight bands, indicative of SNARE-complex formation. The results from both these assays, were therefore consistent with the conclusion that synaptobrevin-binding to the syntaxin1a/SNAP25a/Munc18-1 complex results in SNARE-complex assembly.

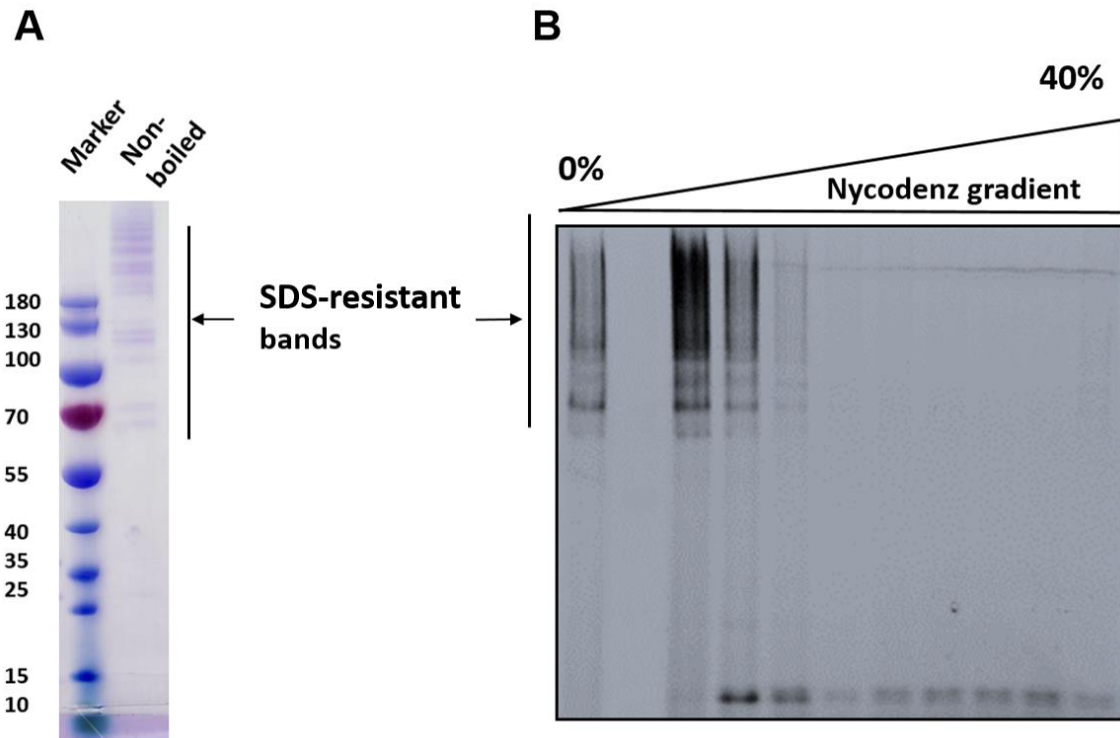


Figure 3.7-5. Assessment of SNARE-complex assembly by SDS-resistance assay.

(A) SDS-PAGE and Coomassie Blue staining of the syntaxin1a/SNAP25a/Munc18-1 complex after its incubation with synaptobrevin. SNARE-complex formation was indicated by the presence of multiple high-molecular weight, SDS-resistant bands. (B) Fluorescence scanning to assess SNARE-complex formation after the incorporation of a pre-incubated mixture of syntaxin1a/SNAP25a/Munc18-1 complex and synaptobrevin into liposomes. Detection of synaptobrevin-fluorescence in the high-molecular weight bands, in the liposomal fractions was indicative of SNARE-complex assembly. The second lane from the left is indicative of the marker lane, and hence shows no fluorescence.

In order to further verify this conclusion, I wanted to attain structural information on SNARE-complex assembly upon binding of synaptobrevin to the syntaxin1a/SNAP25a/Munc18-1, which was attained by the previously described cross-linking assay. Herein, I analyzed the crosslinks obtained between the SNARE-proteins after the addition of synaptobrevin to the syntaxin1a/SNAP25a/Munc18-1 complex. A representative view of the results obtained from the analysis of the

crosslinked peptides obtained by mass spectrometry (MS/MS) has been provided in Figure 3.7-6.

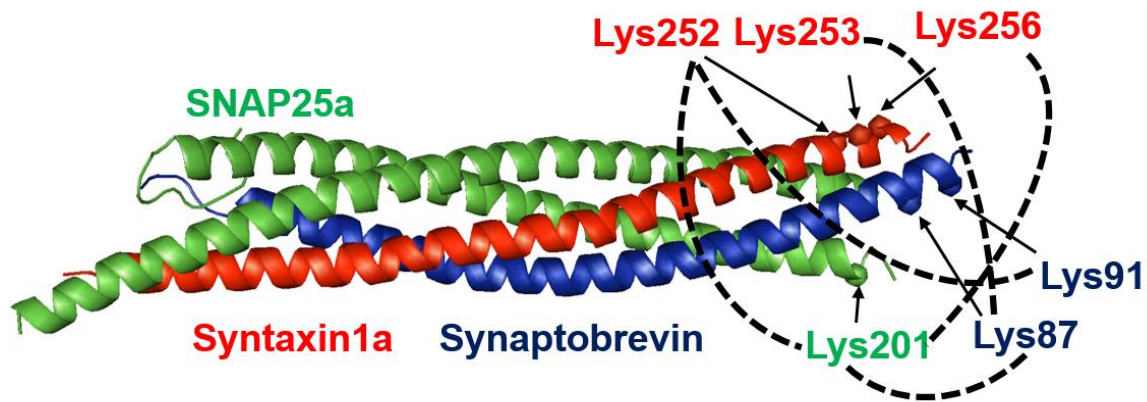


Figure 3.7-6. Synaptobrevin-binding to the syntaxin1a/SNAP25a/Munc18-1 complex leads to the formation of a fully-zipped SNARE-complex.

Inter-crosslinks obtained between the SNARE-proteins upon addition of synaptobrevin to the syntaxin1a/SNAP25a/Munc18-1 complex. The C-termini of all the three SNARE-proteins were found to be crosslinked to each other indicating the formation of a fully-zipped SNARE-complex. [This experiment was performed in collaboration with Dr. Chung-Tien Lee].

Inter-crosslinks were obtained between the C-termini of all the three SNARE-proteins namely syntaxin1a, SNAP25a and synaptobrevin. The amino-acid residues lysine 252 and lysine 253 on syntaxin1a were seen to be crosslinked with lysine 91 and lysine 87 on synaptobrevin, respectively.



Additionally, crosslinks were found between lysine 256 of syntaxin1a and lysine 201 of SNAP25a. Lysine 87 of synaptobrevin was also seen to be crosslinked with lysine 201 of SNAP25a. Since crosslinks could be obtained between the extreme C-termini of syntaxin1a, SNAP25a and synaptobrevin, it was safe to conclude that synaptobrevin-binding to the syntaxin1a/SNAP25a/Munc18-1 complex leads to the formation of a fully-zippered SNARE-complex.

As a final step towards validating SNARE-complex formation, I wanted to test whether NSF and α SNAP can disassemble the complex formed upon the addition of synaptobrevin to the syntaxin1a/SNAP25a/Munc18-1 complex. NSF is a AAA-ATPase and α SNAP is its co-factor, which together constitute the disassembly machinery for the SNARE-complex, to recycle the SNARE-proteins for subsequent rounds of fusion (5).

To this end, I applied a straightforward approach for monitoring the anisotropy of fluorescently-labeled synaptobrevin upon the addition of the syntaxin1a/SNAP25a/Munc18-1 complex and thereafter, upon the subsequent addition of NSF- α SNAP to the reaction mixture. As depicted in Figure 3.7-7, the addition of syntaxin1a/SNAP25a/Munc18-1 complex resulted in an increase in the anisotropy of synaptobrevin, indicating SNARE-complex formation. The subsequent addition of NSF- α SNAP to the reaction in the presence of ATP and magnesium resulted in a decrease in the anisotropy of synaptobrevin (*black curve*). This decrease in anisotropy was indicative of an increase in the rotational motion of synaptobrevin, which, in turn, could be explained by the disassembly of the previously assembled SNARE-complex by NSF- α SNAP. As a control reaction, the addition of NSF- α SNAP was performed in the absence of ATP and magnesium. In this case, no decrease in the anisotropy of synaptobrevin was observed (Figure 3.7-7, *red curve*), thereby highlighting that the decrease in the anisotropy of synaptobrevin observed in the previous case (*black curve*) was caused specifically by the action of NSF- α SNAP on the SNARE-complex.

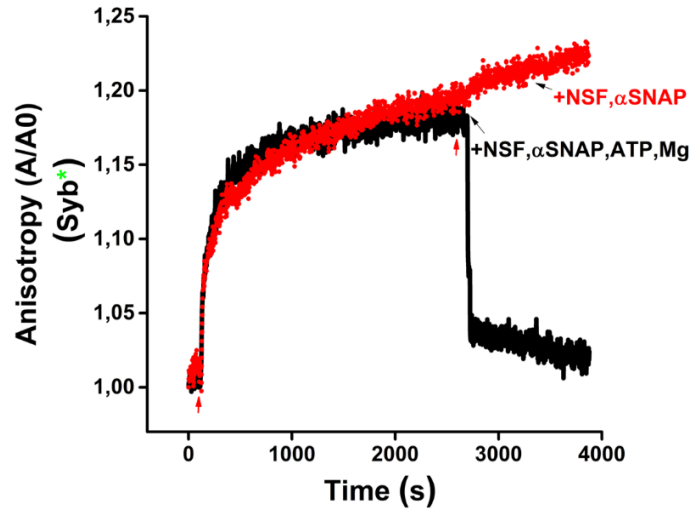


Figure 3.7-7. Fully assembled SNARE-complex can be disassembled by NSF- α SNAP.

The addition of the syntaxin1a/SNAP25a/Munc18-1 complex to fluorescently-labeled synaptobrevin resulted in an increase in the anisotropy of synaptobrevin (the initial phases of both *black curve* and the *red curve*). Subsequent addition of NSF- α SNAP (in the presence of ATP and magnesium) to the complex resulted in a decrease in the anisotropy, indicating subsequent disassembly of the previously formed SNARE-complex (after 2000s, *black curve*). No decrease in the anisotropy of synaptobrevin was observed when NSF- α SNAP was added in the absence of ATP and magnesium (*red curve*).



3.8 Full-length synaptobrevin is required for efficient binding to the syntaxin1a/SNAP25a/Munc18-1 complex.

Extensive efforts have been made in the past to track the details of the progression from the initial contact between the SNARE-proteins to a fully assembled SNARE-complex (85). SNARE-zippering has been hypothesized to proceed from the N-termini towards the C-termini of the SNARE-proteins (101). An understanding of this mechanism has been obtained by monitoring the binding behavior of truncated synaptobrevin fragments to the C-terminally stabilized Δ N-complex (101). Efficient synaptobrevin-binding could be observed to complexes containing syntaxin1a and SNAP25a that were stabilized by a short C-terminal synaptobrevin fragment (such as Syb 60-96, Syb 49-96 or Syb 42-96, whereas the binding was totally abolished when N-terminally longer fragments such as Syb 25-96 or Syb 39-96 were used (101). These observations implicated that the N-terminus of the acceptor complex is largely specific for synaptobrevin-binding (101).

On similar lines, I employed different N-terminal and C-terminal truncations of the cytoplasmic fragment of synaptobrevin to monitor their binding behavior to the syntaxin1a/SNAP25a/Munc18-1 complex. The synaptobrevin fragments for this study included single-cysteine mutants (C28) of two C-terminally truncated synaptobrevin fragments, Syb 1-65 and Syb1-52. A single-cysteine mutant (C79) of an N-terminally truncated fragment of synaptobrevin containing residues 49-96 was also used. All of the above mentioned fragments were fluorescently labeled with the dye Oregon Green.

As a first step, I tried to monitor the binding of the labeled synaptobrevin fragments to unlabeled syntaxin1a/SNAP25a/Munc18-1 complex by recording the fluorescence anisotropy of synaptobrevin. The results obtained from these experiments have been depicted in Figure 3.8-1. The experiments indicated that the full-length cytoplasmic fragment of synaptobrevin (Syb 1-96) binds efficiently to the syntaxin1a/SNAP25a/Munc18-1 complex (*red curve*). This reaction could be completely inhibited when an excess of unlabeled synaptobrevin was added to the reaction mixture (*black curve*), thereby indicating the SNARE-specificity of the reaction. A truncation of 31 amino-acid residues from the C-terminus of synaptobrevin (Syb 1-65), however, resulted in a much slower binding as compared to Syb 1-96 (*green curve*). Additionally, a deletion of the last 44 amino-acid residues from the C-terminus of synaptobrevin (Syb 1-52) resulted in an apparent loss of binding to the syntaxin1a/SNAP25a/Munc18-1 complex (*blue curve*). Similar to Syb 1-52, a truncation of the first 48 amino-acid residues of synaptobrevin (Syb 49-96) resulted in a complete loss of binding to the syntaxin1a/SNAP25a/Munc18-1 complex (*magenta curve*).

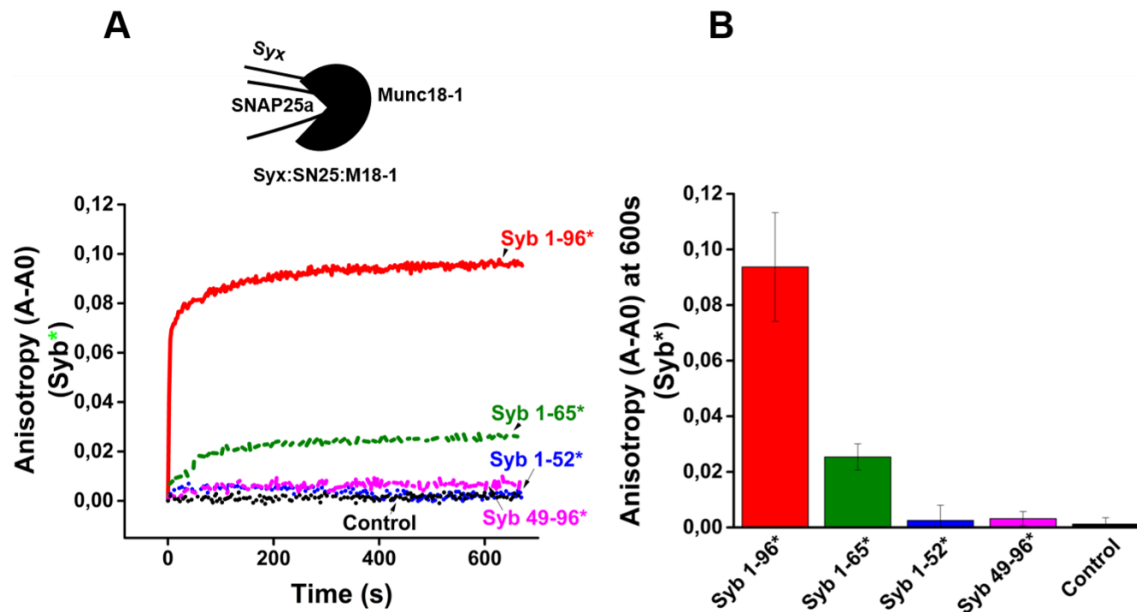


Figure 3.8-1. Fluorescence anisotropy measurements to monitor the binding of C-terminally and N-terminally truncated fragments of synaptobrevin to the syntaxin1a/SNAP25a/Munc18-1 complex.

(A) A full-length cytoplasmic fragment of synaptobrevin (Syb 1-96) binds very efficiently to the syntaxin1a/SNAP25a/Munc18-1 complex (*red curve*), in contrast to the C-terminally and N-terminally truncated fragments used for the assay. Syb 1-65 was able to bind to the syntaxin1a/SNAP25a/Munc18-1 complex *albeit* with much lower affinity (*green curve*) as compared to Syb 1-96. Syb 1-52 (*blue curve*) and Syb 49-96 (*magenta curve*) showed no apparent binding to the syntaxin1a/SNAP25a/Munc18-1 complex. The binding reaction with the full-length cytoplasmic fragment of synaptobrevin could be inhibited when an excess of unlabeled synaptobrevin was added to the reaction mixture (*black curve*). (B) Quantification of the anisotropy measurements performed at 600 seconds, from three independent experiments. Error bars indicate the range of values.

In order to validate the functionality of the synaptobrevin fragments used for the study, I used the same synaptobrevin fragments to check their binding to a previously established acceptor complex, the Δ N-complex (84). As shown in Figure 3.8-2, the pattern of binding of the synaptobrevin fragments to the Δ N-complex was slightly different from the syntaxin1a/SNAP25a/Munc18-1 complex, and was consistent with the earlier studies performed with the Δ N-complex (93). Unlike the syntaxin1a/SNAP25a/Munc18-1 complex, both the C-terminally truncated synaptobrevin fragments (Syb 1-65 and Syb 1-52) showed binding to the Δ N-complex. The efficiency of binding was, however, different for each of these fragments. The full-

length synaptobrevin fragment showed the most efficient binding to the Δ N-complex (Figure 3.8-2 A, *red curve*). A truncation of 31 amino-acid residues from the C-terminus (Syb 1-65) showed a slower binding to the complex (*green curve*). A truncation of 44 residues from the C-terminus (Syb1-52) further reduced the binding affinity (*blue curve*). This decrease in the binding behavior is observed due to the decreased ability of the smaller synaptobrevin-fragments in displacing the downstream Syb 49-96 in the Δ N-complex (93). The N-terminally truncated fragment Syb 49-96, as expected, showed no binding to the Δ N-complex (*magenta curve*).

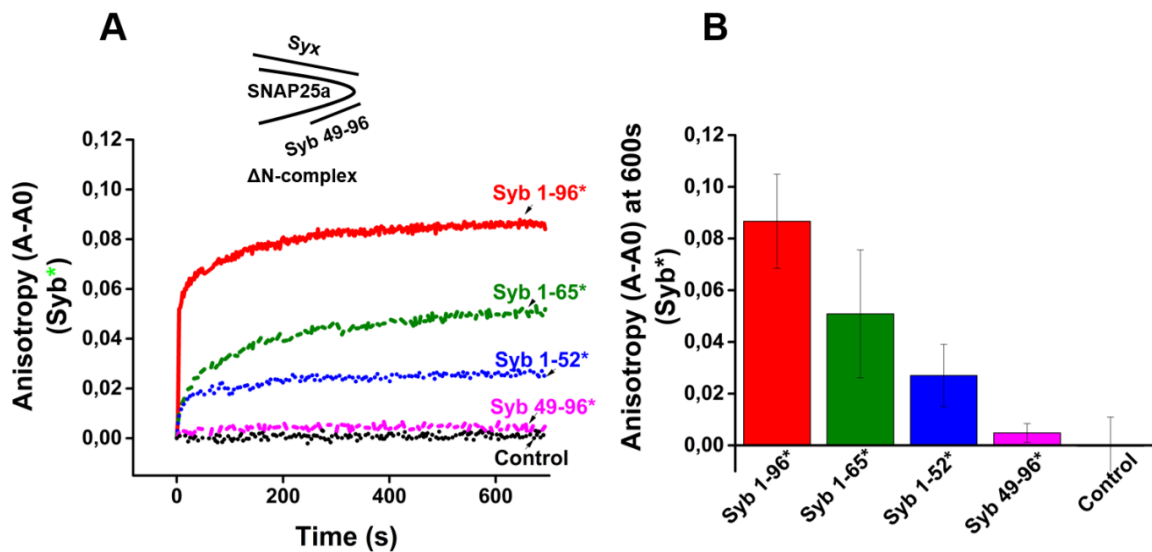


Figure 3.8-2. Binding of fluorescently-labeled synaptobrevin fragments to the C-terminally stabilized Δ N-complex.

(A) Fluorescence anisotropy measurements for the binding of the different synaptobrevin fragments to the Δ N-complex. All the C-terminally truncated synaptobrevin fragments showed binding to the Δ N-complex. The binding of the C-terminally truncated fragments, Syb 1-65 (*green curve*) and Syb 1-52 (*blue curve*), however, proceeded at a slower time-scale as compared to the full cytoplasmic fragment of synaptobrevin (*red curve*). The binding reaction with the full cytoplasmic fragment of synaptobrevin could be inhibited when an excess of unlabeled synaptobrevin was added to the reaction mixture (*black curve*). (B) Quantification of the fluorescence anisotropy using the different synaptobrevin fragments, obtained from three independent experiments. Quantifications were performed at 600 seconds after addition of the acceptor complex. Error bars indicate the range of values.

A comparison of the binding behavior of the synaptobrevin fragments to the Δ N-complex and the syntaxin1a/SNAP25a/Munc18-1 complex indicated a difference in the binding behavior of Syb 1-52. This fragment was able to bind to the Δ N-complex, but exhibited no binding to the syntaxin1a/SNAP25a/Munc18-1, as indicated by fluorescence anisotropy. It therefore became apparent to conclude that although both of the above-mentioned acceptor complexes serve as versatile templates for binding to the full-length cytoplasmic fragment of synaptobrevin, the precise mechanistic details underlying the transition of these complexes to a fully assembled SNARE-complex might be different.

Again, since the anisotropy measurements only give us an idea about the rotational flexibility of a molecule, I tried to validate these results with an alternative approach. I used FRET-measurements to monitor SNARE-zippering between the above-mentioned synaptobrevin fragments and the acceptor complexes, i.e., the syntaxin1a/SNAP25a/Munc18-1 complex or the Δ N-complex. In order to perform FRET measurements, fluorescently-labeled acceptor complexes were purified. The fluorescent label on the acceptor complexes was obtained by using a single-cysteine mutant of SNAP25a (C130), which had been labeled with the fluorophore, Texas Red. This fluorescent version of SNAP25a was used for the assembly and purification of the syntaxin1a/SNAP25a/Munc18-1 complex and the Δ N-complex. FRET between SNAP25a and synaptobrevin was used as a read-out to monitor SNARE-zippering and subsequent SNARE-complex assembly. The quenching of the donor emission upon the addition of acceptor complexes was used as an indicator of FRET. The results of the FRET experiments performed with the syntaxin1a/SNAP25a/Munc18-1 are shown in Figure 3.8-3.

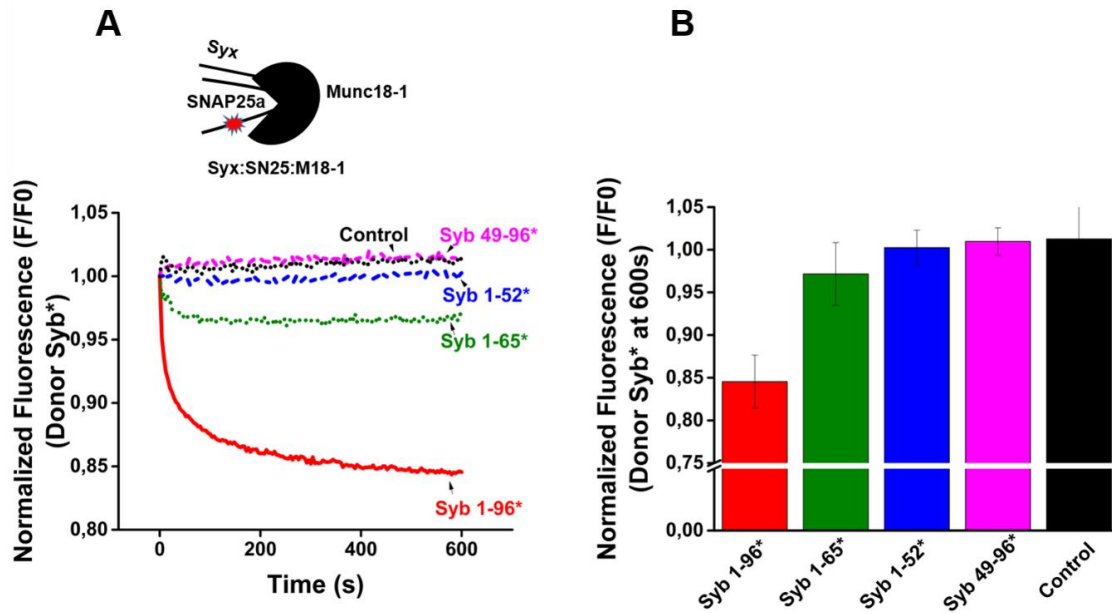


Figure 3.8-3. FRET measurements between the different synaptobrevin fragments and the syntaxin1a/SNAP25a/Munc18-1 complex.

(A) The addition of the acceptor complex to Syb 1-96 showed efficient binding (*red curve*), indicated by a fast quenching of the donor emission. The C-terminally truncated Syb 1-65 (*green curve*) showed binding, *albeit* at a much slower rate as compared to Syb 1-96. Syb1-52 (*blue curve*) and Syb 49-96 (*magenta curve*) showed no binding to the syntaxin1a/SNAP25a/Munc18-1 complex. The reaction with Syb1-96 could be completely inhibited with an excess of unlabeled synaptobrevin (*black dotted curve*). (B) Quantifications of three independent FRET experiments described in (A). Quantifications were performed at 600 seconds after the addition of the acceptor complex. Error bars indicate the range of values.

As shown in Figure 3.8-3 A, the addition of fluorescently-labeled syntaxin1a/SNAP25a/Munc18-1 complex to the full-length cytoplasmic fragment of synaptobrevin resulted in a fast decrease in the donor emission (*red curve*). No decrease in the donor emission was observed when the syntaxin1a/SNAP25a/Munc18-1 complex was added in the presence of a large excess of unlabeled synaptobrevin (*black curve*). This indicated that the decrease in donor emission observed previously was exclusively due to SNARE-specificity of the reaction. In comparison to this, the C-terminally truncated fragment, Syb 1-65 (*green curve*)

resulted in a much slower decrease in the donor emission upon the addition of the syntaxin1a/SNAP25a/Munc18-1 complex. Additionally, quenching of the donor emission could not be observed when either Syb1-52 (*blue curve*) or the N-terminally truncated fragment Syb 49-96 (*magenta curve*) were mixed with the syntaxin1a/SNAP25a/Munc18-1 complex. The results of the FRET experiments were much in line with the anisotropy experiments, largely indicating that a full-length synaptobrevin fragment is required for efficient binding to the syntaxin1a/SNAP25a/Munc18-1 complex. As a step to validate the FRET-measurements, I used the same fragments to monitor SNARE-zippering with the fluorescently-labeled Δ N-complex.

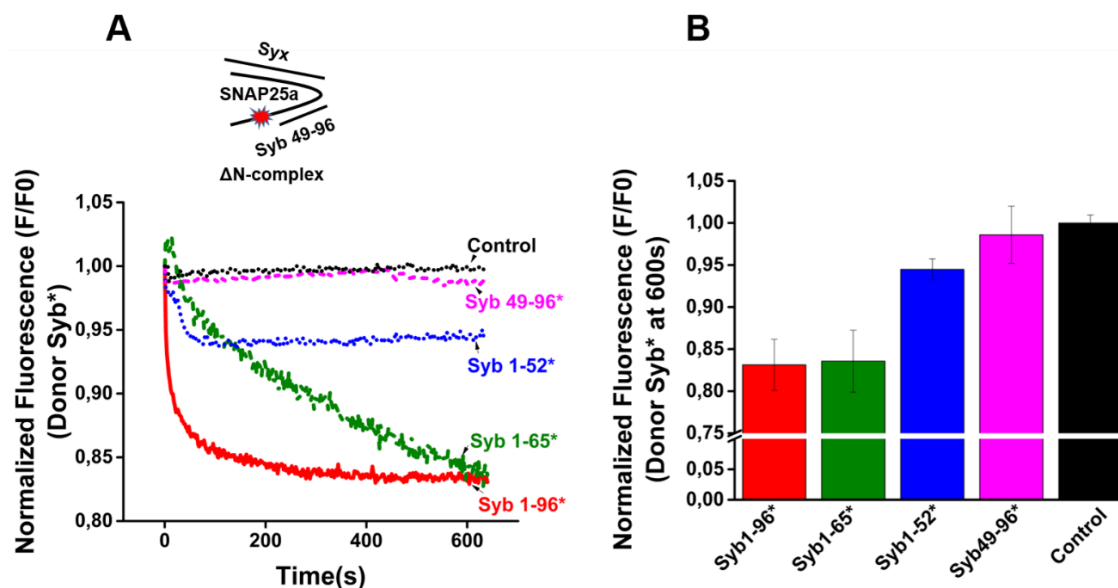


Figure 3.8-4. Binding of different synaptobrevin-fragments to the fluorescently labeled Δ N-complex, measured by FRET.

(A) Addition of Δ N-complex to Syb1-96 was marked by a fast quenching of the donor emission (*red curve*), as compared to the C-terminally truncated Syb 1-65 (*green curve*), which reached the same final state but at a much slower rate. Syb 1-52 (*blue curve*) showed a marked decrease in donor quenching upon addition of the Δ N-complex. No change in the donor emission was observed upon the addition of the complex to Syb 49-96 (*magenta curve*). The reaction with Syb 1-96 showed a complete inhibition when an excess of unlabeled synaptobrevin was added to the reaction mixture (*black curve*). (B) Quantifications of FRET measurements at 600 seconds after the addition of the acceptor complex. Error bars indicate the range of values from three independent experiments.



FRET-measurements indicated that the most efficient binding to the Δ N-complex could be observed when a full-length cytoplasmic fragment of synaptobrevin was used (Figure 3.8-4 A, *red curve*). The C-terminally truncated fragments, Syb 1-65 (*green curve*) and Syb 1-52 (*blue curve*) also showed binding to the Δ N-complex, however, at a much slower rate as compared to the full-length cytoplasmic fragment. Syb 49-96 showed no apparent FRET with the Δ N-complex (*magenta curve*), since this fragment is already present in the Δ N-complex.

The results obtained from the experiments performed in this section clearly indicated that a full-length cytoplasmic fragment of synaptobrevin is required to facilitate efficient binding to the syntaxin1a/SNAP25a/Munc18-1 complex. In addition to this, a progressive truncation of amino-acids from the C-terminus of synaptobrevin was seen to adversely affect the binding efficiency of synaptobrevin to this complex. A truncation from the N-terminus also seemed to lower the apparent binding affinity of synaptobrevin to the syntaxin1a/SNAP25a/Munc18-1 complex. These results provided very interesting insights into the mechanistic details of SNARE-complex assembly, starting with syntaxin1a/SNAP25a/Munc18-1 complex. The implications of these findings have been discussed in broad details in section 4.

3.9 Is the syntaxin1a/SNAP25a/Munc18-1 complex resistant to disassembly by NSF and α SNAP?

After having established the architecture and the biochemical behavior of the syntaxin1a/SNAP25a/Munc18-1 complex, I wanted to check whether the association of Munc18-1 with syntaxin1a and SNAP25a can protect the ternary syntaxin1a/SNAP25a/Munc18-1 complex against disassembly by NSF- α SNAP. To answer this question, I again resorted to a FRET-based approach, wherein, I labeled a single - cysteine mutant of SNAP25a (1-206, C130) and a single-cysteine mutant of full-length syntaxin1a (1-288, C197) with the fluorescent dyes Texas Red and Oregon Green, respectively. These fluorescently-labeled proteins were used to purify a double-labeled syntaxin1a (C197-Oregon Green):SNAP25a (C130-Texas Red):Munc18-1 complex.

This complex was then used as a tool to study the effect of the SNARE-disassembly machinery (NSF and α SNAP) in the given system. The changes in the donor emission observed upon addition of NSF- α SNAP to this complex was used as a read-out to study the effect of these proteins on the syntaxin1a/SNAP25a/Munc18-1 complex. The results from these experiments have been depicted in Figure 3.9-1.

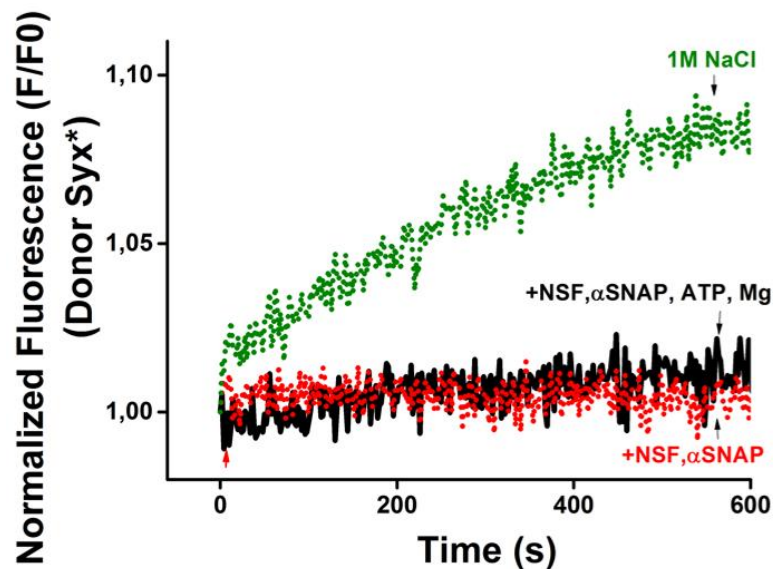


Figure 3.9-1. Effect of NSF- α SNAP on the syntaxin1a/SNAP25a/Munc18-1 complex.

No increase in the donor emission was observed when NSF- α SNAP was added to the syntaxin1a/SNAP25a/Munc18-1 complex in the absence of ATP and magnesium (*red curve*). Incorporation of ATP and magnesium to the reaction mixture also did not result in any changes in the donor emission (*black curve*). A slow increase in the donor emission was, however, observed when a highly concentrated salt solution (1M NaCl) was added to the reaction mixture (*green curve*).

The results from the above experiments gave a very interesting insight into the property of the syntaxin1a/SNAP25a/Munc18-1 complex as an acceptor complex. The unchanged donor emission upon the addition of NSF- α SNAP (in the presence of ATP and magnesium) to the syntaxin1a/SNAP25a/Munc18-1 complex (Figure 3.9-1 A, *black curve*) was a clear indication of the resistance of the syntaxin1a/SNAP25a/Munc18-1 complex to disassembly by NSF- α SNAP.

However, in order to further establish the validity of the experimental system discussed above, I used the fluorescently-labeled syntaxin1a (C197-Oregon Green) and SNAP25a (C130-Texas Red) proteins to assemble and purify a double-labeled syntaxin1a/SNAP25a (2:1) complex. The effect of NSF- α SNAP on this double-labeled acceptor complex was also monitored by measuring the dequenching of the donor emission. As shown in Figure 3.9-2 (*black curve*), a sharp increase in the donor emission was observed when NSF- α SNAP was added to the syntaxin1a/SNAP25a (2:1) complex in the presence of ATP and magnesium. As a negative control, the reaction was performed in the absence of ATP and magnesium. No increase in the donor emission was recorded in this case (Figure 3.9-2, *red curve*), indicating that the effect was exclusive to the effect of NSF- α SNAP on the complex. These experiments led to the conclusion that NSF- α SNAP can efficiently disassemble the syntaxin1a/SNAP25a (2:1) complex but not the ternary syntaxin1a/SNAP25a/Munc18-1 complex.

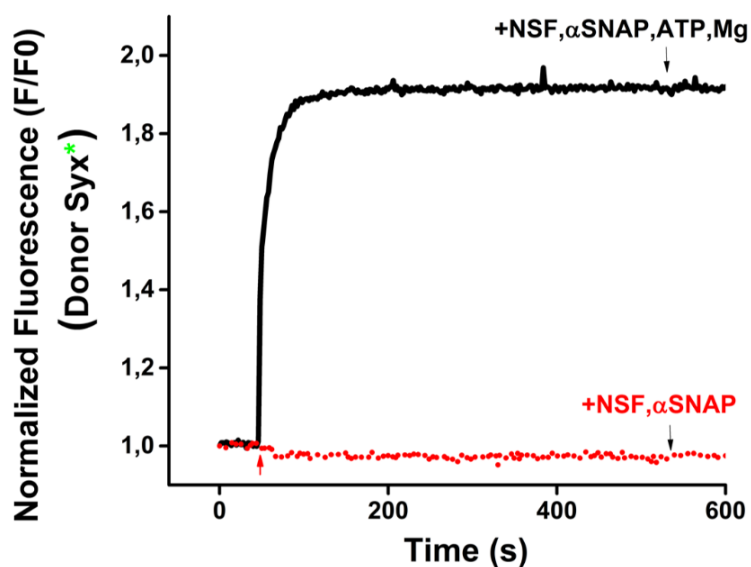


Figure 3.9-2. NSF- α SNAP can disassemble the syntaxin1a/SNAP25a (2:1) complex.

Addition of NSF- α SNAP to the syntaxin1a/SNAP25a complex, in the presence of ATP and magnesium resulted in a very fast increase in the donor emission (*black curve*). This increase could be completely blocked when the addition of NSF- α SNAP was performed in the absence of ATP and magnesium (*red curve*).

To gain additional support for the resistance of the syntaxin1a/SNAP25a/Munc18-1 complex to NSF- α SNAP, I tried to study the reaction using an alternative approach. The syntaxin1a/SNAP25a/Munc18-1 complex was incorporated on small unilamellar vesicles (SUVs) and the proteoliposomes were incubated with NSF- α SNAP in the presence of ATP and magnesium.

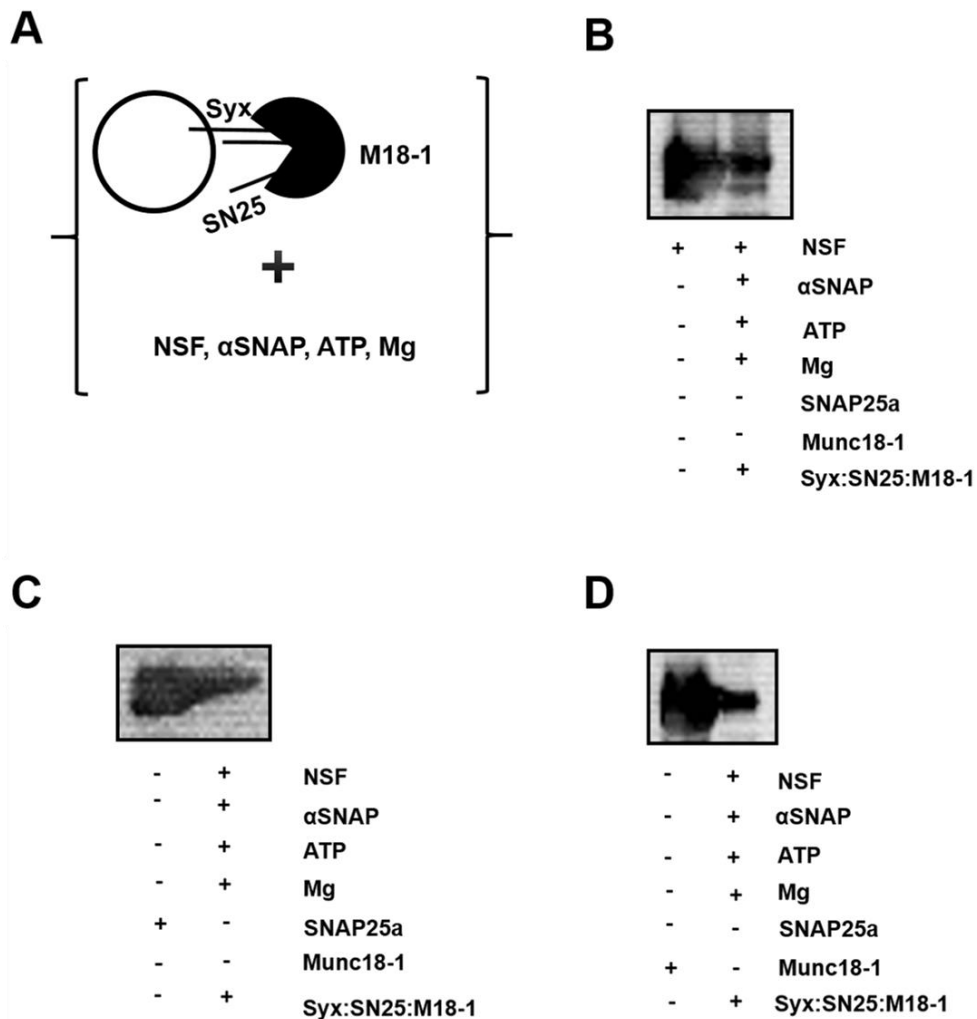


Figure 3.9-3. NSF- α SNAP does not disassemble the syntaxin1a/SNAP25a/Munc18-1 complex.

(A) Incubation of SUVs containing the syntaxin1a/SNAP25a/Munc18-1 complex with NSF, α SNAP, ATP and magnesium. Subsequent co-floitation analysis and western blotting showed the presence of (B) NSF, (C) SNAP25a and (D) Munc18-1 on the top liposomal fractions. The left lane in each blot indicates purified monomeric proteins and the right lanes indicate the liposomal fractions containing the syntaxin1a/SNAP25a/Munc18-1 complex after incubation with NSF- α SNAP.



The proteoliposomes were separated from the unbound/displaced proteins by co-floitation analysis and the top liposomal fractions were analyzed by SDS-PAGE, followed by western blotting against NSF, Munc18-1 and SNAP25a. As a positive control for western blotting, purified monomeric proteins were added alongside each liposomal fraction being analyzed.

As clearly shown in Figure 3.9-3, all the three tested proteins, namely NSF, Munc18-1 and SNAP25a were seen to be present in the liposomal fractions. The presence of NSF in the liposomal fraction implicated that NSF is able to bind to the membrane-incorporated syntaxin1a/SNAP25a/Munc18-1 complex but is unable to disassemble this complex, as indicated by the presence of both Munc18-1 and SNAP25a in the liposomal fractions. These observations corroborated the results from the FRET experiment, thereby validating the resistance of the syntaxin1a/SNAP25a/Munc18-1 complex to disassembly by NSF- α SNAP.

At this point, it however, becomes worthwhile to mention that the incorporation of protein/protein complexes into liposomes can result in the formation of liposomes with proteins being oriented either in a '*right-side out*' or an '*inside-out*' orientation. In order to properly interpret the results of the co-floitation assay discussed above, it became important to assess the orientation of the syntaxin1a/SNAP25a/Munc18-1 complex after their incorporation into liposomes. Therefore, in order to exclude any ambiguities pertaining to the resistance of the syntaxin1a/SNAP25a/Munc18-1 complex to NSF- α SNAP, I performed a concluding experiment using the limited proteolysis assay described in section 2.17. In this assay, the proteolysis of membrane-incorporated syntaxin1a/SNAP25a/Munc18-1 complex by the protease, trypsin was monitored in the presence or absence of a detergent (*TritonX-100*). After the proteolysis reaction, the liposomes were analyzed by SDS-PAGE, followed by western blotting against Munc18-1. As shown in Figure 3.9-4, Munc18-1 was only seen to be present on the liposomal fraction when both trypsin and TritonX-100 were missing from the reaction mixture (*lane 1 from the left*). However, when either trypsin alone or in combination with the detergent was present in the reaction mixture, Munc18-1 was seen to be absent from the liposomes (*lanes 2 and 3 from the left*). These observations indicated complete proteolysis of Munc18-1 both in the absence and presence of the detergent. The complete cleavage of Munc18-1 in the absence of detergent indicated that the entire population of Munc18-1 was accessible to the protease, without being protected by the liposomal membrane. These observations established that the syntaxin1a/SNAP25a/Munc18-1 complex gets incorporated with an almost 100% '*right-side out*' orientation on the liposomes.

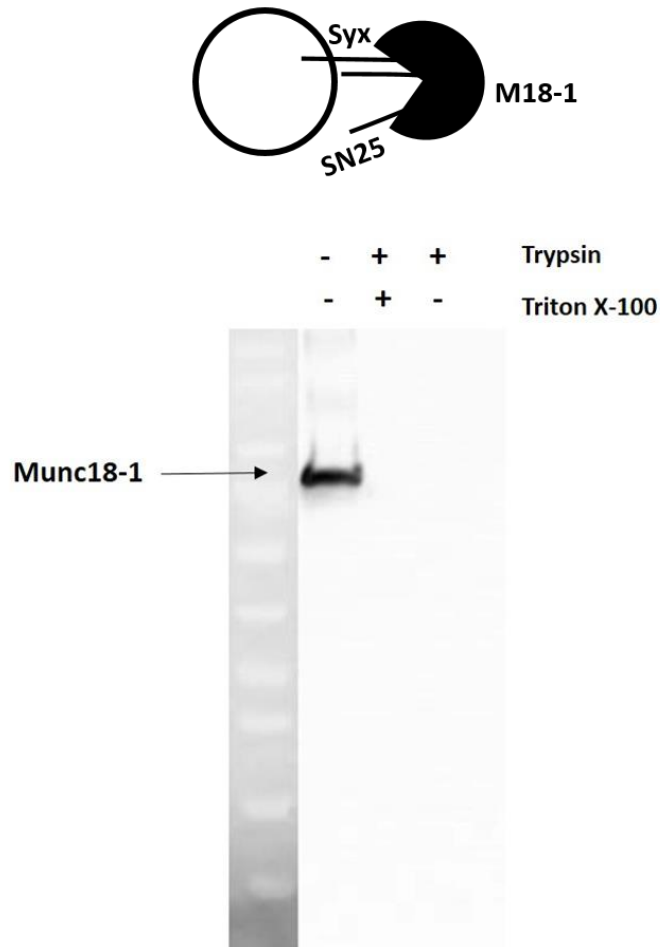


Figure 3.9-4. Determination of the orientation of the syntaxin1a/SNAP25a/Munc18-1 complex after its incorporation into liposomes.

The presence of Munc18-1 on the liposomes only in the absence of both trypsin and TritonX-100 was indicative of ~100% 'right-side-out' orientation of the syntaxin1a/SNAP25a/Munc18-1 complex after their incorporation into liposomes.

The overall experiments performed in this section established the syntaxin1a/SNAP25a/Munc18-1 complex as an acceptor complex that is resistant to disassembly by NSF- α SNAP.



4 Discussion

In this work, I have thoroughly characterized a novel complex containing syntaxin1a (1-288), SNAP25a and Munc18-1 and established it as an efficient acceptor complex for synaptobrevin-binding, using several biochemical and biophysical techniques. The use of all full-length proteins provide tremendous strength to the study, giving it a '*near-native*' scenario for the behaviors of the proteins being discussed.

In addition to understanding the functional importance of this complex, I also attained its structural overview using chemical crosslinking assays. And, finally, by testing the resistance of this complex to disassembly by NSF- α SNAP, I could establish that the syntaxin1a/SNAP25a/Munc18-1 complex can allow SNARE-assembly to proceed in an NSF- α SNAP-resistant manner.

4.1 Structural precision fine-tunes protein-protein interactions.

SNARE-complex assembly proceeds through distinct stages involving a series of intermediates. The SM-protein, Munc18-1 has been implicated to have a crucial role in synaptic vesicle exocytosis, with its involvement being crucial at multiple steps of the process. It has, till date, been difficult to understand whether Munc18-1 functions to support SNAREs or whether it itself, constitutes an integral part of the SNARE-engine (121).

Despite extensive research performed with Munc18-1 in the past few decades, a clear view on its mechanism of action remains vague. The body of evidence for the involvement of Munc18-1 at the early stages (docking, priming) of neuronal exocytosis, however, appear to outweigh the evidence supporting its role at later stages of the pathway (fusion). The work done in this thesis has provided a deeper insight into the mechanistic details of the interaction of Munc18-1 with the Q-SNAREs, and has implicated a physiological role of Munc18-1 in priming the synaptic vesicles to the neuronal plasma membrane.

It has been established for a very long time that syntaxin1a and Munc18-1 exhibit very high affinity for one another (39), and enter into a tight syntaxin1a/Munc18-1 complex (39, 73), where syntaxin1a is incompatible for SNARE-complex assembly (122). This tight interaction between syntaxin1a and Munc18-1 has been shown to exist in the intracellular compartments to prevent futile interactions with other SNAREs during the transport of syntaxin1a from the endoplasmic reticulum to the plasma membrane (40).

The tight binding of syntaxin1a to Munc18-1 can be abolished by mutating two residues (L165A, E166A) lying in the linker region of syntaxin1a, that connects its Habc-domain to its SNARE-motif (122). These two mutations have been proposed to cause a conformational switch in syntaxin1a from its '*closed*' to '*open*' conformation,

consequently causing a loss in its binary interaction with Munc18-1 (122). Consistent with the conformational switch, the LE-mutant of syntaxin1a also partially bypasses the need for Munc13-1 for synaptic vesicle priming in *C.elegans* (123).

The transition of syntaxin1a from its 'closed' to 'open' conformation has also been seen to result from a deletion of the Habc-domain of syntaxin1a (124). A deletion of the Habc-domain is, however, accompanied by a decrease in the intracellular levels of Munc18-1 (unlike the LE- mutation), indicating the importance of this interaction in maintaining the stability of Munc18-1 (124). Interestingly, even though the Habc-domain deletion and the LE-mutation had similar effects on syntaxin1a conformation, they were seen to produce contrary effects on synaptic vesicle fusion in intact cells. Experiments performed *in-vivo* indicated that the L165A, E166A mutation increases the levels of synaptic vesicle fusion, but a deletion of the Habc-domain of syntaxin1a results in decreased levels of synaptic vesicle exocytosis (124), thereby attributing additional functions to the Habc-domain in the process of SNARE-mediated neurotransmitter release.

Likewise, a double knock-out of Munc18-1 in mice was seen to cause a tremendous reduction in the intracellular levels of syntaxin1a (83). The interaction between syntaxin1a and Munc18-1, thus appears to be important for the stability of both syntaxin1a and Munc18-1 and also, for maintaining the readily releasable pool for synaptic vesicle exocytosis. The tight association between these two proteins has, however, been proposed to undergo changes upon reaching the plasma membrane (115, 123, 126) making the syntaxin1a in the syntaxin1a/Munc18-1 complex available for SNARE-complex assembly. Although considerable progress has been made in understanding the role of Munc18-1 in the process of synaptic vesicle exocytosis, the field remains surrounded by conflicting views on the precise function of this protein. (39, 75, 80). A closer look at the experimental systems used in the different reports can, however, provide a reasonable explanation for the observed discrepancies.

At this point, it needs to be highlighted that during the characterization of the interaction between syntaxin1a and Munc18-1, a cytoplasmic fragment of syntaxin1a, lacking its transmembrane domain (Syx 1-262) had been used. Although the cytoplasmic fragment of syntaxin1a provides the ease of handling for *in-vitro* studies, it depicts a deviation from the *in-vivo* situation, where the SNARE-motif of syntaxin1a is connected to the transmembrane domain by a linker region. The transmembrane segment of syntaxin1a has been shown to modulate its interactions with the partner proteins (114). The presence of the transmembrane segment of syntaxin1a has been implicated in lowering its affinity for Munc18-1 and SNAP25a and, to increase its interaction with synaptotagmin and synaptobrevin (114). Additionally, reconstitution studies have shown that syntaxin1a/Munc18-1 complexes with syntaxin1a lacking its transmembrane domain are unable to facilitate SNARE-complex assembly (127), whereas syntaxin1a/Munc18-1 complexes with syntaxin1a containing its transmembrane domain can interact with SNAP25a and synaptobrevin to form SNARE-complexes (113). These observations clearly highlighted the importance of the C-



terminal transmembrane segment of syntaxin1a in mediating protein-protein interactions.

Similar observations have been made for the syntaxin3/Munc18-2 and syntaxin4/Munc18-3 interactions. Munc18-2 has been reported to bind to a preassembled SNARE-complex consisting of syntaxin3, SNAP23 and VAMP8, only when syntaxin3 C-terminus was immobilized on affinity beads (128). Similarly, a binary complex of syntaxin4/Munc18-3 could be driven into SNARE-complex assembly only when syntaxin4 was immobilized into affinity beads via its C-terminus (77).

Another important feature of syntaxin1a that has been reported to have a key effect on its interaction with Munc18-1, is the N-peptide. The N-peptide of syntaxin1a has been speculated to regulate the gating of syntaxin1a/Munc18-1 complexes into functional SNARE-complexes. The presence of the N-peptide of syntaxin1a in the syntaxin1a/Munc18-1 complex has an inhibitory effect on *in-vitro* SNARE-complex assembly, with its truncation causing a complete relief of the inhibition (39). This observation was, however, contradictory to another study performed with the cytoplasmic variant of the core-SNARE complex and Munc18-1, which suggested that Munc18-1 can interact with a fully assembled SNARE-complex, with a continued association between the N-peptide and Munc18-1 throughout the assembly process (88).

The physiological importance of the interaction between the N-peptide and Munc18-1 is, however, debatable. Mutations of Munc18-1 (L130K and F115E) designed to impair binding to the N-peptide, tend to disrupt the binding of Munc18-1 to the neuronal SNARE-complex *in-vitro*, but support normal docking, priming and fusion *in-vivo* (41). The synaptic plasticity in these mutants also remains unaltered (27).

Reconciling the role of N-peptide from different studies (41, 42, 80, 124), it has been collectively proposed that the N-peptide might disengage from Munc18-1 in the syntaxin1a/Munc18-1 complex and rebind Munc18-1 after the association of syntaxin1a with SNAP25a (39). The continued association of Munc18-1 with the SNAREs, however, appears to be dispensable after SNARE-complex assembly. A pictorial representation of this hypothesis has been provided in Figure 4.1-1.

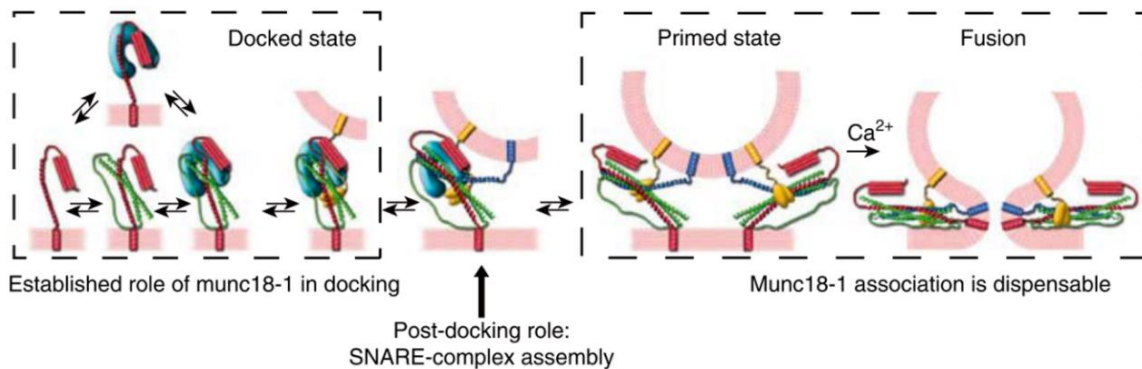


Figure 4.1-1. The association between syntaxin1a and Munc18-1 is indispensable for synaptic vesicle docking and priming, but becomes dispensable at a later stage in synaptic vesicle exocytosis.

Left panel. The association of Munc18-1 (shown in cyan) with syntaxin1a (shown in red) in its 'closed' conformation is considered as an important regulatory step to prevent the syntaxin1a from assembling into large multimers on the neuronal plasma membrane. The conformation of syntaxin1a in the syntaxin1a/Munc18-1 complex then changes (by yet unclear mechanisms) to mediate interaction with SNAP25a (shown in green), resulting in the formation of a syntaxin1a/SNAP25a/Munc18-1 complex. This complex can then act as an acceptor for the initial binding of synaptotagmin (shown in yellow), causing vesicle docking. The binding of synaptobrevin (shown in blue) to this complex then results in the formation of a partially zippered SNARE-complex, causing vesicle priming. *Right panel.* The continued association of Munc18-1 with syntaxin1a or the partially assembled trans-SNARE complex, however, appears to be dispensable for synaptic vesicle exocytosis. [Adapted from (41)].

The syntaxin1a used for the assembly of the syntaxin1a/SNAP25a/Munc18-1 complex characterized in this study, contained both N-peptide and the C-terminal transmembrane domain thereby, ruling out any artifacts in protein-protein interactions arising from the use of truncated proteins.



Moreover, it becomes compelling to state that, although a ternary association between syntaxin1a, SNAP25a and Munc18-1 had been proposed almost a decade ago (126), a complex containing these three proteins could not be characterized till date, probably due to a lack of using full-length syntaxin1a. Identifying the importance of these domains and incorporating it in the experimental system has, however, helped me in achieving this long-sought goal.

The most direct support for the existence of this complex in intact neuronal cells has been obtained by studies of the neuronal plasma membrane using ultra-high resolution microscopy, which indicate micro-domains containing syntaxin1a, SNAP25a and Munc18-1 (46). Additionally, assemblies of the syntaxin1a/Munc18-1 complexes on plasma membrane sheets from PC12-cells had earlier been shown to be driven into SNARE-complex assembly upon addition of synaptobrevin (126). A pre-association of SNAP25a with the syntaxin1a/Munc18-1 complex in these studies could, however, not be deduced. A recent study using electron paramagnetic resonance has reported that the association of Munc18-1 with the syntaxin1a/SNAP25a complex can result in the formation of a complex containing syntaxin1a, SNAP25a, Munc18-1 in a 1:1:1 stoichiometry, which in turn, can act as an acceptor complex for SNARE-mediated neuronal exocytosis (79).

The functional characterization of the syntaxin1a/SNAP25a/Munc18-1 complex in this thesis has established this complex as an efficient acceptor for synaptobrevin-binding (see Figure 3.4-2), with kinetics similar to the C-terminally stabilized Δ N-complex (101). This finding has been an important step forward in understanding the positive role of Munc18-1 in synaptic vesicle exocytosis.

Moreover, using mass spectrometry (MS/MS), I could establish the structural details underlying the functional efficiency of the syntaxin1a/SNAP25a/Munc18-1 complex (see Figure 3.6-2). The close association between SNAP25a and Munc18-1 in this ternary complex is indicative of an N-terminal association of Munc18-1 with syntaxin1a, making the SNARE-motif of syntaxin1a, available for interaction with its partner SNARE, SNAP25a. It is conceivable that in this complex, syntaxin1a exists in a partially 'open' conformation, which allows it to enter into a loose association with SNAP25a, while still maintaining a binding site for Munc18-1 (with *albeit* much lower affinity as compared to the binary syntaxin1a/Munc18-1 interaction). The syntaxin1a in the syntaxin1a/SNAP25a/Munc18-1 complex can be speculated to be only partially open, because Munc18-1 does not bind to a constitutively 'open' mutant of syntaxin1a (126). This explains how Munc18-1 could interact with the Q-SNAREs to form an intermediate that sets the stage for SNARE-complex assembly.

The versatility of the syntaxin1a/SNAP25a/Munc18-1 complex for synaptobrevin-binding can be attributed to two possible roles of Munc18-1 in this complex. First, the association of Munc18-1 with syntaxin1a/SNAP25a could prevent the formation of the "off-pathway" 2:1 syntaxin1a/SNAP25a complex (89). Alternatively, Munc18-1 could

induce helicity in the C-terminus of the Q-SNAREs, thereby providing a smooth template for SNARE-complex assembly (129).

4.2 Munc18-1 as a key player for SNARE-complex assembly.

An important point in understanding SNARE-mediated exocytosis, is to decipher how the assembly of the SNARE-complex proceeds in the presence of the AAA-ATPase, NSF and its co-factor α SNAP, which together, constitute the disassembly machinery of the SNARE-apparatus (5). NSF- α SNAP have been shown to dismantle the syntaxin1a/SNAP25a complex (106) as well as the fully assembled SNARE-complex (130).

The susceptibility of the syntaxin1a/SNAP25a complex to NSF-mediated disassembly questions its role as an acceptor complex for synaptobrevin-binding. The only complex that has, till date, been reported to be resistant to disassembly by NSF- α SNAP is the binary syntaxin1a/Munc18-1 complex (85). This makes the syntaxin1a/Munc18-1 complex, a strong candidate for serving as the starting point of SNARE-complex assembly (43). Interestingly, the syntaxin1a/SNAP25a/Munc18-1 complex characterized in this study also shows resistance to disassembly by NSF- α SNAP (see Figure 3.9-1 and Figure 3.9-3), indicating that the association of Munc18-1 with the Q-SNARE complex (syntaxin1a/SNAP25a) might help in shielding it from the dismantling effect of NSF and α SNAP. A similar role has recently been hinted for Vps33, which is the vacuolar orthologue of the SM-protein Munc18-1 (87). In the light of current and earlier research, it thus becomes intuitive to speculate that one of the additional roles of Munc18-1 in SNARE-complex assembly would be to shield the assembling SNARE-complexes against disassembly by NSF and α SNAP.

The function of Munc18-1 in synaptic vesicle exocytosis, however, might not be limited to the above-mentioned roles. In addition to its interaction with syntaxin1a (39, 47, 113) and the syntaxin1a/SNAP25a complex (30, 31, 61, *this work*), Munc18-1 has been proposed to interact with the R-SNARE synaptobrevin (44, 74, 131, 132) and also with the fully-assembled SNARE-complexes (42, 75, 133).

Studies with cross-linking provided evidence for the interaction of the domain3a of Munc18-1 with the membrane-proximal residues of synaptobrevin, placing Munc18-1, at the site of membrane-fusion (74). Four years later, a specific region in the domain3a of Munc18-1, helix 12, was shown to undergo a conformational switch during synaptic vesicle exocytosis, promoting both an 'open' conformation of syntaxin1a and activating synaptobrevin-2 for SNARE-complex assembly (86). Additionally, a single point mutation in the helix 12, L348R, has been shown to abolish both the binding of Munc18-1 to synaptobrevin-2, as well as the stimulatory effect of Munc18-1 on membrane-fusion (86). Alternatively, another point mutation, P335A at the N-terminus of the helix 12 was shown to result in an extended conformation of this



helix, favoring an 'open' conformation of syntaxin1a, allowing it to bind to SNAP25a (86). The effects of these mutations have only recently been tested in Munc18-1 *null* mouse adrenal chromaffin cells, rescued with either L348R or P335A mutants of Munc18-1 (132). Consistent with the results from the *in-vitro* experiments, a decrease in vesicle priming was observed for L348R, whereas P335A showed an increase in the secretory amplitude, indicative of increased vesicle priming. However, neither of these mutants showed a change in the fusion kinetics, indicating that the interaction of synaptobrevin with Munc18-1 is critical for vesicle priming, but not for fusion (132).

On similar lines, a recent study has reported that Munc18-1 can provide a template for SNARE-complex assembly through simultaneous interactions with syntaxin1a and synaptobrevin (44). In this study, single-molecule force-measurements were used to study SNARE-complex assembly in the presence of SNAP25a and Munc18-1, starting with a construct containing crosslinked syntaxin1a and synaptobrevin. The use of a crosslinked construct, however, made the system quite constrained, making it nearly impossible to detect any intermediate states containing syntaxin1a, SNAP25a and Munc18-1 (as reported in this study), that could form during SNARE-complex assembly.

An analogous mechanism has lately been proposed for Vps33, the SM-protein which forms a part of the HOPS complex to facilitate vacuolar fusion in yeast (87). Crystal structures of Vps33 have been obtained in complex with the Qa-SNARE, Vam1 and the R-SNARE, Nyv1. An overlay of these structures have implicated the involvement of Vps33 in providing a template for SNARE-complex assembly by interacting simultaneously with both of these SNAREs (87). However, since these conclusions have been made only by overlaying two separate structures and not by obtaining a single complex containing Vps33, Vam3 and Nyv1, the conclusions derived from this study remain dubious. Also, the conclusions obtained from this study cannot be directly extrapolated for the mammalian syntaxin1a/Munc18-1 system. This is mainly because the R-SNARE-binding site on Munc18-1 is not accessible in the syntaxin1a/Munc18-1 complex, thereby posing an additional regulatory step before synaptobrevin-binding can occur (87). A comparison of the structure of Vps33/Vam3 complex and the syntaxin1a/Munc18-1 complex has been shown in Figure 4.2-1. The R-SNARE-binding site on Munc18-1 only becomes exposed when syntaxin1a transitions from a 'closed' to an 'open' state. It can thus be speculated that upon 'opening', the syntaxin1a could possibly bind first to SNAP25a, resulting in a syntaxin1a/SNAP25a/Munc18-1 intermediate (as shown in this study), to which synaptobrevin-binding can be facilitated via an SM-template.

Alternatively, interactions between Munc18-1 and the fully-assembled SNARE-complex have also been established (40, 74, 75, 80), indicating that the interaction of Munc18-1 with the fully-assembled SNARE complex on the plasma membrane could accelerate fusion by causing the expansion of the fusion-pore. A major support from this hypothesis came from *in-vitro* lipid-mixing assays, where Munc18-1 was reported to cause acceleration of fusion between liposomes containing neuronal SNAREs (31). A

closer look at the experimental system, however, revealed that this accelerating effect could be observed only when the liposomes containing reconstituted SNAREs were pre-incubated with Munc18-1 for several hours. The pre-requisite of long incubations in these experiments indicate that the effect of Munc18-1 could possibly have been observed due to a rearrangement of the Q-SNAREs by Munc18-1 and not by its effect on an already assembled trans-SNARE-complex.

The fine experimental details in the different studies have thus helped us to reconcile the regulatory role of Munc18-1, underlining its critical importance mainly in the early stages (docking, priming) of SNARE-complex assembly.

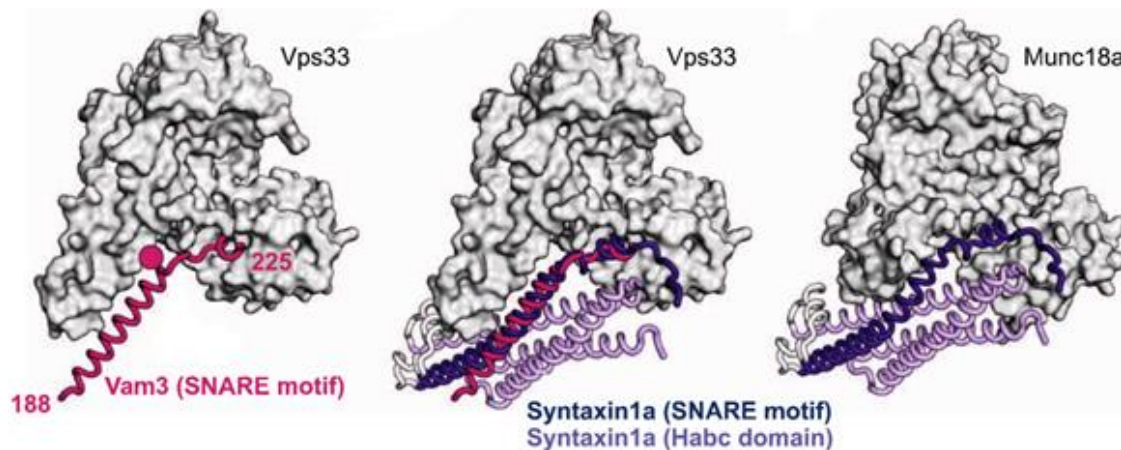


Figure 4.2-1. Crystal structure of Vps33 with the SNARE-motif of the Qa-SNARE, Vam3 and its comparison with Munc18-1/syntaxin1a interaction.

Left. Crystal structure of Vps33 (grey) and the SNARE-motif of Vam3 (shown in pink). The pink sphere indicates the residue of Vam3 that forms the zero-layer in the SNARE-complex. *Middle.* A superimposition of syntaxin1a containing its SNARE-motif (shown in dark blue) and the Habc domain (shown in purple) on the structure of Vps33-Vam3. Vam3 has been shown in pink. *Right.* Crystal structure of Munc18-1/syntaxin1a complex. The R-SNARE binding-site on Munc18-1 is not accessible in this binary complex and becomes accessible only upon ‘opening’ of syntaxin1a. [Adapted from (87)].



4.3 Understanding the transition of an acceptor-complex to a fully-assembled SNARE-complex.

SNARE-zippering is speculated to proceed from the N-termini of the SNARE-proteins towards their C-termini, slowly bringing the two opposing membranes in close apposition for membrane-fusion (134). *In-vitro* studies in a membrane environment have indicated that the SNAREs zipper at their membrane-distal ends, with the membrane proximal ends remaining unassembled, due to opposing forces from the juxtaposed membranes (135).

In this study, I attempted to study the mechanism of SNARE-zippering, starting with the ternary syntaxin1a/SNAP25a/Munc18-1 complex, by using different truncations of the cytoplasmic fragment of synaptobrevin. The results obtained in this thesis indicated that a truncation of 44 residues from the C-terminus (Syb 1-52) and a truncation of 48 residues from the N-terminus (Syb 49-96) of the cytoplasmic fragment of synaptobrevin results in a complete loss of binding to the syntaxin1a/SNAP25a/Munc18-1 complex. This result was very intriguing and provided clues for the existence of an alternative zippering mechanism, where SNARE-zippering would nucleate not at the conventionally proposed N-terminus, but somewhere downstream, and then proceed bi-directionally in a co-operative fashion.

The results from these experiments can, however, also be interpreted in the light of a recent report for Vps33 (87). A deletion of the N-terminal and the C-terminal residues of Nyv1 (R-SNARE), was shown to result in reduced affinities for binding to the SM-protein, Vps33 (87). A similar trend was observed in response to the truncation of the neuronal R-SNARE, synaptobrevin in this study. In addition to the complete loss of binding observed for Syb 1-52 and Syb 49-96, a considerable decrease was observed in the binding kinetics of a fragment (Syb 1-65) in which 31 residues from the C-terminus of synaptobrevin had been truncated. The complete cytoplasmic fragment of synaptobrevin, however, exhibited fast binding kinetics to the syntaxin1a/SNAP25a/Munc18-1 complex. These observations could therefore, be indicative of SNARE-complex assembly via an R-SNARE-SM-protein intermediate.

A very interesting question with respect to Munc18-1 that still remains unclear is its mode of interaction with the SNARE-protein(s) after SNARE-complex assembly. Some studies indicate that SNARE-complex assembly can cause the dissociation of Munc18-1 from the neuronal SNAREs (78, 126), whereas others indicate that Munc18-1 can remain attached to the fully-assembled SNARE-complex, either by a close interaction with the core SNARE-complex (42, 75, 80) or, through a distal interaction with the N-terminus of syntaxin1a (39, 41). The work done in this thesis supports the latter hypothesis by providing evidence for a continued association of Munc18-1 with the SNARE-complex via the N-terminus of syntaxin1a (see Figure 3.7-2 and Figure 3.7-4). However, as indicated in one of the previous sections, the physiological relevance of this interaction still remains to be deciphered.

4.4 Physiological relevance of the syntaxin1a/SNAP25a/Munc18-1 complex.

Almost forty years of intensive research in the SNARE-field has provided immense progress in the understanding of the details that define the spatial and temporal precision of SNARE-mediated membrane fusion. However, a clear step-by-step transition of the complexes in the SNARE-pathway remains missing. To cite an example, a consensus mechanism underlying the transition of syntaxin1a from its 'closed' conformation (in the intracellular compartments) to an 'open' conformation (on the neuronal plasma membrane), largely remains unknown.

There are three major candidates for the so-called '*plasma-membrane factors*' that could be responsible for bringing about this transition. The first and one of the most well-characterized factor is the CATCH-R protein, Munc13-1. *In-vitro* studies have indicated that the incubation of syntaxin1a/Munc18-1 complexes with Munc13-1 can result in a conformation of syntaxin1a which is compatible for SNARE-complex assembly (54). A closer look at the mechanistic details of this transition has been reported only recently, where two residues in the linker region of syntaxin1a, R151 and I155, were identified to be critical for the interaction of Munc13-1 with the syntaxin1a/Munc18-1 complex (136). These residues were shown to be crucial for the formation of a ternary complex between syntaxin1a, Munc13-1 and Munc18-1, where syntaxin1a still exists in a 'closed' conformation, but structural changes in its linker region promoted by Munc13-1, allows the gating of the syntaxin1a/Munc18-1 complex for functional SNARE-complex assembly (136).

Former studies have attributed the key function of Munc13- to its MUN-domain, which has been shown to completely rescue neurotransmitter release in hippocampal neurons lacking Munc13-1/2 (52). In contradiction to this observation, a recent study has reported that rescue experiments performed with the MUN-domain in autaptic neuronal cultures from Munc13-1/2 double knock-out mice, could rescue neurotransmitter release only by a very small level in comparison to the wild-type (32). The discrepancies observed in these two reports was found to result from differential levels of protein expression. The rescue experiment in the latter study was performed with a lentiviral expression vector, which results in moderate levels of protein expression as compared to the Semliki Forest Virus that causes protein expression much above the intracellular levels. This fact underlined any artifacts caused due to extremely high levels of proteins in the study reported earlier (52). Additionally, a fragment of Munc13-1 encompassing the region C1C2BMUNC2C of Munc13-1 was seen to cause much higher levels of rescue as compared to the MUN-domain, indicating a functional synergy between the different domains to promote the function of Munc13-1 in neurotransmitter release (32).

Another candidate which is considered important for altering the interaction between syntaxin1a and Munc18-1 is protein kinase C (PKC), a second messenger that has been proposed to play a key role during neuronal exocytosis. Two sites on Munc18-1, serine 306 and serine 313 can be phosphorylated by protein kinase C *in-vitro*, which in turn,



has been reported to attenuate the interaction of Munc18-1 with syntaxin1a (137). The phosphorylation of serine 313 in intact chromaffin cells has also been shown to affect kinetics of vesicle fusion and release (137). On similar lines, Munc18-1 has been reported to show redistribution and clustering at the synapse upon calcium influx and phosphorylation by PKC (138). In fact, a direct correlation has been obtained between synaptic strength and the PKC-dependent clustering of Munc18-1 at the synapse (138). Other studies, however, indicate that the facilitation of vesicle docking by Munc18-1 is independent of phosphorylation by protein kinase C, but the phosphorylation could play a post-docking role by potentiating vesicle pool replenishment (139). In a non-neuronal system, another kinase, Cdk5, has been speculated to weaken the interactions between syntaxin3 and Munc18-2, making way for a tripartite complex containing syntaxin3, SNAP25 and Munc18-2. The so formed syntaxin3/SNAP25/Munc18-2 complex is hypothesized to function as an intermediate for SNARE-complex assembly and subsequent secretion of gastric acid in epithelial cells (76). The interaction with plasma membrane Q-SNAREs can therefore be considered to be a universal feature of the mammalian SM-proteins.

A third candidate which has been proposed to have a role in altering syntaxin1a/Munc18-1 interaction for promoting SNARE-complex assembly is arachidonic acid. Arachidonic acid is a poly-unsaturated fatty acid that has been shown to increase SNARE-complex formation in chromaffin cells and bovine cortical brain extracts in a dose-dependent manner (140). It has also been shown to promote long-term plasticity in hippocampal neurons (141). Arachidonic acid can be released from the plasma membrane phospholipids by the action of phospholipases and can act as a potential second messenger in a micro-molar concentration range (115). Other studies have reported that the stimulatory effect of arachidonic acid on SNARE-mediated fusion can be blocked by the use of botulinum neurotoxins (142), thereby indicating that arachidonic acid acts by modulating the SNARE-machinery and not by increasing the general fusogenicity of the membrane lipids. Arachidonic acid has been speculated to positively regulate membrane fusion by relieving the inhibition of syntaxin1a by Munc18-1 (115, 140, 143). Studies using synaptosomes from rat brains indicated that the arachidonic acid could activate SNARE-complex assembly by causing the dissociation of syntaxin1a from Munc18-1 (115). Subsequent studies with more detailed characterizations, however, suggested that the effect of arachidonic acid is brought by causing a conformational change in syntaxin1a, allowing syntaxin1a to assemble into a tripartite complex containing syntaxin1a, SNAP25a and Munc18-1 (143). This mechanism of action for arachidonic acid appears to be consistent in other syntaxin isoforms like syntaxin3 and syntaxin4 (143). Yet another study has proposed that an additional binding site on Munc18-1 can be exposed upon the action of arachidonic acid on the syntaxin1a/Munc18-1 complex (140), thereby facilitating the interaction of syntaxin1a with its partner SNAREs.

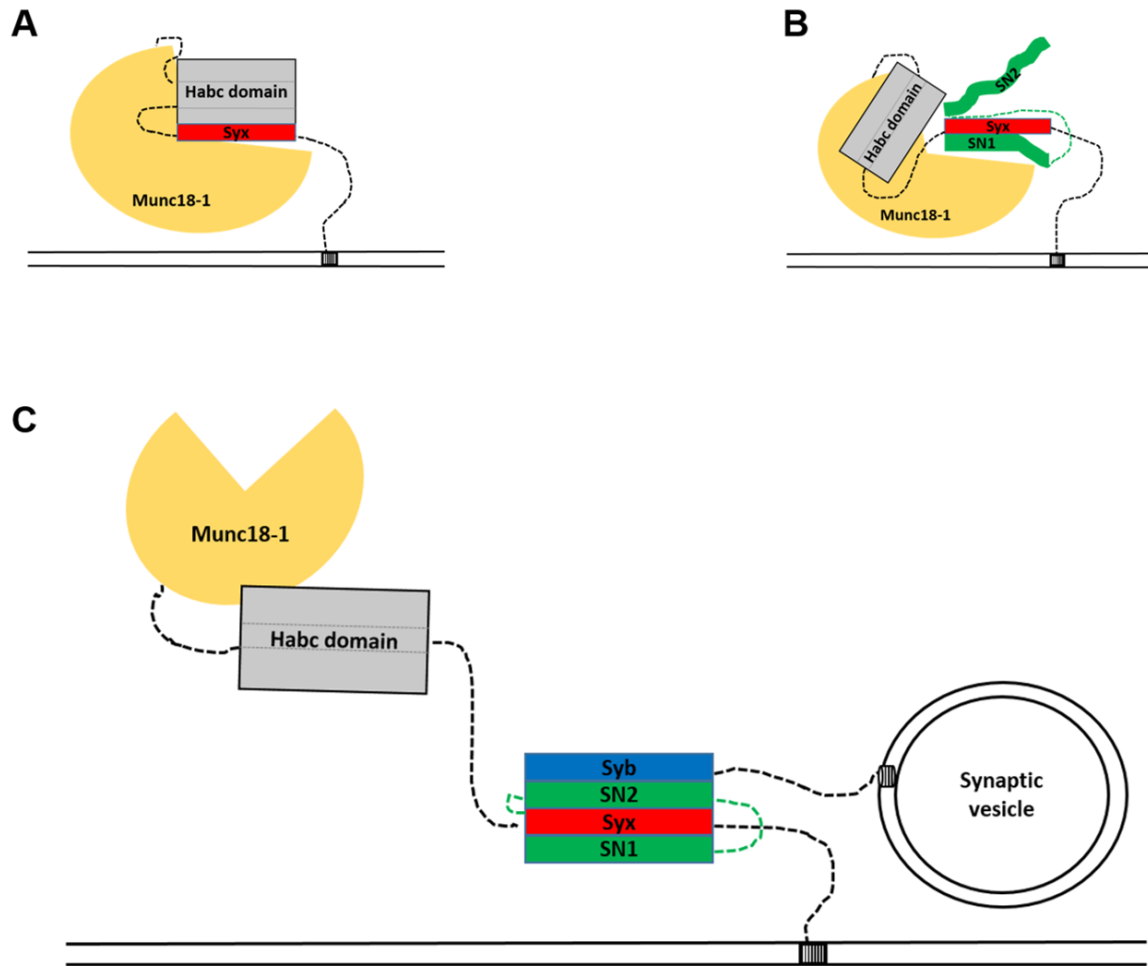


Figure 4.4-1. Schematic model representing the association of Munc18-1 with the SNARE-proteins at different stages of SNARE-complex assembly.

(A) The classical interaction of syntaxin1a with Munc18-1 in the binary syntaxin1a/Munc18-1 complex, with syntaxin1a being in a 'closed' conformation. (B) The syntaxin1a/Munc18-1 complex can be acted upon by certain 'in-vivo' factors to alter the tight association of syntaxin1a and Munc18-1, making way for the association of syntaxin1a with SNAP25a, within a ternary syntaxin1a/SNAP25a/Munc18-1 complex. Syntaxin1a in this ternary complex is speculated to exist in a 'partially open' conformation. (C) Upon synaptobrevin-binding to this complex, syntaxin1a transitions to a 'fully open' conformation, leading to SNARE-complex assembly. This transition is accompanied by major structural rearrangements, causing the translocation of Munc18-1 to the N-terminus of syntaxin1a.



Taken together, it becomes conceivable, that the interaction between syntaxin1a and Munc18-1 gets altered by some *in-vivo* factors upon reaching the plasma membrane, resulting in the formation of an intermediate consisting of syntaxin1a, SNAP25a and Munc18-1 that forms a template for synaptobrevin-binding and SNARE-complex assembly. A cartoon representation of the associations of Munc18-1 with the SNARE-proteins at different stages in SNARE-complex assembly has been shown in Figure 4.4-1.

Several studies performed earlier had highlighted the role of Munc18-1 in structuring the t-SNAREs for SNARE-complex assembly and, this study has helped in advancement of this understanding by providing direct mechanistic details underlying this function of Munc18-1.

The conclusions from this study have highlighted the syntaxin1a/SNAP25a/Munc18-1 complex as a strong candidate for a physiological intermediate in the SNARE-assembly pathway. The role of other accessory proteins such as Munc13-1, synaptotagmin and complexin, however, remain to be encompassed, to reconcile the significance of each of these components to specific stages of the SNARE-pathway.

5 Conclusions and perspectives

This thesis has aimed at defining the long-speculated role of Munc18-1 during the early steps of synaptic vesicle exocytosis. The characterization of the novel syntaxin1a/SNAP25a/Munc18-1 complex has provided tremendous support to the speculations on the progress of SNARE-complex assembly via a Q-SNARE/SM-protein template. Precise details of synaptobrevin-binding to this complex via interactions with Munc18-1, however, need to be unraveled.

The use of full-length proteins in this study has provided a closer understanding of the physiological behaviors of the proteins. Most of the experiments in this study were, however, performed using detergent micelles, without the use of lipid bilayers or vesicles. The role of protein-lipid interactions thus, remained ignored in this work. An effort to optimize the system in a membrane-environment would strengthen the conclusions obtained from this study and would help to faithfully extend the conclusions towards a physiological scenario.

Additionally, due to technical limitations of the experimental system, it was only possible to obtain an overview of the architecture of the syntaxin1a/SNAP25a/Munc18-1 complex using chemical crosslinking assays. In future, it would be interesting to figure out if the syntaxin1a/SNAP25a/Munc18-1 complex can be stabilized by other accessory factors (for example, Munc13-1) and to probe the structural details of this macromolecular assembly using a more precise structural technique, such as X-ray crystallography.

The spatial and temporal coupling of calcium-influx on the arrival of an action potential and synaptic vesicle exocytosis is achieved by the calcium-sensor synaptotagmin (56). Another protein, complexin has also been speculated to undergo conformational changes to promote SNARE-mediated fusion upon increase in the intra-cellular calcium levels (144). Therefore, a next big step for future research would be to figure out the role of these accessory proteins in the system. This would help us in obtaining a closer look at the intermediate steps, highlighting precisely at which step the trans-SNARE complex gets clamped and how the influx of calcium helps in promoting membrane fusion and neurotransmitter release.

One of the major aims of this work was to detect the functional significance of association of Munc18-1 with the Q-SNAREs, syntaxin1a and SNAP25a. It still remains unknown when and how exactly during the process of neuronal exocytosis this interaction comes into play. Nonetheless, the work done in this thesis has, in the least, been able to establish that the association between the Q-SNAREs and Munc18-1 helps in greasing the wheels of the SNARE-engine and the subsequent binding of synaptobrevin to this complex sets the wheels rolling, resulting in SNARE-complex assembly. The resistance of the syntaxin1a/SNAP25a/Munc18-1 complex to disassembly by NSF- α SNAP has also highlighted an additional role of Munc18-1, in



Conclusions and Perspectives

providing a protective shield against disassembly for the intermediates formed in the SNARE-pathway.

The work done in this thesis has thus provided a step forward in understanding the pre-fusion role of Munc18-1 in neuronal exocytosis. Subsequent progress will help in further unraveling the secrets that underlie the beauty of the exquisitely regulated process of synaptic vesicle exocytosis.

6 References

1. P. Novick, C. Field, R. Schekman, Identification of 23 complementation groups required for post-translational events in the yeast secretory pathway. *Cell*. **21**, 205–215 (1980).
2. A. Stein, G. Weber, M. C. Wahl, R. Jahn, Helical extension of the neuronal SNARE complex into the membrane. *Nature*. **460**, 525–528 (2009).
3. R. B. Sutton, D. Fasshauer, R. Jahn, A. T. Brunger, Crystal structure of a SNARE complex involved in synaptic exocytosis at 2.4 angstrom resolution. *Nature*. **395**, 347–353 (1998).
4. S. Gonzalo, M. E. Linder, SNAP-25 palmitoylation and plasma membrane targeting require a functional secretory pathway. *Mol. Biol. Cell*. **9**, 585–597 (1998).
5. R. Jahn, R. H. Scheller, SNAREs--engines for membrane fusion. *Nat. Rev. Mol. cell Biol*. **7**, 631–43 (2006).
6. Gabor Nagy et al *et al.*, The SNAP-25 Linker as an Adaptation Toward Fast Exocytosis. *Mol. Biol. Cell*. **19**, 3769–3781 (2008).
7. R. Fukuda *et al.*, Functional architecture of an intracellular membrane t-SNARE. *Nature*. **407**, 198–202 (2000).
8. F. Wang, A. Whynot, M. Tung, V. Denic, The Mechanism of Tail-Anchored Protein Insertion into the ER Membrane. *Mol. Cell*. **43**, 738–750 (2011).
9. S. O. Rizzoli, W. J. Betz, Synaptic vesicle pools. *Nat. Rev. Neurosci*. **6**, 57–69 (2005).
10. T. C. Südhof, J. Rizo, Synaptic vesicle exocytosis. *Cold Spring Harb. Perspect. Biol*. **3**, 1–14 (2011).
11. D. Fasshauer, R. B. Sutton, A. T. Brunger, R. Jahn, Conserved structural features of the synaptic fusion complex: SNARE proteins reclassified as Q- and R-SNAREs. *Proc. Natl. Acad. Sci. U. S. A*. **95**, 15781–6 (1998).
12. F. Parlati *et al.*, Topological restriction of SNARE-dependent membrane fusion. *Nature*. **407**, 194–198 (2000).
13. J. a McNew *et al.*, Compartmental specificity of cellular membrane fusion encoded in SNARE proteins. *Nature*. **407**, 153–159 (2000).
14. S. J. Scales *et al.*, SNAREs contribute to the specificity of membrane fusion. *Neuron*. **26**, 457–64 (2000).
15. G. Schiavo *et al.*, Tetanus and botulinum-B neurotoxins block neurotransmitter release by proteolytic cleavage of synaptobrevin. *Nature*. **359**, 832–835 (1992).
16. J. M. Hunt *et al.*, A post-docking role for synaptobrevin in synaptic vesicle fusion.



- Neuron*. **12**, 1269–1279 (1994).
17. C. Imig *et al.*, The Morphological and Molecular Nature of Synaptic Vesicle Priming at Presynaptic Active Zones. *Neuron*. **84**, 416–431 (2014).
 18. B. L. Grosshans, D. Ortiz, P. Novick, Rabs and their effectors: achieving specificity in membrane traffic. *Proc. Natl. Acad. Sci. U. S. A.* **103**, 11821–7 (2006).
 19. N. J. Pavlos, R. Jahn, Distinct yet overlapping roles of Rab GTPases on synaptic vesicles. *Small GTPases*. **2**, 77–81 (2011).
 20. A. G. Leenders, F. H. Lopes da Silva, W. E. Ghijsen, M. Verhage, Rab3a is involved in transport of synaptic vesicles to the active zone in mouse brain nerve terminals. *Mol. Biol. Cell*. **12**, 3095–102 (2001).
 21. Y. A. Chen, R. H. Scheller, SNARE-mediated membrane fusion. *Nat. Rev. Mol. Cell Biol.* **2**, 98–106 (2001).
 22. Y. A. Chen, R. H. Scheller, Snare-mediated membrane fusion [Review]. *Nat. Rev. Mol. Cell Biol.* **2**, 98–106 (2001).
 23. G. van den Bogaart *et al.*, One SNARE complex is sufficient for membrane fusion. *Nat. Struct. Mol. Biol.* **17**, 358–64 (2010).
 24. C. G. Schuette *et al.*, Determinants of liposome fusion mediated by synaptic SNARE proteins. *Proc. Natl. Acad. Sci. U. S. A.* **101**, 2858–63 (2004).
 25. J. M. Hernandez *et al.*, Membrane Fusion Intermediates via Directional and Full Assembly of the SNARE Complex. *Science (80-.)*. **336**, 1581–1584 (2012).
 26. K. Bacia, C. G. Schuette, N. Kahya, R. Jahn, P. Schwille, SNAREs prefer liquid-disordered over “raft” (liquid-ordered) domains when reconstituted into giant unilamellar vesicles. *J. Biol. Chem.* **279**, 37951–37955 (2004).
 27. L. L. G. Schwenen *et al.*, Resolving single membrane fusion events on planar pore-spanning membranes. *Sci. Rep.* **5**, 12006 (2015).
 28. H. von Gersdorff, G. Matthews, Electrophysiology of Synaptic Vesicle Cycling. *Annu. Rev. Physiol.* **61**, 725–752 (1999).
 29. M. Wolfel, R. Schneggenburger, Presynaptic Capacitance Measurements and Ca²⁺ Uncaging Reveal Submillisecond Exocytosis Kinetics and Characterize the Ca²⁺ Sensitivity of Vesicle Pool Depletion at a Fast CNS Synapse. *J. Neurosci.* **23**, 7059–7068 (2003).
 30. A. Stein, A. Radhakrishnan, D. Riedel, D. Fasshauer, R. Jahn, Synaptotagmin activates membrane fusion through a Ca²⁺-dependent trans interaction with phospholipids. *Nat Struct Mol Biol.* **14**, 904–911 (2007).
 31. J. Shen, D. C. Tareste, F. Paumet, J. E. Rothman, T. J. Melia, Selective activation of cognate SNAREpins by Sec1/Munc18 proteins. *Cell*. **128**, 183–95 (2007).
 32. X. Liu *et al.*, Functional synergy between the Munc13 C-terminal C1 and C2

- domains. *Elife*. **5**, 1–27 (2016).
33. S. Brenner, The genetics of *Caenorhabditis elegans*. *Genetics*. **77**, 71–94 (1974).
 34. P. Novick, R. Schekman, Secretion and cell-surface growth are blocked in a temperature-sensitive mutant of *Saccharomyces cerevisiae*. *Proc. Natl. Acad. Sci. U. S. A.* **76**, 1858–1862 (1979).
 35. S. D. Harrison, K. Broadie, J. Van De Goor, G. M. Rubin, Mutations in the *Drosophila* Rop gene suggest a function in general secretion and synaptic transmission. *Neuron*. **13**, 555–566 (1994).
 36. F. F. Assaad, Y. Huet, U. Mayer, G. Jürgens, The cytokinesis gene KEULE encodes a Sec1 protein that binds the syntaxin KNOLLE. *J. Cell Biol.* **153**, 531–543 (2001).
 37. J. T. Tellam, S. McIntosh, D. E. James, Molecular identification of two novel Munc-18 isoforms expressed in non-neuronal tissues. *J. Biol. Chem.* **270** (1995), pp. 5857–5863.
 38. M. Verhage *et al.*, Synaptic assembly of the brain in the absence of neurotransmitter secretion. *Science (80-.)*. **287**, 864–869 (2000).
 39. P. Burkhardt, D. A. Hattendorf, W. I. Weis, D. Fasshauer, Munc18a controls SNARE assembly through its interaction with the syntaxin N-peptide. *EMBO J.* **27**, 923–933 (2008).
 40. C. Rickman, C. N. Medine, A. Bergmann, R. R. Duncan, Functionally and spatially distinct modes of munc18-syntaxin 1 interaction. *J. Biol. Chem.* **282**, 12097–12103 (2007).
 41. M. Meijer *et al.*, Munc18-1 mutations that strongly impair SNARE-complex binding support normal synaptic transmission. *EMBO J.* **31**, 2156–2168 (2012).
 42. M. Khvotchev *et al.*, Dual modes of Munc18-1/SNARE interactions are coupled by functionally critical binding to syntaxin-1 N terminus. *J. Neurosci. Off. J. Soc. Neurosci.* **27**, 12147–12155 (2007).
 43. C. Ma, L. Su, A. B. Seven, Y. Xu, J. Rizo, Reconstitution of the Vital Functions of Munc18 and Munc13 in Neurotransmitter Release. *Science (80-.)*. **339**, 421–425 (2013).
 44. L. Ma *et al.*, Munc18-1-regulated stage-wise SNARE assembly underlying synaptic exocytosis. *Elife*. **4**, 1–30 (2015).
 45. K. Weninger, M. E. Bowen, U. B. Choi, S. Chu, A. T. Brunger, Accessory Proteins Stabilize the Acceptor Complex for Synaptobrevin, the 1:1 Syntaxin/SNAP-25 Complex. *Structure*. **16**, 308–320 (2008).
 46. A. Pertsinidis *et al.*, Ultrahigh-resolution imaging reveals formation of neuronal SNARE/Munc18 complexes in situ. *Proc. Natl. Acad. Sci. U. S. A.* **110**, E2812–20 (2013).
 47. K. M. Misura, R. H. Scheller, W. I. Weis, Three-dimensional structure of the



- neuronal-Sec1-syntaxin 1a complex. *Nature*. **404**, 355–362 (2000).
48. I. Augustin *et al.*, Differential expression of two novel Munc13 proteins in rat brain. *Biochem. J.* **337** (Pt 3, 363–71 (1999).
 49. S. Kalla *et al.*, Molecular Dynamics of a Presynaptic Active Zone Protein Studied in Munc13-1 – Enhanced Yellow Fluorescent Protein Knock-In Mutant Mice. *J. Neurosci.* **26**, 13054–13066 (2006).
 50. L. Sheu *et al.*, Regulation of insulin exocytosis by Munc13-1. *J. Biol. Chem.* **278**, 27556–27563 (2003).
 51. Varoqueaux, Frederique *et al.*, Total arrest of spontaneous and evoked synaptic transmission but normal synaptogenesis in the absence of Munc13-mediated vesicle priming. *Proc. Natl. Acad. Sci. U. S. A.* **99**, 9037–42 (2002).
 52. J. Basu *et al.*, A minimal domain responsible for Munc13 activity. *Nat. Struct. Mol. Biol.* **12**, 1017–8 (2005).
 53. X. Yang *et al.*, Syntaxin opening by the MUN domain underlies the function of Munc13 in synaptic-vesicle priming. *Nat. Struct. Mol. Biol.* **22**, 1–10 (2015).
 54. C. Ma, W. Li, Y. Xu, J. Rizo, Munc13 mediates the transition from the closed syntaxin-Munc18 complex to the SNARE complex. *Nat. Struct. Mol. Biol.* **18**, 542–9 (2011).
 55. E. A. Nalefski, J. J. Falke, The C2 domain calcium-binding motif: structural and functional diversity. *Protein Sci.* **5**, 2375–2390 (1996).
 56. N. Brose, a G. Petrenko, T. C. Südhof, R. Jahn, Synaptotagmin: a calcium sensor on the synaptic vesicle surface. *Science*. **256**, 1021–1025 (1992).
 57. Y. Park *et al.*, Synaptotagmin-1 binds to PIP2-containing membrane but not to SNAREs at physiological ionic strength. *Nat. Struct. Mol. Biol.* (2015), doi:10.1038/nsmb.3097.
 58. E. R. Chapman, S. An, J. M. Edwardson, R. Jahn, A novel function for the second C2 domain of synaptotagmin. Ca²⁺- triggered dimerization. *J Biol Chem.* **271**, 5844–5849 (1996).
 59. M. C. Chicka, E. Hui, H. Liu, E. R. Chapman, Synaptotagmin arrests the SNARE complex before triggering fast, efficient membrane fusion in response to Ca²⁺. *Nat Struct Mol Biol.* **15**, 827–835 (2008).
 60. and T. H. S. Florian Seiler, Jörg Malsam, Jean Michel Krause, A role of complexin-lipid interactions in membrane fusion Florian. *FEBS Lett.* **583**, 2343–2348 (2009).
 61. C. G. Giraud *et al.*, Alternative zippering as an on-off switch for SNARE-mediated fusion. *Science (80-.)*. **323**, 512–516 (2009).
 62. D. Kümmel *et al.*, Complexin cross-links prefusion SNAREs into a zigzag array. *Nat. Struct. Mol. Biol.* **18**, 927–933 (2011).

63. D. J. Woodbury, Is it zippered? Does it flare? That darn complexin clamping SNARE. *Biophys. J.* **105**, 835–836 (2013).
64. R. Jahn, D. Fasshauer, Molecular machines governing exocytosis of synaptic vesicles. *Nature.* **490**, 201–7 (2012).
65. K. Reim *et al.*, Complexins regulate a late step in Ca²⁺-dependent neurotransmitter release. *Cell.* **104**, 71–81 (2001).
66. M. Weber-Boyvart, N. Aro, K. G. Chernov, T. Nyman, J. Jääntti, Sec1p and Mso1p C-terminal tails cooperate with the SNAREs and Sec4p in polarized exocytosis. *Mol. Biol. Cell.* **22**, 230–244 (2011).
67. A. Bracher, W. Weissenhorn, Structural basis for the Golgi membrane recruitment of Sly1p by Sed5p. *EMBO J.* **21**, 6114–6124 (2002).
68. R. Peng, D. Gallwitz, Sly1 protein bound to Golgi syntaxin Sed5p allows assembly and contributes to specificity of SNARE fusion complexes. *J. Cell Biol.* **157**, 645–655 (2002).
69. L. N. Carpp, L. F. Ciuffo, S. G. Shanks, A. Boyd, N. J. Bryant, The Sec1p/Munc18 protein Vps45p binds its cognate SNARE proteins via two distinct modes. *J. Cell Biol.* **173**, 927–936 (2006).
70. B. T. Lobingier, A. J. Merz, Sec1/Munc18 protein Vps33 binds to SNARE domains and the quaternary SNARE complex. *Mol. Biol. Cell.* **23**, 4611–22 (2012).
71. M. Weber-Boyvart *et al.*, The Sec1/Munc18 Protein Groove plays a Conserved Role in Interaction with Sec9p/SNAP-25. *Traffic.* **17**, 131–53 (2015).
72. C. M. Carr, E. Grote, M. Munson, F. M. Hughson, P. J. Novick, Sec1p binds to SNARE complexes and concentrates at sites of secretion. *J. Cell Biol.* **146**, 333–344 (1999).
73. K. M. Misura, R. H. Scheller, W. I. Weis, Three-dimensional structure of the neuronal-Sec1-syntaxin 1a complex. *Nature.* **404**, 355–62 (2000).
74. Y. Xu, L. Su, J. Rizo, Binding of Munc18-1 to synaptobrevin and to the SNARE four-helix bundle. *Biochemistry.* **49**, 1568–1576 (2010).
75. I. Dulubova *et al.*, Munc18-1 binds directly to the neuronal SNARE complex. *Proc. Natl. Acad. Sci. U. S. A.* **104**, 2697–2702 (2007).
76. Y. Liu *et al.*, A Mechanism of Munc18b-Syntaxin 3-SNAP25 complex assembly in regulated epithelial secretion. *FEBS Lett.* **581**, 4318–4324 (2007).
77. C. F. Latham *et al.*, Molecular dissection of the Munc18c/syntaxin4 interaction: implications for regulation of membrane trafficking. *Traffic.* **7**, 1408–1419 (2006).
78. R. F. G. Toonen, M. Verhage, Munc18-1 in secretion: lonely Munc joins SNARE team and takes control. *Trends Neurosci.* **30**, 564–572 (2007).



79. D. Dawidowski, D. S. Cafiso, Munc18-1 and the Syntaxin-1 N Terminus Regulate Open-Closed States in a t-SNARE Complex. *Structure*. **24**, 392–400 (2016).
80. F. Deák *et al.*, Munc18-1 binding to the neuronal SNARE complex controls synaptic vesicle priming. *J. Cell Biol.* **184**, 751–764 (2009).
81. S. R. Pfeffer, Transport-vesicle targeting: tethers before SNAREs. *Nat. Cell Biol.* **1**, E17-22 (1999).
82. L. Arunachalam *et al.*, Munc18-1 Is Critical for Plasma Membrane Localization of Syntaxin1 but Not of SNAP-25 in PC12 Cells. *Mol. Biol. Cell.* **19**, 722–734 (2008).
83. R. F. G. Toonen, K. J. De Vries, R. Zalm, T. C. Südhof, M. Verhage, Munc18-1 stabilizes syntaxin 1, but is not essential for syntaxin 1 targeting and SNARE complex formation. *J. Neurochem.* **93**, 1393–1400 (2005).
84. C. Ma, L. Su, A. A. B. Seven, Y. Xu, J. Rizo, Reconstitution of the vital functions of Munc18 and Munc13 in neurotransmitter release. *Science (80-.)*. **339**, 421–5 (2013).
85. C. Ma, L. Su, A. B. Seven, Y. Xu, J. Rizo, Reconstitution of the vital functions of Munc18 and Munc13 in neurotransmitter release. *Sci. New York NY.* **339**, 421–5 (2013).
86. D. Parisotto *et al.*, An extended helical conformation in domain 3a of Munc18-1 provides a template for SNARE (soluble N-ethylmaleimide-sensitive factor attachment protein receptor) complex assembly. *J. Biol. Chem.* **289**, 9639–50 (2014).
87. R. W. Baker *et al.*, A direct role for the Sec1/Munc18-family protein Vps33 as a template for SNARE assembly. *Science (80-.)*. **349**, 1111–1114 (2015).
88. M. Khvotchev *et al.*, Dual modes of Munc18-1/SNARE interactions are coupled by functionally critical binding to syntaxin-1 N terminus. *J. Neurosci.* **27**, 12147–55 (2007).
89. M. Margittai, D. Fasshauer, S. Pabst, R. Jahn, R. Langen, Homo- and Heterooligomeric SNARE Complexes Studied by Site-directed Spin Labeling. *J. Biol. Chem.* **276**, 13169–13177 (2001).
90. D. Fasshauer, W. Antonin, M. Margittai, S. Pabst, R. Jahn, Mixed and Non-cognate SNARE Complexes. *Biochemistry.* **274**, 15440–15446 (1999).
91. Y. Park *et al.*, α -SNAP interferes with the zippering of the SNARE protein membrane fusion machinery. *J. Biol. Chem.* **289**, 16326–16335 (2014).
92. A. V. Pobbati, N- to C-Terminal SNARE Complex Assembly Promotes Rapid Membrane Fusion. *Science (80-.)*. **313**, 673–676 (2006).
93. K. Wiedelhold, D. Fasshauer, Is assembly of the SNARE complex enough to fuel membrane fusion? *J. Biol. Chem.* **284**, 13143–13152 (2009).
94. J. Matias, H. Amezquita, Reconstituted SNARE-mediated fusion: towards a

- mechanistic understanding (2011).
95. T. D. Pollard, A guide to simple and informative binding assays. *Mol. Biol. Cell.* **21**, 4061–4067 (2010).
 96. S. F. Martin, M. H. Tatham, R. T. Hay, I. D. W. Samuel, Quantitative analysis of multi-protein interactions using FRET: application to the SUMO pathway. *Protein Sci.* **17**, 777–84 (2008).
 97. J. R. Lakowicz, *Principles of fluorescence spectroscopy, 3rd Edition*, Joseph R. Lakowicz, editor (2006).
 98. D. Shrestha, A. Jenei, P. Nagy, G. Vereb, J. Szoellosi, *Understanding FRET as a research tool for cellular studies* (2015), vol. 16.
 99. G. W. Vuister, A. Bax, Resolution enhancement and spectral editing of uniformly ^{13}C -enriched proteins by homonuclear broadband ^{13}C decoupling. *J. Magn. Reson.* **98**, 428–435 (1992).
 100. D. Doyle, The Fine Structure of the Nervous System: The Neurons and Supporting Cells. *J. Neurol. Neurosurg. Psychiatry.* **41**, 191–192 (1978).
 101. A. V Pobbati, A. Stein, D. Fasshauer, N- to C-terminal SNARE complex assembly promotes rapid membrane fusion. *Science.* **313**, 673–676 (2006).
 102. H. Zhao, P. Lappalainen, A simple guide to biochemical approaches for analyzing protein-lipid interactions. *Mol. Biol. Cell.* **23**, 2823–30 (2012).
 103. H. Yu, S. S. Rathore, E. M. Davis, Y. Ouyang, J. Shen, Doc2b promotes GLUT4 exocytosis by activating the SNARE-mediated fusion reaction in a calcium- and membrane bending-dependent manner. *Mol. Biol. Cell.* **24**, 1176–84 (2013).
 104. A. L. Shapiro, E. Viñuela, J. V Maizel, Molecular weight estimation of polypeptide chains by electrophoresis in SDS-polyacrylamide gels. *Biochem. Biophys. Res. Commun.* **28**, 815–820 (1967).
 105. A. Penna, M. Cahalan, Western Blotting using the Invitrogen NuPage Novex Bis Tris minigels. *J. Vis. Exp.*, 264 (2007).
 106. H. Otto, P. I. Hanson, R. Jahn, Assembly and disassembly of a ternary complex of synaptobrevin, syntaxin, and SNAP-25 in the membrane of synaptic vesicles. *Proc Natl Acad Sci U S A.* **94**, 6197–6201 (1997).
 107. J. Pevsner *et al.*, Specificity and regulation of a synaptic vesicle docking complex. *Neuron.* **13**, 353–361 (1994).
 108. J. M. Walker, *Mass Spectrometry of Proteins and Peptides Series Editor* (2009).
 109. A. Shevchenko, H. Tomas, J. Havli^[sbreve], J. V Olsen, M. Mann, In-gel digestion for mass spectrometric characterization of proteins and proteomes. *Nat. Protoc.* **1**, 2856–2860 (2007).
 110. T. J. Siddiqui *et al.*, Determinants of Synaptobrevin Regulation in Membranes.



- Mol. Biol. Cell.* **18**, 2037–2046 (2007).
111. P. Hoopmann *et al.*, Endosomal sorting of readily releasable synaptic vesicles. *Proc. Natl. Acad. Sci. U. S. A.* **107**, 19055–19060 (2010).
112. T. Söllner, M. K. Bennett, S. W. Whiteheart, R. H. Scheller, J. E. Rothman, A Protein Assembly-Disassembly Pathway In Vitro That May Correspond to Sequential Steps of Synaptic Vesicle Docking , Activation , and Fusion. *Cell.* **75**, 409–418 (1993).
113. S.-H. Hu *et al.*, Possible roles for Munc18-1 domain 3a and Syntaxin1 N-peptide and C-terminal anchor in SNARE complex formation. *Proc. Natl. Acad. Sci. U. S. A.* **108**, 1040–5 (2011).
114. J. L. Lewis, M. Dong, C. A. Earles, E. R. Chapman, The Transmembrane Domain of Syntaxin 1A Is Critical for Cytoplasmic Domain Protein-Protein Interactions. *J. Biol. Chem.* **276**, 15458–15465 (2001).
115. C. Rickman, B. Davletov, Arachidonic acid allows SNARE complex formation in the presence of Munc18. *Chem. Biol.* **12**, 545–553 (2005).
116. U. Winter, X. Chen, D. Fasshauer, A conserved membrane attachment site in α -SNAP facilitates N-ethylmaleimide-sensitive factor (NSF)-driven SNARE complex disassembly. *J. Biol. Chem.* **284**, 31817–31826 (2009).
117. E. Rusinova, V. Tretyachenko-Ladokhina, O. E. Vele, D. F. Seneor, J. B. Alexander Ross, Alexa and Oregon Green dyes as fluorescence anisotropy probes for measuring protein-protein and protein-nucleic acid interactions. *Anal. Biochem.* **308**, 18–25 (2002).
118. D. Fasshauer, Structural insights into the SNARE mechanism. *Biochim. Biophys. Acta - Mol. Cell Res.* **1641**, 87–97 (2003).
119. D. Dawidowski, D. S. Cafiso, Allosteric control of syntaxin 1a by munc18-1: Characterization of the open and closed conformations of syntaxin. *Biophys. J.* **104**, 1585–1594 (2013).
120. R. Guan, H. Dai, J. Rizo, Binding of the Munc13-1 MUN domain to membrane-anchored SNARE complexes. *Biochemistry.* **47**, 1474–1481 (2008).
121. T. C. Südhof, J. E. Rothman, Membrane fusion: grappling with SNARE and SM proteins. *Science.* **323**, 474–7 (2009).
122. I. Dulubova, S. Sugita, S. Hill, M. Hosaka, A conformational switch in syntaxin during exocytosis: role of munc18. *EMBO* **18**, 4372–4382 (1999).
123. J. E. Richmond, R. M. Weimer, E. M. Jorgensen, An open form of syntaxin bypasses the requirement for UNC-13 in vesicle priming. **412**, 338–341 (2008).
124. P. Zhou *et al.*, Syntaxin-1 N-peptide and Habc-domain perform distinct essential functions in synaptic vesicle fusion. *EMBO J.* **32**, 159–71 (2013).
125. T. Sasaki, Phosphorylation of Munc-18/n-Sec1/rbSec1 by Protein Kinase C. *J.*

- Biol. Chem.* **271**, 7265–7268 (1996).
126. F. E. Zilly, J. B. Sørensen, R. Jahn, T. Lang, Munc18-bound syntaxin readily forms SNARE complexes with synaptobrevin in native plasma membranes. *PLoS Biol.* **4**, 1789–1797 (2006).
127. Y. Zhang *et al.*, Munc18a does not alter fusion rates mediated by neuronal SNAREs, synaptotagmin, and complexin. *J. Biol. Chem.* **290**, 10518–10534 (2015).
128. R.-W. Peng, C. Guetg, E. Abellan, M. Fussenegger, Munc18b regulates core SNARE complex assembly and constitutive exocytosis by interacting with the N-peptide and the closed-conformation C-terminus of syntaxin 3. *Biochem. J.* **431**, 353–61 (2010).
129. F. Li, N. Tiwari, J. E. Rothman, F. Pincet, Kinetic barriers to SNAREpin assembly in the regulation of membrane docking/priming and fusion. *Proc. Natl. Acad. Sci.* **113**, 10536–10541 (2016).
130. S. Vivona *et al.*, Disassembly of all snare complexes by N-ethylmaleimide-sensitive factor (NSF) is initiated by a conserved 1:1 interaction between ??-soluble NSF attachment protein (SNAP) and SNARE complex. *J. Biol. Chem.* **288**, 24984–24991 (2013).
131. D. Parisotto, J. Malsam, A. Scheutzow, J. M. Krause, T. H. Söllner, SNAREpin assembly by Munc18-1 requires previous vesicle docking by synaptotagmin 1. *J. Biol. Chem.* **287**, 31041–9 (2012).
132. A. S. Munch *et al.*, Extension of Helix 12 in Munc18-1 Induces Vesicle Priming. *J. Neurosci.* **36**, 6881–91 (2016).
133. F. Deak *et al.*, Munc18-1 binding to the neuronal SNARE complex controls synaptic vesicle priming. *J. Cell Biol.* **184**, 751–764 (2009).
134. R. Jahn, T. Lang, T. C. Südhof, Membrane fusion. *Cell.* **112**, 519–533 (2003).
135. Y. Gao *et al.*, Single Reconstituted Neuronal SNARE Complexes Zipper in Three Distinct Stages. *Science (80-.)*. **337**, 1340–1343 (2012).
136. S. Wang *et al.*, Conformational change of syntaxin linker region induced by Munc 13 s initiates SNARE complex formation in synaptic exocytosis. **36**, 816–829 (2017).
137. J. W. Barclay *et al.*, Phosphorylation of Munc18 by protein kinase C regulates the kinetics of exocytosis. *J. Biol. Chem.* **278**, 10538–10545 (2003).
138. T. Cijssouw *et al.*, Munc18-1 redistributes in nerve terminals in an activity- and PKC-dependent manner. *J. Cell Biol.* **204**, 759–75 (2014).
139. U. Nili *et al.*, Munc18-1 phosphorylation by protein kinase C potentiates vesicle pool replenishment in bovine chromaffin cells. *Neuroscience.* **143**, 487–500 (2006).



140. C. F. Latham, S. L. Osborne, M. J. Cryle, F. A. Meunier, Arachidonic acid potentiates exocytosis and allows neuronal SNARE complex to interact with Munc18a. *J. Neurochem.* **100**, 1543–1554 (2007).
141. J. H. Williams, M. L. Errington, M. a Lynch, T. V Bliss, Arachidonic acid induces a long-term activity-dependent enhancement of synaptic transmission in the hippocampus. *Nature.* **341**, 739–742 (1989).
142. P. Ray, J. D. Berman, W. Middleton, J. Brendle, Botulinum toxin inhibits arachidonic acid release associated with acetylcholine release from PC12 cells. *J. Biol. Chem.* **268**, 11057–11064 (1993).
143. E. Connell *et al.*, Mechanism of arachidonic acid action on syntaxin-Munc18. *EMBO Rep.* **8**, 414–9 (2007).
144. A. Stein, R. Jahn, Complexins living up to their name--new light on their role in exocytosis. *Neuron.* **64**, 295–297 (2009).

Appendix

Appendix Table 1. A representative view of the crosslinks obtained upon the chemical crosslinking and MS/MS analysis of the syntaxin1a/SNAP25a/Munc18-1 complex.

Type	Protein 1	Protein 2	Residue 1	Residue 2
Inter	SNAP25a	Syntaxin1a	40	94
Inter	SNAP25a	Syntaxin1a	96	94 252 256 260
Inter	SNAP25a	Syntaxin1a	102	94 252
Inter	SNAP25a	Syntaxin1a	103	94 252 260
Inter	SNAP25a	Syntaxin1a	189	252 260
Inter	Munc18-1	SNAP25a	46	72
Inter	Munc18-1	SNAP25a	13	103
Inter	Munc18-1	Syntaxin1a	125	3
Intra	Munc18-1	Munc18-1	125	92 98 120 294 583
Intra	Munc18-1	Munc18-1	294	125 277



				294 308 526 562
Intra	Munc18-1	Munc18-1	583	125 587
Intra	SNAP25a	SNAP25a	40	102 103
Intra	SNAP25a	SNAP25a	96	103 201
Intra	SNAP25a	SNAP25a	102	40 103 201
Intra	SNAP25a	SNAP25a	103	40 96 102 103 184 201
Intra	Syntaxin1a	Syntaxin1a	1	70 117
Intra	Syntaxin1a	Syntaxin1a	12	88 94 117
Intra	Syntaxin1a	Syntaxin1a	84	46 88
Intra	Syntaxin1a	Syntaxin1a	88	12 37 63 70 83



				94 118
Intra	Syntaxin1a	Syntaxin1a	83	75 79 117



Appendix Table 2. A representative view of the peptide-crosslinks obtained upon the chemical crosslinking and MS/MS analysis of the syntaxin1a/SNAP25a/Munc18-1 complex after addition of synaptobrevin.

Type	Protein 1	Protein 2	Residue 1	Residue 2
Inter	SNAP25a	Syntaxin1a	96	94 260
Inter	SNAP25a	Syntaxin1a	102	94 260
Inter	SNAP25a	Syntaxin1a	103	94 252 260
Inter	SNAP25a	Syntaxin1a	201	94 252 260
Inter	Synaptobrevin 2	Syntaxin1a	87	252 260
Inter	Synaptobrevin 2	Syntaxin1a	91	252 260
Inter	Synaptobrevin 2	SNAP25a	87	96 103 201
Inter	Syntaxin1a	Synaptobrevin 2	252	87 94
Inter	Munc18-1	Syntaxin 1a	384	70
Inter	Munc18-1	Syntaxin 1a	461	92
Intra	SNAP25a	SNAP25a	103	40 96 184 201

Intra	SNAP25a	SNAP25a	201	96 103
Intra	Syntaxin 1a	Syntaxin 1a	63	46 88 94
Intra	Syntaxin 1a	Syntaxin 1a	70	83 88 94
Intra	Syntaxin 1a	Syntaxin 1a	46	37 63 83
Intra	Syntaxin 1a	Syntaxin 1a	88	37 63 70 83 94
Intra	Syntaxin 1a	Syntaxin 1a	83	12 46 8
Intra	Syntaxin 1a	Syntaxin 1a	94	1 12 63 70 88 94 108 260
Intra	Syntaxin 1a	Syntaxin 1a	108	12 94
Intra	Syntaxin 1a	Syntaxin 1a	117	1 46
Intra	Syntaxin 1a	Syntaxin 1a	252	253 256 260



Intra	Syntaxin 1a	Syntaxin 1a	253	252 256 260
Intra	Syntaxin 1a	Syntaxin 1a	256	252 253 256 260
Intra	Syntaxin 1a	Syntaxin 1a	251	94 252 253 256 260
Intra	Synaptobrevin 2	Synaptobrevin 2	87	94
Intra	Munc18-1	Munc18-1	20	25 294
Intra	Munc18-1	Munc18-1	25	20 277
Intra	Munc18-1	Munc18-1	120	125 461
Intra	Munc18-1	Munc18-1	125	120 294 526
Intra	Munc18-1	Munc18-1	184	294 583
Intra	Munc18-1	Munc18-1	196	213
Intra	Munc18-1	Munc18-1	277	25 294 461
Intra	Munc18-1	Munc18-1	294	20 98 125 184 277



				294 526
Intra	Munc18-1	Munc18-1	308	332 333
Intra	Munc18-1	Munc18-1	314	332 333
Intra	Munc18-1	Munc18-1	461	120 277
Intra	Munc18-1	Munc18-1	526	125 294
Intra	Munc18-1	Munc18-1	583	184 587



List of Figures

INTRODUCTION

FIGURE 1.1-1. SNARE-PROTEINS INVOLVED AT DIFFERENT STEPS OF INTRACELLULAR TRAFFICKING IN A YEAST CELL AND A MAMMALIAN CELL. 12

FIGURE 1.2-1. SNARE-CORE COMPLEX AND THE CENTRAL LAYERS OF THE INTERACTING SIDE-CHAINS. 14

FIGURE 1.3-1. STEPS INVOLVED IN SNARE-MEDIATED MEMBRANE FUSION. 16

FIGURE 1.4-1. STEPS INVOLVED IN SNARE-COMPLEX ASSEMBLY AND SUBSEQUENT SNARE-RECYCLING..... 17

FIGURE 1.5-1. RIBBON DIAGRAMS OF MUNC18-1, SYNTAXIN1A AND THE SYNTAXIN1A/MUNC18-1 COMPLEX. 20

FIGURE 1.5-2. MUNC13-1 CAUSES THE TRANSITION FROM THE 'CLOSED' SYNTAXIN1A TO 'OPEN'SYNTAXIN1A. 22

FIGURE 1.7-1. SCHEMATIC REPRESENTATIONS OF THE ASSOCIATION OF MUNC18-1 WITH SNARE-PROTEINS DURING THE PROCESS OF SNARE-COMPLEX ASSEMBLY. 27

MATERIALS AND METHODS

FIGURE 2.1-1. WILD-TYPE CONSTRUCTS FOR NEURONAL SNARE PROTEINS AND SM-PROTEIN USED IN THIS STUDY. 31

FIGURE 2.1-2. REPRESENTATION OF THE CYSTEINE MUTANTS OF SYNTAXIN1A AND SNAP25A USED IN THIS STUDY. 32

FIGURE 2.1-3. DIFFERENT FRAGMENTS OF WILD-TYPE SYNAPTOBREVIN AND THE CORRESPONDING CYSTEINE-MUTANTS USED IN THIS STUDY..... 33

FIGURE 2.13-1. SCHEME OF A TYPICAL CO-FLOTATION ASSAY..... 41

RESULTS

FIGURE 3.1-1. EFFECT OF MUNC18-1 ON THE SYNTAXIN1A/SNAP5A (2:1) COMPLEX IN SOLUTION. 46

FIGURE 3.1-2 DETERMINATION OF THE MAGNITUDE OF MUNC18-1 EFFECT ON THE SYNTAXIN1A/SNAP25A COMPLEX.....	47
FIGURE 3.1-3 HSQC-NMR SPECTRA OF ¹⁵ N-SNAP25A UNDER DIFFERENT CONDITIONS.....	49
FIGURE 3.1-4. PEAK ASSIGNMENTS OF SNAP25A FOR THE CROSS-PEAKS OBSERVED IN THE HSQC-NMR SPECTRA.....	51
FIGURE 3.2-1. PURIFICATION OF THE SYNTAXIN1A/SNAP25A/MUNC18-1 COMPLEX.	53
FIGURE 3.3.1-1. SYNTAXIN1A/SNAP25A/MUNC18-1 COMPLEX BINDS EFFICIENTLY TO SYNAPTOBREVIN.	54
FIGURE 3.3.1-2. DOSE-DEPENDENT RESPONSE FOR THE SYNTAXIN1A/SNAP25A/MUNC18-1 COMPLEX.....	55
FIGURE 3.4-1 COMPARISON OF THE SYNTAXIN1A/SNAP25A/MUNC18-1 COMPLEX WITH THE SYNTAXIN1A/SNAP25A (2:1) COMPLEX.....	58
FIGURE 3.4-2 COMPARISON OF THE SYNAPTOBREVIN-BINDING EFFICIENCY BETWEEN THE SYNTAXIN1A/SNAP25A/MUNC18-1 COMPLEX AND THE ΔN-COMPLEX.	59
FIGURE 3.4-3. FRET MEASUREMENTS SHOWING THE KINETICS OF SNARE-COMPLEX FORMATION, USING SYNTAXIN1A/SNAP25A/MUNC18-1 COMPLEX AND THE ΔN-COMPLEX.....	61
FIGURE 3.5-1. THE SYNTAXIN1A/SNAP25A/MUNC18-1 COMPLEX LOSES ITS STABILITY WITH TIME.	62
FIGURE 3.5-2. STABILITY OF THE SYNTAXIN1A/SNAP25A/MUNC18-1 COMPLEX.....	64
FIGURE 3.5-3. SEC-PROFILES OF SYNTAXIN1A, SNAP25A, MUNC18-1, THE BINARY SYNTAXIN1A/SNAP25A COMPLEX AND THE SYNTAXIN1A/MUNC18-1 COMPLEX	65
FIGURE 3.6-1. TITRATION OF THE SYNTAXIN1A/SNAP25A/MUNC18-1 COMPLEX WITH INCREASING AMOUNTS OF THE CHEMICAL CROSS-LINKER, BS3.....	67
FIGURE 3.6-2. INTER CROSS-LINKS OBTAINED BETWEEN SYNTAXIN1A, SNAP25A AND MUNC18-1 UPON CHEMICAL CROSS-LINKING OF THE SYNTAXIN1A/SNAP25A/MUNC18-1 COMPLEX.	68
FIGURE 3.6-3. RIBBON DIAGRAM OF THE SYNTAXIN1A/MUNC18-1 COMPLEX.....	70
FIGURE 3.6-4. REPRESENTATIVE INTRA-CROSSLINKS BETWEEN THE MONOMERIC CONSTITUENTS OF THE SYNTAXIN1A/SNAP25A/MUNC18-1 COMPLEX.....	72
FIGURE 3.7-1. SYNAPTOBREVIN-BINDING TO THE SYNTAXIN1A/SNAP25A/MUNC18-1 COMPLEX CAUSES A DECREASE IN ITS RETENTION VOLUME.....	74



FIGURE 3.7-2. MUNC18-1 DOES NOT GET DISPLACED UPON SYNAPTOBREVIN-BINDING TO THE SYNTAXIN1A/SNAP25A/MUNC18-1 COMPLEX.	75
FIGURE 3.7-3. INTER-CROSSLINKS BETWEEN MUNC18-1 AND SYNTAXIN1A AFTER THE ADDITION OF SYNAPTOBREVIN TO THE SYNTAXIN1A/SNAP25A/MUNC18-1 COMPLEX.....	77
FIGURE 3.7-4. SYNAPTOBREVIN-BINDING TO THE SYNTAXIN1A/SNAP25A/MUNC18-1 COMPLEX LEADS TO AN INCREASE IN ITS MOLECULAR MASS/HYDRODYNAMIC RADIUS.	78
FIGURE 3.7-5. ASSESSMENT OF SNARE-COMPLEX ASSEMBLY BY SDS-RESISTANCE ASSAY.....	80
FIGURE 3.7-6. SYNAPTOBREVIN-BINDING TO THE SYNTAXIN1A/SNAP25A/MUNC18-1 COMPLEX LEADS TO THE FORMATION OF A FULLY-ZIPPERED SNARE-COMPLEX.....	81
FIGURE 3.7-7. FULLY ASSEMBLED SNARE-COMPLEX CAN BE DISASSEMBLED BY NSF-ASNAP.	83
FIGURE 3.8-1. FLUORESCENCE ANISOTROPY MEASUREMENTS TO MONITOR THE BINDING OF C-TERMINALLY AND N-TERMINALLY TRUNCATED FRAGMENTS OF SYNAPTOBREVIN TO THE SYNTAXIN1A/SNAP25A/MUNC18-1 COMPLEX.	85
FIGURE 3.8-2. BINDING OF FLUORESCENTLY-LABELED SYNAPTOBREVIN FRAGMENTS TO THE C-TERMINALLY STABILIZED Δ N-COMPLEX.	86
FIGURE 3.8-3. FRET MEASUREMENTS BETWEEN THE DIFFERENT SYNAPTOBREVIN FRAGMENTS AND THE SYNTAXIN1A/SNAP25A/MUNC18-1 COMPLEX.....	88
FIGURE 3.8-4. BINDING OF DIFFERENT SYNAPTOBREVIN-FRAGMENTS TO THE FLUORESCENTLY LABELED Δ N-COMPLEX, MEASURED BY FRET.....	89
FIGURE 3.9-1. EFFECT OF NSF-ASNAP ON THE SYNTAXIN1A/SNAP25A/MUNC18-1 COMPLEX..	91
FIGURE 3.9-2. NSF-ASNAP CAN DISASSEMBLE THE SYNTAXIN1A/SNAP25A (2:1) COMPLEX.....	92
FIGURE 3.9-3. NSF-ASNAP DOES NOT DISASSEMBLE THE SYNTAXIN1A/SNAP25A/MUNC18-1 COMPLEX.	93
FIGURE 3.9-4. DETERMINATION OF THE ORIENTATION OF THE SYNTAXIN1A/SNAP25A/MUNC18-1 COMPLEX AFTER ITS INCORPORATION INTO LIPOSOMES.....	95

DISCUSSION

FIGURE 4.1-1. THE ASSOCIATION BETWEEN SYNTAXIN1A AND MUNC18-1 IS INDESPENSABLE FOR SYNAPTIC VESICLE DOCKING AND PRIMING, BUT BECOMES DISPENSABLE AT A LATER STAGE IN SYNAPTIC VESICLE EXOCYTOSIS.....	99
---	----

List of Figures



MAX-PLANCK-GESELLSCHAFT

FIGURE 4.2-1. CRYSTAL STRUCTURE OF VPS33 WITH THE QA-SNARE, VAM3 AND ITS COMPARISON WITH MUNC18-1/SYNTAXIN1A INTERACTION. 103

FIGURE 4.4-1. SCHEMATIC MODEL REPRESENTING THE ASSOCIATION OF MUNC18-1 WITH THE SNARE-PROTEINS AT DIFFERENT STAGES OF SNARE-COMPLEX ASSEMBLY. 107

Curriculum Vitae

Name: Shrutee Jakhanwal

Nationality: Indian

Date of Birth: 27.12.1989

E-mail address:
shrutee.jakhanwal@mpibpc.mpg.de



Education

PhD Research

Max Planck Institute for Biophysical chemistry, Department of Neurobiology,
Am Fassberg, Göttingen, Germany.

PhD Supervisor: Prof. Dr. Reinhard Jahn

Title of Thesis: 'Regulation of Neuronal SNARE Complex by Accessory Proteins'

**Sep 2013-
August 2017**

Molecular Biology Course Work

International Max Planck Research School, Molecular Biology,
Göttingen, Germany.

Grade obtained: A

2012-2013

Masters of Science (M.Sc.)

South Campus, University of Delhi, Department of Biochemistry,
New Delhi, India.

Thesis Supervisor: Prof. Dr. Debi P. Sarkar

Title of Thesis: 'Sendai virosome-liver cell interaction: An approach towards understanding alterations in host cell proteome.'

Grade obtained: I (2nd rank in the university)

2010-2012

Bachelors of Science (B.Sc.)

Sri Venkateswara College, University of Delhi, South Campus,
Department of Biochemistry, New Delhi, India.
Grade obtained: I (2nd rank in the university)

2007-2010

Conferences/symposiums attended

Horizons in Molecular Biology, Göttingen, Germany, September 2013.

Turkish –German Graduate Workshop, Istanbul, Turkey, September 2014.

Horizons in Molecular Biology, Göttingen, Germany, September 2014.

Heinrich –Wieland Symposium, Munich, Germany, October 2014

Janelia Farm Conference, Virginia, USA, May 2015

European Biophysical Societies' Association Conference, Dresden, Germany, June 2015.

The Protein Society Symposium, Barcelona, Spain, July 2015

Horizons in Molecular Biology, Göttingen, Germany, October 2015.

Gordon Research Conference, New Hampshire, USA, August 2016.

Life Sciences Open Day, Weizmann Institute of Science, Israel, September 2016.

Horizons in Molecular Biology, Göttingen, Germany, October 2016.

Society for Neuroscience, San Diego, USA, November, 2016.

Organizational/Teaching skills

Organizing committee of the conference: 'Horizons in Molecular Biology' held in Göttingen, Germany (2014).

A selected poster judge at 'Horizons in Molecular Biology' held in Göttingen, Germany (2014).



Organizing committee of the conference: 'Horizons in Molecular Biology' held in Göttingen, Germany (2015).

Supervisor of several lecture tutorials offered by the International Max Planck Research School (IMPRS) for Molecular Biology, Göttingen, Germany.

Supervisor of short methods courses organized in the laboratory of Prof. Reinhard Jahn at Max Planck Institute for Biophysical Chemistry, Göttingen, Germany.

Awards/Honors

2010 – 2012: Mon Santo Scholarship (awarded to the top two university rankers) for Master studies in Biochemistry by the University of Delhi, India.

2012 – 2013: Stipend of the Excellence Foundation for the Promotion of the Max Planck Society, Germany.

2013-2016: Max Planck Society Grants for PhD Students, Goettingen, Germany

September, 2014: Awarded a travel grant to attend the Turkish-German Graduate Workshop on Molecular Neuroscience held in Istanbul (Turkey)

October, 2014: Awarded a travel grant to attend and present scientific research at the 'Heinrich -Wieland Symposium' held in Munich, Germany.

May, 2015: Awarded a travel award (1500 Euros) to attend and present scientific research at a Janelia Farm Conference held in Virginia, USA.

July, 2015: Awarded a travel grant (1500 Euros) to attend and present scientific research at 'The Protein Society Symposium' held in Barcelona, Spain.

October, 2016: Awarded the GGNB travel grant (1900 Euros) to attend and present research at the 'Society for Neuroscience' held in San Diego, USA.

Languages

English: Full proficiency in reading, writing and speaking.

Hindi (Native): Full proficiency in reading, writing and speaking.

German: Elementary level.



List of Publications

Shrutee Jakhanwal¹, Chung-Tien Lee^{2,3}, Henning Urlaub^{2,3}, and Reinhard Jahn¹, An activated Q-SNARE/SM protein complex as a possible intermediate in SNARE assembly. *EMBO J.* **36**, 1788-1802 (2017).

Alex J. B. Kreutzberger^{1,2}, Volker Kiessling^{1,2}, Binyong Liang^{1,2}, Patrick Seelheim^{1,2}, **Shrutee Jakhanwal**³, Reinhard Jahn³, J. David Castle^{1,4}, and Lukas K. Tamm^{1,2}, Reconstitution of Calcium-Mediated Exocytosis of Dense Core Vesicles. *Science Advances.* (2017).